# Cell Quota Based Population Models and their Applications

by

Aaron Packer

A Dissertation Presented in Partial Fulfillment
of the Requirement for the Degree
Doctor of Philosophy

Approved November 2014 by the
Graduate Supervisory Committee:

Yang Kuang, Chair
Eric Kostelich
Yun Kang
John Nagy
Hal Smith

ARIZONA STATE UNIVERSITY

December 2014

ABSTRACT

In 1968, phycologist M.R. Droop published his famous discovery on the functional relationship between growth rate and internal nutrient status of algae in chemostat culture. The simple notion that growth is directly dependent on intracellular nutrient concentration is useful for understanding the dynamics in many ecological systems. The cell quota in particular lends itself to ecological stoichiometry, which is a powerful framework for mathematical ecology. Three models are developed based on the cell quota principal in order to demonstrate its applications beyond chemostat culture.

First, a data-driven model is derived for neutral lipid synthesis in green microalgae with respect to nitrogen limitation. This model synthesizes several established frameworks in phycology and ecological stoichiometry. The model demonstrates how the cell quota is a useful abstraction for understanding the metabolic shift to neutral lipid production that is observed in certain oleaginous species.

Next a producer-grazer model is developed based on the cell quota model and nutrient recycling. The model incorporates a novel feedback loop to account for animal toxicity due to accumulation of nitrogen waste. The model exhibits rich, complex dynamics which leave several open mathematical questions.

Lastly, disease dynamics in vivo are in many ways analogous to those of an ecosystem, giving natural extensions of the cell quota concept to disease modeling. Prostate cancer can be modeled within this framework, with androgen the limiting nutrient and the prostate and cancer cells as competing species. Here the cell quota model provides a useful abstraction for the dependence of cellular proliferation and apoptosis on androgen and the androgen receptor. Androgen ablation therapy is often used for patients in biochemical recurrence or late-stage disease progression and is in general initially effective. However, for many patients the cancer eventually develops resistance months to years after treatment begins. Understanding how and predicting

when hormone therapy facilitates evolution of resistant phenotypes has immediate implications for treatment. Cell quota models for prostate cancer can be useful tools for this purpose and motivate applications to other diseases.

ACKNOWLEDGEMENTS

First and foremost, I would like to thank my advisor Dr. Yang Kuang. Without his continuous support over the many years, I would not be where I am today, in both my academic and professional careers. Dr. Kuang is more than just a great professor; he is a mentor who stands by his students and helps them realize their potential. This and all future (and past) academic work is dedicated to him.

I would also like to thank Debra Olson for her unprecedented support throughout my years at ASU. From registering for classes to meeting deadlines to graduating, Debra has made it possible for me to succeed academically. She goes out of her way to ensure that every graduate student has a successful tenure in the School of Mathematical and Statistical Sciences.

I am also grateful for the support and sacrifices of my parents. They have worked extraordinarily hard to give all four of their children every opportunity possible to succeed. Their compassion has enabled me to be free to pursue my dreams.

Last but certainly not least, I am forever grateful to my beautiful wife Erin. Her love and support have been the true motivators for me to finish my degree. Nothing would have been possible without her by my side. We are expecting a baby boy later this year, just around the same time as graduation. There could not be a better gift.

TABLE OF CONTENTS

CHAPTER Page

LIST OF TABLES

LIST OF FIGURES

Chapter 1

# DROOP (CELL QUOTA) MODEL

## 1.1 Introduction

In 1968, phycologist M.R. Droop published his famous discovery on the functional relationship between growth rate and internal nutrient status of algae in chemostat culture (Droop, 1968). The cell quota is a basic but important concept. This simple notion that growth depends directly on the intracellular level of the limiting nutrient can be a powerful tool for population ecology and ecosystem dynamics.

The experiments in Droop (1968) involved chemostats with varying concentrations of vitamin $B_{12}$ in the growth media. Droop discovered that there was an empirical relationship between algal specific growth rate and the intracellular concentration of vitamin $B_12$ in chemostat culture. This growth model, commonly referred to as the Cell Quota (or Droop) model (Droop, 1983) is a two-parameter curve which maps specific growth rate to intracellular nutrient of a cell,

$$\mu(Q) = \mu_m \left(1 - \frac{q}{Q}\right), \tag{1.1}$$

where the *cell quota* $Q$ is often expressed as units per cell, e.g. the relative mass of some nutrient per unit of biomass. The *subsistence quota* $q$ can be interpreted as the minimum $Q$ required for life. Similarly, it can be interpreted as the conversion ratio for biomass, whereby $Q > q$ implies there is a nutrient pool available for reproduction (Droop, 1983; Leadbeater, 2006).

The Cell Quota model departs from the traditional Monod growth model where

specific growth rate is a function of the extracellular limiting nutrient (Droop, 1983),

$$\mu(S) = \frac{1}{\gamma}\frac{mS}{K_S + S}, \tag{1.2}$$

where $S$ is the nutrient concentration, $m$ is the maximum specific uptake rate of $S$, $K_S$ is the half-saturation constant, and $\gamma$ is the yield constant. $\gamma$ represents the conversion efficiency of nutrient to net biomass production.

The cell quota model has become commonplace in the ecology literature, with a recent and untraditional application by Portz, Kuang and Nagy (2012) to prostate cancer. $Q$ is especially important in the context of ecological stoichiometry because it explicitly quantifies the stoichiometric ratio of an entity, translating the quantity to important processes such as growth.

## 1.2 Derivation of $\frac{dQ}{dt}$

The derivation for $\frac{dQ}{dt}$ is identical for any population model because it follows directly from conservation of mass. Suppose we have a system with three interdependent state variables. Let $\mathbf{X}$ denote a population and $X(t)$ (mass/volume) its density. Denote by $\mu$ and $\delta$ (1/time) the specific growth and death rates, respectively. The specific rate of net change in $X$ is thus $\mu(\cdot) - \delta(\cdot)$. These rates would generally be nonconstant functions dependent on any number of variables including $X$ and/or some external or internal (limiting) factor(s), indicated by the notation $(\cdot)$.

Let $\mathbf{N}$ represent some "nutrient" that is taken up by and assimilated into $\mathbf{X}$. Define $N(t)$ (mass/volume) as the available *external* concentration of $\mathbf{N}$. Further let $N_x(t)$ be the *internal* concentration of $\mathbf{N}$ uniformly distributed in the population $\mathbf{X}$. $Q(t)$ (mass $\mathbf{N}$/mass $\mathbf{X}$), the cell quota for $\mathbf{N}$, is now calculated by

$$Q(t) = N_x(t)/X(t),\ X(t) \neq 0$$
$$\implies N_x(t) = Q(t)X(t).$$

For the sake of argument, suppose $X(t)$ and $N(t)$ have units of (g/L). Then $Q(t)$ is a scalar. Assume that $X$ is in isolation from any other biological species and can only change from proliferation and death. Denote by $v$ the $X$-specific uptake rate of $\mathbf{N}$ and by $w$ the $N_x$-specific loss rate of $N_x$. Similarly, these rates would generally be nonconstant functions dependent on $X$, $N$, and/or any other factors. Whether or not $\mu$ and $\delta$ are nonconstant functions (and regardless of what variables), we have from conservation of mass that

$$X' = \mu X - \delta X, \tag{1.3}$$

$$N_x' = vX - wN_x - \delta N_x, \tag{1.4}$$

$$N' = -vX + wN_x + \delta N_x. \tag{1.5}$$

Since $N_x = QX$, it follows from the product rule that

$$\begin{aligned} Q' &= \frac{1}{X}N_x' - \frac{Q}{X}X' \\ &= v - w\frac{N_x}{X} - \delta\frac{N_x}{X} - (\mu Q - \delta Q) \\ &= v - wQ - \mu Q. \end{aligned} \tag{1.6}$$

Note that in this generalized model, the nutrient $\mathbf{N}$ need not be a limiting factor. To generalize further, $\mu$ and $\delta$ may represent the specific rates of overall "gain" and "loss" of the population $X$, whose units are not necessarily density. $\mu$ encompasses any process that, in the absence of $\delta$, results in a net increase of $X$: birth, some exogenous input flux, etc. Similarly, $\delta$ encompasses any process that, in the absence of $\mu$, results in a net decrease of $X$: death, harvesting, predation, etc.

Conservation of mass has an important implication for the Cell Quota Model and the mathematical expression of $Q'$. Suppose a model is such that $X'$ has the term $\mu_m\left(1 - \frac{q}{Q}\right)X$ and it is possible that $Q < q$. Unlike the generalized formulation, "gain" and "loss" of $X$ are no longer separated into two distinct functions. While

nothing changes for Then in order for the model to respect conservation of mass, $Q'$ (and $N_x'$) must have the piecewise form (1.7) for $\mu$:

$$\mu = \begin{cases} \mu_m \left(1 - \frac{q}{Q}\right) & \text{if } q \leq Q \\ 0 & \text{if } q > Q \end{cases} \tag{1.7}$$

If a model without the property $Q \geq q$ does not distinguish between $\mu < 0$ and $\mu \geq 0$ in $Q'$ then it violates conservation of mass. While this fact does not preclude using the Cell Quota Model for both proliferation and death, it reinforces the inherent problems with extending Droop's relationship beyond microalgae. This observation does not imply it is incorrect to use the Cell Quota Model for death. It simply illustrates that doing so requires careful derivation of $Q'$ and increases the mathematical complexity with regards to analysis.

## 1.3 Ecological Stoichiometry

The concept of the cell quota lends itself in particular to ecological stoichiometry (Sterner and Elser, 2002), which is a powerful framework for mathematical ecology. Ecological stoichiometry is concerned with the underlying elemental balance in organisms and their interactions. By abstracting organisms as collection of elements, ecosystem dynamics can be conceptualized as the flow of elements between species and their environment.

Ecological stoichiometry is applicable to important industrial questions. Biofuels are important for a number of obvious reasons, ranging from scientific to environmental to industrial. Algal-derived biofuels are a byproduct of neutral lipids (NL) which some species upregulate in nitrogen limiting settings. Understanding why these species upregulate NL synthesis is fundamental to improving the feasibility of industrial scale production (Hu et al., 2008). For certain species of green microalgae, nitrogen (N) limitation stimulates NL synthesis. In Chapter 2 models are used to

demonstrate how the mass ratio of nitrogen to carbon (N:C quota) of algal biomass can be used as an underlying mechanism which drives NL synthesis in N-limiting settings. Combining ecological stoichiometry with the cell quota provides a simple formulation for complicated biological processes.

Ecological stoichiometry is equally effective for multi-species systems. The elemental imbalance between an organism and its food is a fundamental observation in ecological stoichiometry. Animals generally maintain a relatively fixed elemental composition whereas photoautotrophs such as phytoplankton and plants exhibit a highly variable elemental composition (Sterner and Elser, 2002). In a simple plant-herbivore system, this imbalance produces rich and biologically meaningful dynamics (Kuang, Huisman and Elser, 2004).

In Chapter 3 a stoichiometric producer-consumer model is used to investigate the effects of N-based toxicity on producer health. In ecological terms, the recycling of N is an important mechanism in driving dynamics for a producer-consumer system. The model was motivated in part by aquaculture ponds, where accumulation of inorganic N, specifically ammonia, inhibits animal growth and survival.

## 1.4 Cell Quota Model Versus the Cell Quota

It is proposed here that a distinction should be made between the Cell Quota (Droop) Model and the cell quota. Henceforth the Cell Quota Model refers to the functional relationship $\mu_m \left(1 - \frac{q}{Q}\right)$ discovered by Droop whereas cell quota refers to $Q$. More generally, the cell quota is the ratio of the total amount of an intracellular entity and the population. In the context of cell populations such as microalgae or human epithelial cells, it is the per-cell measure of an entity. From this understanding, the cell quota is simply a quantitative tool for relating intracellular biochemical processes to population dynamics.

The notion of a subsistence quota should also be decoupled from the concept of the cell quota. The distinction is needed when attempting to extend the "cell quota" concept to models beyond algae. In the Droop Model, the minimum (or subsistence) quota $q$ is the amount of nutrient ($\mathbf{N}$) required for a single unit of biomass production. If $Q > q$ then there is material available for growth. Conversely, $Q < q$ is open to interpretation. It could represent a form of "starvation" which causes loss of biomass. It could also be argued that $Q < q$ is impossible because the proportion of biomass constituted by $\mathbf{N}$ is no less than $q$. Indeed, typical models with the Droop Model for phytoplankton growth should have the mathematical property that if $Q(0) \geq q$ then $Q(t) \geq q$ for all forward time. This conforms to the idea that $q$ represents the minimum $\mathbf{N}$ needed in a building block of biomass.

In other words, there are subtle intricacies that complicate how exactly the cell quota can or should be applied to different problems. As will be shown in Chapter 4, relaxation of the cell quota's definition gives rise to natural applications for prostate cancer modeling. Since (cancerous) prostate epithelial cells depend on androgen signaling for proliferation and survival, the "cell quota" is defined as the intracellular androgen content. Strictly speaking, in this case the "traditional" cell quota would be a misnomer: the androgens are not "building blocks" that become assimilated into biomass *per se*. The minimum quota $q$ is instead interpreted as a theoretical, homoeostatic intraprostatic androgen concentration at which natural cell turnover and proliferation are balanced on the population level.

# Chapter 2

# NEUTRAL LIPID SYNTHESIS IN GREEN MICROALGAE

## 2.1 Introduction

Algal-derived biofuels show potential as alternative sources of fuel. However, industrial-scale biodiesel production from microalgae still has many open problems and as such is an active research area (Rawat et al., 2013; Mata, Martins and Caetano, 2010). The successful realization of algal biofuel in large, commercial settings is undoubtedly tied to scientific progress in many areas of biology and engineering. The work in this chapter is grounded in both theoretical and applied phycology and explores several pertinent questions concerning algal biofuel.

Many species of microalgae have propensity for synthesizing high levels of neutral lipids (NL), which can then be harvested and used for biofuel production (Hu et al., 2008). It has been observed that many of these "oligeneous" species upregulate lipid synthesis under stressed conditions, particularly during nitrogen limitation. Greater light intensity is also observed to increase NL synthesis. Under conditions low nitrogen and high light, there is an inherent danger for photo-oxidative stress caused by excessive buildup of reducing energy in the photosystems. As algae and higher plants deploy many strategies to protect against photoinhibition and oxidative stress, the phenomenon of extreme NL accumulation is suggested to be one such adaptive response (Hu et al., 2008; Mata, Martins and Caetano, 2010). The synthesis of high-energy NL compensates for the decrease in growth, sustaining an energy sink.

The mathematical model presented in Packer et al. (2011) was the first known model in the literature for lipid production in algae with respect to both light and nu-

trient (nitrogen) limitation. The brief paper stemmed from a much larger, multi-year research effort that began with research interests in mathematical ecology, ecological stoichiometry, and phycology. The original work, elaborated here in greater detail, is independent research.

## 2.2 Data Insights

While the model employs a careful mechanistic derivation, it is also highly data-driven. It is built on underlying biological processes general to oleaginous green microalgae but is formulated specifically for microalgae grown in batch culture. This allowed it to be adapted to and empirically tested against a controlled experiment. The research experiment, outlined in Li et al. (2011), is briefly summarized and discussed here because its data give useful insight into growth and lipid dynamics with respect to nitrogen limitation.

Li et al. (2011) cultivated oleaginous species (Hu, Han and Summerfeld, 2010) of the genus *Pseudochlorococcum* (Archibald, 1970) in rectangular cuboid photobioreactors with constant irradiance on a single side. Reactors contained 1.5 L of the standard BG-11 growth medium (Stanier et al., 1971) prepared with varying $NaNO_3$ concentrations in order to achieve three different nitrogen treatments (0.24, 0.06, and 0 g N $L^{-1}$ corresponding to 100%, 25%, and 0% of the full 1.5 g $L^{-1}$ $NaNO_3$ concentration). Algal dry weight, neutral lipid content, and extracellular nitrogen concentration were measured over the course of 12 days and subsequently used to find best-fit parameters for the model.

The data, illustrated in Figs. 2.1 and 2.2, help give a visual overview of the relationship between growth, NL synthesis, and nitrogen availability. Figure 2.2(a)-(b) demonstrates that neutral lipid synthesis accounted for nearly all biomass productivity after nitrogen was depleted from the media. Figure 2.2(c)-(d) shows the non-NL

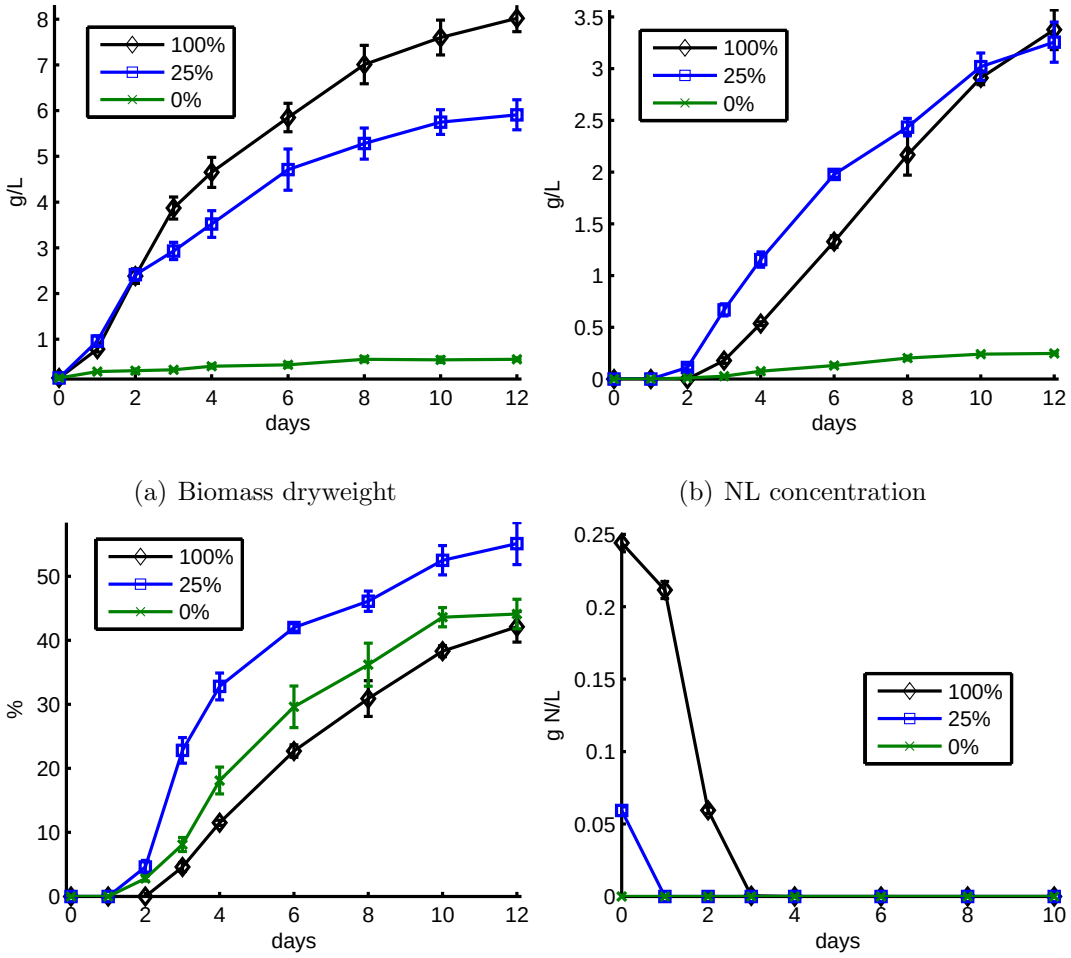


(a) Biomass dryweight

(b) NL concentration

(c) NL content

(d) Extracellular N concentration

**Figure 2.1:** Data from Li et al. (2011). The three lines distinguish cultures with 100%, 25%, and 0% of the 1.5 g $L^{-1}$ $NaNO_3$ concentration of standard BG11 growth medium (0.24, 0.06, and 0 g N $L^{-1}$, respectively).

biomass, calculated by subtracting the measured dryweight densities from the measured NL densities. The negative productivity values for non-NL biomass (Fig. 2.2(c)) are due to net decreases in non-NL mass (e.g. from respiration). Since NL productivity is positive, the decrease in non-NL biomass occurred simultaneously with an increase in NLs. The new NLs could have been synthesized from newly fixed carbon and/or have been converted from existing assimilated carbon. The latter is suggested by Li et al. (2011), as externally induced inhibition of starch synthesis and degradation

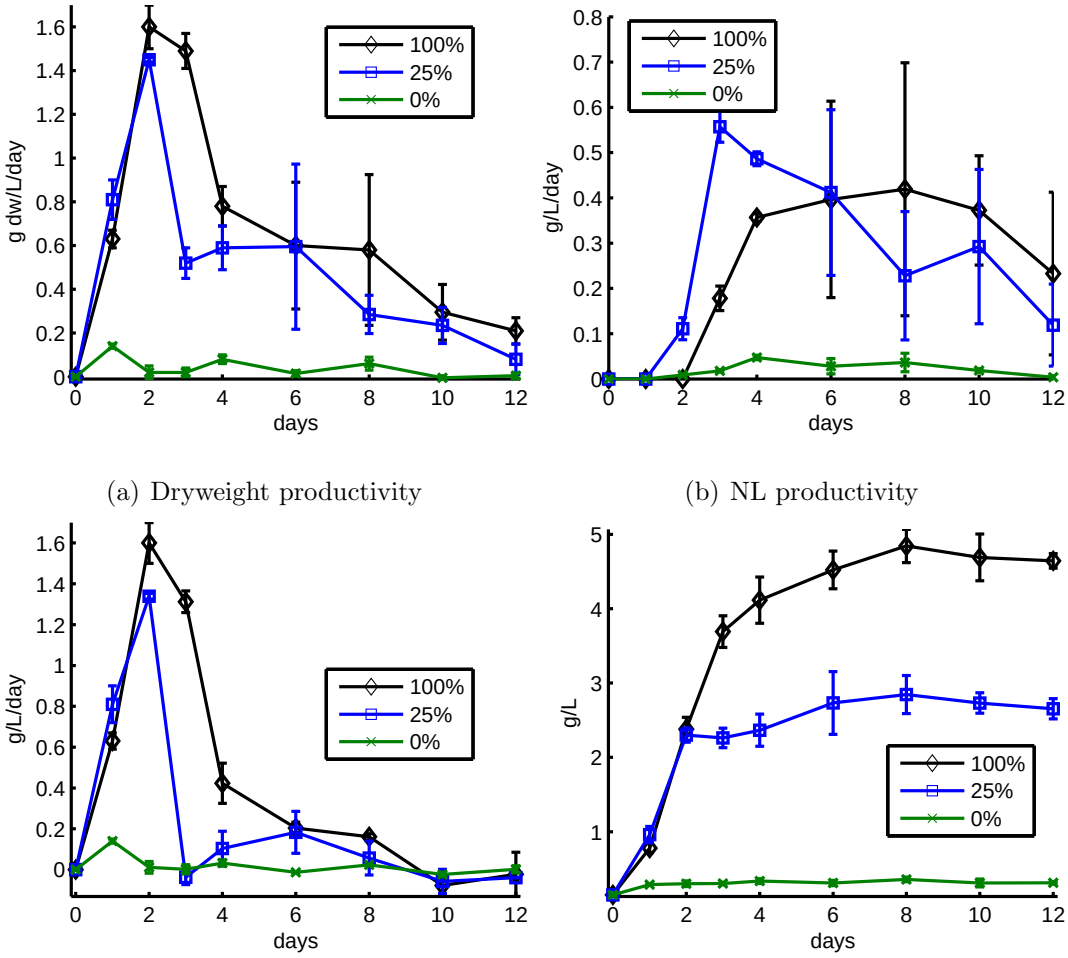


(a) Dryweight productivity

(b) NL productivity

(c) Non-NL productivity

(d) Non-NL biomass

**Figure 2.2:** (a)-(c) Productivity (g $L^{-1}$ $d^{-1}$) calculated from the data using the backward difference. (d) The non-NL biomass density, calculated as the difference of the dry weight and neutral lipid densities.

correlated to decreases in NL production.

### *2.2.1 Cell Quota Implications*

Quantitatively describing a mechanism for this switch from non-NL production to NL production is important for optimizing lipid yield. The cell quota for nitrogen (N-quota) may drive this metabolic transition. As such, it is important to link the data with the N-quota. Although the intracellular N was not directly measured, it

can be estimated using the fact that the system is closed under N. Let $T$ be the total N in the system and $N(t)$ be the extracellular N concentration at time $t$. Then the intracellular N concentration at any time $t$ is given by $T - N(t)$.

Next define $A(t)$ as the non-NL biomass density and $L(t)$ as the lipid density. Thus the total dry weight density is the sum of $A(t)$ and $L(t)$. Also define $Q(t)$ as the N-quota with respect to of $A(t)$. So $Q$ is the ratio of intracellular N to non-NL biomass and $Q(t)A(t)$ is the intracellular N concentration. Therefore,

$$T = Q(t)A(t) + N(t) = Q(0)A(0) + N(0),$$

and $Q(t)$ can be expressed in terms of the unknown initial value $Q(0)$,

$$Q(t) = \frac{Q(0)A(0) + N(0) - N(t)}{A(t)}. \tag{2.1}$$

Finally, let $\widetilde{Q}$ be the N-quota with respect to total biomass. Then

$$\widetilde{Q}(t) = \frac{Q(t)A(t)}{A(t) + L(t)} = \frac{Q(0)A(0) + N(0) - N(t)}{A(t) + L(t)}. \tag{2.2}$$

The rationale for considering both $Q(t)$ and $\widetilde{Q}(t)$ stems from the following observations. First, consider the "normal" state when N is not limiting. Algal growth is due to non-NL biomass production, and NL synthesis is insignificant. Second, consider the state where N is depleted. NL synthesis greatly increases while the production of non-NL biomass is essentially zero. The third and final observation is that the empirical growth rate function discovered by Droop (1968) was the cell-specific growth rate. The cell quota measured and used by Droop (1968) in the function was the N:cell ratio.

It stands to reason that the NL synthesis rate and cell-specific growth rate of *Pseudochlorococcum* sp. were inversely correlated across the two states considered above. Given the experimental observations of $A$ and $L$, it is not unfeasible to assume

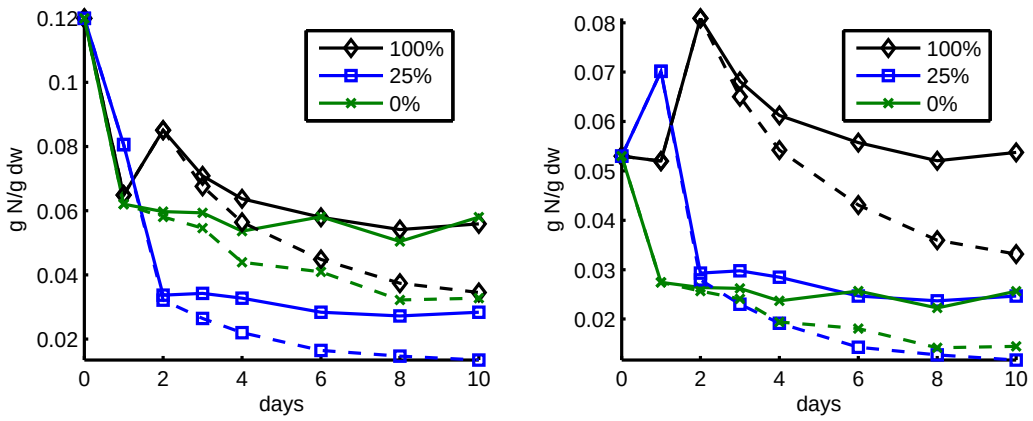


(a) $Q(0) = 0.12$ (b) $Q(0) = 0.053$

**Figure 2.3:** Calculated $Q$ and $\widetilde{Q}$ from the data assuming different values of $Q(0)$. (a) This case would suggest that NL synthesis was upregulated around $Q = 0.07$ and that the 25% culture maintained cell growth at values of $Q$ significantly smaller than 0.07. (b) This case would suggest that $q \approx 0.028$ but that the 100% culture was not N-limited.

that the non-NL biomass density is positively correlated to the cellular density. (This is equivalent to assuming that large variations in an alga's mass are largely due to variations in its NL content.)

It follows that the transition to extreme NL accumulation during N-deprivation is also the transition from positive to extremely low cellular growth. The classic Droop model describes cell-specific growth, and so the switch to complete NL synthesis and zero cellular growth occurs when the N:cell ratio is equal to the minimum quota. Therefore $Q$ is more indicative than $\widetilde{Q}(t)$ of the metabolic switch to NL production. Modeling $A$-specific growth using the $Q$ and the Droop model is consistent with observation.

Figure 2.3 shows the calculated values for $Q$ and $\widetilde{Q}$ using the data with different values for $Q(0)$. If a relatively large $Q(0) > 0.09$ is assumed, the data show that $\widetilde{Q}$ of the 100% and 0% cultures are close in value whereas $\widetilde{Q}$ of the 25% culture decreases to significantly smaller values. This behavior would be consistent with the similar

relationship between the NL content of the three cultures. It would also suggest that NL synthesis in the 0% culture is inhibited despite rapid N-depletion, while NL synthesis in the 100% culture is inhibited due to N-replete conditions. There would be some mechanism by which the 25% culture upregulates NL production during N-depletion, beyond the limit of the 0% culture. A possible explanation would be greater sustained photosynthesis due to the N-availability during the first two days in juxtaposition to the extreme N-starvation of the 0% culture. The problem with this case is that it would suggest $q \approx 0.06$ but that in the 25% culture $Q < q$. If instead $q \approx 0.03$ then both the 0% and 100% cultures would have arrested growth for $Q \approx 2q$. Although it is very likely that the 100% culture is not N-limited, the 0% culture has more extreme N-limitation than that of the 25% culture.

If $Q(0)$ is smaller, e.g. 0.053, then $\widetilde{Q}$ of the 0% and 25% cultures are closely linked whereas $\widetilde{Q}$ of the 100% culture remains significantly greater. In this case the data are fully consistent with the hypothesis that the NL transition occurs as $Q$ decreases towards $q$, and that for $Q = q$ net primary production is almost entirely due to NL synthesis. The data imply that $q \approx 0.027$. While the 0% and 25% data align with this theoretical model, the 100% culture is entirely inconsistent. NL production would have began between days 2 and 3 when $Q > 0.068 > 2.5q$. However, measured NL productivity would have been 0 for $Q > 0.05$ in both the 25% and 100% cultures prior to day 1 and day 2, respectively. If the 100% was indeed N-limited then one could argue that the "premature" decoupling of growth and carbon fixation would have been due to photoacclimation-induced increases in photosynthesis. This could occur if the stock culture was acclimated to low light conditions and/or the initial N-availability facilitated photoacclimation to increase in the rate of photosynthesis. But since the cultures were stocked from the same control suspension, such "premature" decoupling of photosynthesis and growth would have been expected in the 25%

culture, too—especially since its growth was more N-limited.

In the more likely case that the 100% culture was not N-limited, the data support the model. Indeed, with four times the available extracellular nitrogen the 100% culture (non-NL) biomass averaged only (1.70) 1.36 times that of the 25% culture by day 12. Algal uptake fully depleted nitrogen from the growth medium before day 4 (Fig. 2.1). In contrast, the 25% culture (non-NL) biomass averaged (7.97) 10.55 times that of the 0% culture. Coincidentally, if it is assumed that the ratio of $T$ for the two treatments is 7.97 then $Q(0) = 0.057$. In this case the calculated $Q$ and $\widetilde{Q}$ are fully consistent with the discussed example $Q(0) = 0.053$ (Fig. 2.3). If the 100% culture was not N-limited its observed dynamics are still consistent with the theoretical model of NL production by *Pseudochlorococcum* sp. When the limiting nutrient is depleted, cellular growth becomes uncoupled from photosynthesis and the excess carbon influx is devoted to NL synthesis. More experimental work would be required to identify the limiting nutrient and test the model.

## 2.3 Model derivation

A system of 4 ODEs is developed to described the biomass, neutral lipid, and nitrogen dynamics as observed in Li et al. (2011) in addition to chlorophyll *a*. Denote by the following,

| | | |
|---|---|---|
| $A(t)$: | algal dry weight density, ***excluding* neutral lipids** | (g dw $m^{-3}$) |
| $L(t)$: | neutral lipid density | (g C $m^{-3}$) |
| $H(t)$: | Chl *a* quota | (g Chl *a* $g^{-1}$ dw) |
| $Q(t)$: | nitrogen quota of $A$ | (g N $g^{-1}$ dw) |
| $N(t)$: | extracellular nitrogen concentration | (g N $m^{-3}$) |

Algal biomass is split into two pools: NLs and non-NLs, namely $L(t)$ and $A(t)$. Thus the total biomass concentration is the sum $A(t) + L(t)$. The NL pool is considered a transient, C-rich form of biomass that accumulates under stressed conditions. The non-NL pool is assumed to be coupled with the cell-based population, and cell mass changes due to changes in $L(t)$. For consistency with the experimental data and much of the other existing, relevant data, $A$ is defined in terms of dry weight.

Model (2.3) below has similar structure to a generic model of algae suspended in batch culture, but adds two new state variables, $H(t)$ and $L(t)$, for the cellular quota of chlorophyll $a$ and the NL concentration, respectively. The cellular growth rate is a function of both $Q$ and irradiance $I_0$. The rate of neutral lipid synthesis is also a function of $Q$ and $I_0$, as is the rate of Chl $a$ synthesis. The minimum quota $q$ serves as the metabolic switch from cellular proliferation to lipid accumulation.

$$\begin{aligned} A' &= \mu(Q, I_0)A, \\ L' &= f(\mu)A, \\ Q' &= v_m \frac{q_m - Q}{q_m - q} \frac{N}{N + v_h} - \mu(Q, I_0)Q, \\ H' &= h(Q, I_0) - \mu(Q, I_0)H, \\ N' &= -v_m \frac{q_m - Q}{q_m - q} \frac{N}{N + v_h} A \end{aligned} \tag{2.3}$$

Note that $AH$ gives the chlorophyll $a$ concentration just as $QA$ gives the intracellular nitrogen concentration. As before, define by $T$ the total nitrogen in the system. Since the system is closed under nitrogen, only one of $N$ or $Q$ is needed, since $T$ is a constant and for all $t$:

$$(Q \cdot A)(t) + N(t) = T. \tag{2.4}$$

The exact expressions for the functions $\mu$, $f$, and $h$ are systematically derived from both theoretical biology and existing, empirically-driven phytoplankton models

in the literature. Ecological stoichiometry (Sterner and Elser, 2002) then provides the overarching framework for linking the biology, data, and mathematics.

**Assumption 1.** *The cell-specific growth rate, $\mu$, is either N-limited or light-limited.*

Following Liebig's Law of the Minimum, growth can only be limited by a single resource at any given time. If biomass production requires two resources, A and B, then it is limited to the minimum of the two production capacities afforded by A and B. Therefore if $\mu_N$ and $\mu_L$ are the nitrogen- and light-limited growth rates, respectively, then

$$\mu = \min\{\mu_N, \mu_L\}. \tag{2.5}$$

When nitrogen is the only limiting nutrient for growth, $\mu$ is simply the well-established and empirically-supported Droop (Cell Quota) model (Leadbeater, 2006),

$$\mu_N = \mu_m \left(1 - \frac{q}{Q}\right). \tag{2.6}$$

**Assumption 2.** *The rate of C fixation is determined by the rate of photosynthesis, expressed as g C $g^{-1}$ Chl a, and the Chl a content of biomass, $H(t)$.*

Commonly used phytoplankton models of photosynthesis can be mechanistically derived from first order principles. The following formulation from Sakshaug, Andresen and Kiefer (1989) as reviewed in Cullen (1990), relates the quantum yield (mol C $mol^{-1}$ photons) to the mean photon absorption and turnover rates of the photosynthetic unit (PSU). While a PSU is processing an absorbed photon, any subsequently absorbed photons by the PSU are not used. This excess absorption decreases the effective quantum yield. If $\sigma$ ($m^2$ $mol^{-1}$ PSU) is the mean absorption cross-section of the PSU and $I_0$ is the irradiance (mol photons $m^{-2}$ $s^{-1}$) then $\sigma I_0$ is the mean PSU specific absorption rate. Suppose $\tau$ (s) is the turnover time for the PSU (i.e. the time required to process an absorbed photon). Then on average, $\sigma\tau I_0$

photons are absorbed by a PSU while processing a photon. Using a Poisson distribution with mean $\sigma\tau I_0$, the probability of absorbing at least one photon during this period is $1 - e^{-\sigma\tau I_0}$. Since only the first photon is used, the proportion of photons absorbed during a period of length $\tau$ that contribute to the net photosynthesis rate is $(1 - e^{-\sigma\tau I_0})/(\sigma\tau I_0)$.

The theoretical quantum yield $\Phi$ (mol C mol$^{-1}$ photons) is a measure of how much C is fixed relative to absorbed photons if every photon is utilized. Multiplying by the mean proportion of absorbed photons that are used for C fixation gives the effective quantum yield,

$$\Phi \frac{1 - e^{-\sigma\tau I_0}}{\sigma\tau I_0}. \tag{2.7}$$

Phytoplankton models of photosynthesis are often formulated in terms of primary production (e.g. g C m$^{-2}$ d$^{-1}$ or g C m$^{-3}$ d$^{-1}$) and chlorophyll (e.g. g Chl m$^{-2}$ and g Chl m$^{-3}$), as these data are measured in the field (Behrenfeld and Falkowski, 1997b,a; Friedrichs et al., 2009). The result is a function which gives the rate of C fixation relative to chlorophyll (g C g$^{-1}$ Chl d$^{-1}$). If the absorption coefficient of chlorophyll is $a$ (m$^2$ g$^{-1}$ Chl) then the Chl-specific rate of photon absorption is $aI_0$ (mol photons g$^{-1}$ Chl d$^{-1}$). Together with the quantum yield (Eq. (2.7)), the chlorophyll-specific photosynthesis rate $p^H$ can be modeled (Cullen, 1990; Sakshaug, Andresen and Kiefer, 1989) as

$$p^H = aI_0\Phi \frac{1 - e^{-\sigma\tau I_0}}{\sigma\tau I_0} = \frac{a\Phi}{\sigma\tau}\left(1 - e^{-\sigma\tau I_0}\right). \tag{2.8}$$

As a function of $I_0$, Eq. (2.8) is monotonically increasing towards the upper bound $\frac{a\Phi}{\sigma\tau}$. Define $p_m = \frac{a\Phi}{\sigma\tau}$. Then Eq. (2.8) can be expressed as

$$p^H = p_m\left(1 - e^{-\sigma\tau I_0}\right).$$

For $I_0 < {}^1/_{\sigma\tau}$, $p^H$ is approximated by the linear function $p^H(I_0) \approx p_m\sigma\tau I_0$. This approximation is evident by expanding the Taylor series of $p^H$ about 0. Define $I_k :=$

$p_m/a\Phi = 1/\sigma\tau$. Then Eq. (2.8) can be re-expressed again in the equivalent form(s),

$$p^H = p_m \left(1 - e^{-a\Phi I_0/p_m}\right) = p_m \left(1 - e^{-I_0/I_k}\right). \tag{2.9}$$

Field data and models of photosynthesis are often parameterized in terms of $p_m$ and $I_k$ (Cullen, 1990; MacIntyre et al., 2002; Geider, MacIntyre and Kana, 1998; Behrenfeld et al., 2004). The rate $p_m$ ($d^{-1}$) is commonly called the light-saturated rate of photosynthesis, and the value $I_k$ (mol photons $m^{-2}$ $d^{-1}$) the "light saturation parameter" (Platt, Gallegos and Harrison, 1980). For $I_0 < I_k$, the linear approximation above can be written as

$$p^H(I) \approx a\Phi I\big|_{I<I_k}, \quad I_k = \frac{p_m}{a\Phi}, \tag{2.10}$$

which is the numerator in the exponent in Eq. (2.9). For $I = I_k$, Eq. (2.10) gives $p^H(I_k) \approx p_m$, at which point $p^H$ is considered light saturated. As such, $a\Phi I_0$ is referred to as the light-limited rate and $a\Phi$ the light-limited initial slope (MacIntyre et al., 2002; Geider, MacIntyre and Kana, 1996).

With the new formulation in Eq. (2.9), the parameter $p_m$—while mechanistically derived in Eq. (2.8)—represents the adapted maximum photosynthesis rate. Based on observations under nutrient-replete growth conditions, $p_m$ is generally considered to be limited downstream of PSII by the dark reactions (Sukenik, Bennett and Falkowski, 1987; MacIntyre et al., 2002; Behrenfeld et al., 2004) and largely independent of growth irradiance. When different cultures from the same species were photoacclimated to varying levels of irradiance, the corresponding values of $p_m H$ ($h^{-1}$) were not correlated to growth irradiance (MacIntyre et al., 2002). Since $H$ depends largely on growth irradiance (i.e. light history), $p_m$ (g C $g^{-1}$ Chl $a$) may correlate more strongly with growth irradiance.

In Geider, MacIntyre and Kana (1998) $p_m$ is a linear function of $Q$ with $p_m = 0$ when $Q = q$ whereas it is nonlinear in the photoinhibition model of Marshall, Geider

and Flynn (2000). Here $p_m$ is modeled as an increasing nonlinear function of algal N:C with properties given in Eq. (2.11). Since the total biomass $X = A + L$, the N:C is given by the proportion of intracellular N concentration and $X$.

$$\begin{aligned} &p_m\left(Q = q\right) > 0, \quad p_m\left(0\right) = 0, && p_m'\left(\widetilde{Q}\right) \geq 0, \\ &p_m''\left(\widetilde{Q} < q\right) > 0, \quad p_m''\left(\widetilde{Q} > q\right) < 0, && \widetilde{Q} = \frac{AQ}{A+L}. \end{aligned} \tag{2.11}$$

The reason for the formulation in Eq. (2.11) is that $Q(t) \geq q$ for all $t > 0$ and $\lim_{t\to\infty} Q(t) = q$. As the data reveal, $Q$ reaches $q$ in finite time. If $p_m$ were a function of $Q$ then it would remain constant ($p_m(q)$) for all forward time. However, $Q = q$ indicates N-depletion during which $p_m$ should decrease with respect to time. The reason is that during N-stress, down-regulation of the Calvin Cycle coupled with accumulation of inactive/damaged PSII has an inhibitory effect on $p_m$. In addition, the data suggest that after a certain time nearly all increases in biomass can be attributed to the increases in neutral lipids. If $p_m(q) = 0$ then the model would not agree with the observed behavior of lipid production during N-stress. Instead, $p_m$ should rapidly decrease with respect to decreases in $\widetilde{Q}$ when $Q = q$. These properties are adequately described by Eq. (2.12):

$$p_m(\widetilde{Q}) = p_0 \frac{\widetilde{Q}^2}{\widetilde{Q}^2 + q^2} \tag{2.12}$$

Using $I_0$ for $I$ is problematic because it neglects light attenuation and self shading which may limit photosynthesis. It is also important to consider the photobioreactor because light dynamics are fundamentally linked to its design. Technically, the irradiance is a spatial function $I : \Re^3 \to [0, I_0]$ such that the irradiance available for photosynthesis at one position in the reactor may be different than that of another position. In this particular application, the photobioreactor design gives rise to a simple formulation for $I$. With constant irradiance through a single side of the

cuboid-shaped and flat-panel reactor, only one spatial dimension is considered. Further, it is assumed that algal density is spatially homogeneous due to mixing. At a depth $x$ from the light-facing side of the reactor, the Lambert-Beer law is used to estimate $I(x) = I_0 e^{-aHAx}$. If the total depth of the reactor is $z$ then the average irradiance is

$$\begin{aligned} \overline{I} &= \frac{1}{z}\int_0^z I(x)dx \\ &= \frac{1}{z}\int_0^z I_0 e^{-aHAx}dx \\ &= \frac{I_0}{aHAz}\left(1 - e^{-aHAz}\right). \end{aligned} \tag{2.13}$$

This simplification does not consider light attenuation due to non-algal chemical species and assumes that light attenuation from algae is due only to chlorophyll $a$. Since the parameter $a$ is decoupled from $p_m$, it can account for the attenuation due to non-chlorophyll $a$ biomass with a coordinated decrease of the quantum yield $\Phi$.

With $I$, the full expression for the photosynthesis rate can be written. Since $p^H$ is the rate of carbon fixation normalized to Chl $a$ (g C $g^{-1}$ Chl $a$ $d^{-1}$), multiplication by $H$ gives the rate specific to $A$ and the full photosynthesis model is given by,

$$\begin{aligned} p &= Hp_m\left(1 - e^{-a\Phi I/p_m}\right), \\ p_m &= p_0\frac{\widetilde{Q}^2}{\widetilde{Q}^2 + q^2}, \quad \widetilde{Q} = \frac{AQ}{A+L} \\ I &= \frac{I_0}{aHAz}\left(1 - e^{-aHAz}\right). \end{aligned} \tag{2.14}$$

Armed with Eq. (2.14), the remaining model equations can be found.

**Assumption 3.** *The amount of carbon that is required per unit of non-lipid biomass production, $c$, is constant.*

From this assumption the expression for $\mu_L$ can be derived. $c$ serves as a conversion factor between carbon and $A$, similar to $Q$ and intracellular nitrogen— $cA$ is the

intracellular C concentration (excluding neutral lipids) while $QA$ is the intracellular N concentration. Multiplying the rate of C fixation by $c^{-1}$ is the maximum possible growth rate specific to $A$, or

$$\mu_L = p\left(A, L, Q, H\right)/c.$$

**Assumption 4.** *When C intake exceeds that needed for cellular growth and maintenance, neutral lipids are synthesized at a rate proportional to that of excess C intake.*

The decoupling of cellular growth and photosynthesis results in an increased carbon flux that cannot be used for cell growth. There are many mechanisms by which algae deal with the excess photosynthetic activity including excretion of photosynthetically derived dissolved organic compounds and increased synthesis of carotenoids (Berman-Frank and Dubinsky, 1999).

The utilization rate of C for cell growth is $c\mu$ because $c$ is the carbon required per unit of $A$ and $\mu$ is the $A$-specific growth rate. $p$ is the rate of C fixation normalized to $A$. Excess carbon assimilation is therefore quantified as the difference of these two rates: $p - c\min\left\{\mu_N, c^{-1}p\right\}$. When growth is not N-limited, $\mu = c^{-1}p$ and the difference is zero—neutral lipids are only synthesized when $\mu_m\left(1 - \frac{q}{Q}\right) < c^{-1}p$. It is assumed that all excess carbon is used for *de novo* neutral lipid synthesis and that it occurs on the same time scale as $\mu$ and $p$. The full equation for $L'(t)$ simply follows as

$$\begin{aligned} L' &= (p - c\mu)A \\ &= \left(p - \min\left\{c\mu_N, p\right\}\right)A \\ &= \max\left\{p - c\mu_N, 0\right\}A. \end{aligned} \tag{2.15}$$

**Assumption 5.** *Nitrogen uptake and assimilation is a function of the extracellular nitrogen concentration and is regulated by $Q$.*

The standard MichaelisMenten kinetics (Monod) model for nitrogen uptake is used. However, the uptake rate function is multiplied by the function $(q_m - Q)/(q_m - q)$ which is linear and decreasing in $Q$ (Geider, MacIntyre and Kana, 1998). Doing so adds regulation of $Q$ and imposes the mathematical property $Q < q_m$. Although luxury uptake of limiting nutrients is a common strategy amongst green algae, there are significant metabolic costs associated with nitrate uptake and assimilation.

**Assumption 6.** *A variable chlorophyll a content of biomass is used to incorporate photoacclimation. A portion of nitrogen uptake and assimilation is partitioned to chlorophyll a synthesis in order to regulate photosynthesis with respect to the internal cellular state and the environment.*

Photoacclimation is a fundamental process of algal photosynthesis and growth. The chlorophyll $a$ content of green microalgae varies within and across species (Behrenfeld et al., 2004; MacIntyre et al., 2002). The Chl $a$:dw ratio in batch culture has been observed to increase from less than 0.01 to over 0.03 during the course of several days (Li et al., 2008; Geider, MacIntyre and Kana, 1998) which suggests chlorophyll $a$ may play an important role in the transient dynamics modeled here.

Since $H = \text{Chl } a : A$, the chlorophyll $a$ content of $A$, the $H'$ equation follows from the same method used to derive $Q'$. Note that $HA$ is the phytoplankton chlorophyll $a$ concentration: $(HA)'$ is easily derived then used to find $H'$. Namely, $(HA)'$ is the difference of the synthesis and loss rates of chlorophyll $a$.

The synthesis rate of $HA$ is directly tied to nitrogen uptake and assimilation in that a proportion of nitrogen intake is partitioned to chlorophyll $a$ synthesis (Geider, MacIntyre and Kana, 1998). This proportion is given by the function $\rho$, which is dependent on the effectiveness of photosynthesis relative to the energy (C) demands of cellular growth and maintenance. $\rho$ also directly regulates $H$ in the model and thus

its image $[0, \rho_m]$ (g Chl $a$ $g^{-1}$ N), where the parameter constant $\rho_m$ is the maximum observed Chl $a$:N ratio for a specific species of green algae. Although such data were not measured for *Pseudochlorococcum*, the model values were derived from those presented in the literature for other species.

It is assumed that net chlorophyll $a$ degradation can be omitted due to the short duration of the experiments and model (10-12 days). In Geider, MacIntyre and Kana (1998), chlorophyll $a$ degradation was set to 0 for three of the four species data used to validate the model. Further, in Li et al. (2008) the chlorophyll content was measured for an oleaginous species, and such data did not suggest a significant loss of chlorophyll due to degradation. This contrasts the authors' conclusions that chlorophyll $a$ degradation not only was significant but also provided an intracellular nitrogen pool during N-depletion. However, the observed decreases in the algal chlorophyll $a$ content instead could be explained by the observed increases in biomass. The data presented was for the equivalent of $H$, the relative Chl $a$ proportion of biomass. Since $H = \text{Chl } a : A$, any net increases in $A$ relative to net changes in Chl $a$ subsequently decrease $H$. The data instead suggested that chlorophyll $a$ synthesis is arrested during N-depletion, and that continued biomass productivity (due to non-NL or NL production) dilutes the chlorophyll $a$ content (Li et al., 2008).

The derivative for $AH$, the Chl $a$ concentration, is simply the rate of N uptake multiplied by the ratio controlling how much Chl $a$ is produced per unit N. The equation for $H'$ then follows from the product rule, as shown in Eq. (2.16). $v$ is the N-uptake rate function (g N $g^{-1}$ dw $d^{-1}$) and $\rho$ is the proportion of N-assimilation directed to chlorophyll $a$ synthesis.

$$\begin{aligned} (AH)' &= \rho v A, \\ \Rightarrow H' &= \rho v - \mu H. \end{aligned} \tag{2.16}$$

It remains to define $\rho$, which serves as the regulation mechanism for $H$. The

model assumes that regulation of chlorophyll $a$ synthesis, and thus photoacclimation, is inextricably linked to the interplay of carbon fixation and cell growth. (The model does not consider non-chlorophyll $a$ pigments such as those used for photoprotection.) Under low irradiance and N-replete conditions, cells upregulate pigment synthesis in order to meet the demands of growth. Under high irradiance phytoplankton downregulate chlorophyll $a$ synthesis in order to protect from photoinhibition and reduce excess C-fixation relative to growth. Similarly, in N-limited conditions the downregulation of chlorophyll $a$ synthesis reflects unavailability of N.

This regulatory feedback is modeled using a function which is based on the aptly-named "regulatory ratio" presented in Geider, MacIntyre and Kana (1997). This ratio, which drives photoacclimation in the model, quantifies the relative degree of light limitation or light saturation of photosynthesis. It is the ratio of the actual rate to the maximum potential rate of photosynthesis, or

$$\rho = \rho_m \frac{p}{a\Phi IH}. \tag{2.17}$$

The parameter $\rho_m$ is the maximum Chl $a$:N observed for a particular species and the equation $a\Phi IH$ is the light-dependent photosynthesis rate, as described in the derivation of $p(I)$ Eq. (2.14). For non-saturating irradiance, the chlorophyll-specific photosynthesis rate is approximately a linear function of $I$ with slope $a\Phi$ (Eq. (2.10)). Hence $a\Phi IH$ also represents the light harvesting capacity of the algae. For saturating $I$, $p(I)$ is bounded above by the maximum rate $p_m$, which is necessarily less than $a\Phi IH$ (2.14). In this case, light absorption potentially exceeds what an alga can handle downstream of the light reactions. Since $p_m$ is N-dependent but not light-dependent, increasing the light harvesting capacity $a\Phi IH$ would not prove strategic for increasing $p$. To increase $a\Phi IH$ without a relatively equal increase in $p_m$ would worsen the state of excess energy influx.

The parameterization of $\rho$ used for the neutral lipid model (2.3) differs slightly from Eq. (2.17). As originally defined (Geider, MacIntyre and Kana, 1997), the regulatory ratio is the utilization rate of energy relative to the intake rate of energy. However, here utilization is not carbon fixation but instead cell growth, i.e. $c\mu$. Energy refers to organic carbon (or more abstractly light energy) from photosynthesis. $\rho$ now quantifies the degree of the decoupling of growth and photosynthesis, instead of the decoupling of light harvesting capacity and photosynthesis:

$$\rho = \rho_m \frac{c\mu}{p}, \tag{2.18}$$

where $\rho$ declines when photosynthesis $p$ is uncoupled from cell growth $\mu$. Since $\mu = \min\{\mu_N, {}^{p}/_{c}\}$, $p \geq c\mu$ and $\rho \leq \rho_m$.

Both approaches in Eq. (2.17) and Eq. (2.18) are similar because of the relation between $\mu$, $p$ (more specifically $p_m$), and $Q$. Decreases in $Q$ cause parallel changes in $\mu$ and $p_m$ for both models, and when $p > c\mu$, photosynthesis is in excess of growth demands. This would also be indicative of excess light harvesting relative to utilization. Another difference in the model presented here is that $p_m$ is normalized to chlorophyll $a$ rather than algal carbon Geider, MacIntyre and Kana (1997, 1998). In Geider, MacIntyre and Kana (1997) and Geider, MacIntyre and Kana (1998), increasing $H$ decreases $\rho$ (2.17). Here, $p$ is the product of $H$ with the chlorophyll $a$ specific photosynthesis rate. Thus if the same $\rho$ were used for the neutral lipids model (2.20), changes in $H$ would be negated due to it appearing on the numerator and denominator (2.17).

With the new $\rho$ in Eq. (2.18), $H'$ can be fully expressed:

$$\begin{aligned} H' &= \rho v - \mu H = \rho_m \frac{c\mu}{p} v - \mu H \\ &= \mu \\ &= \min\left\{\frac{c\mu_N}{p}, 1\right\}\left(\rho_m v - c^{-1} p H\right) \end{aligned} \tag{2.19}$$

| Parameter | Description | Units |
|---|---|---|
| $A(t)$ | non-NL biomass | g dw $L^{-1}$ |
| $L(t)$ | NL concentration | g NL $L^{-1}$ |
| $N(t)$ | extracellular N concentration | g N $L^{-1}$ |
| $Q(t)$ | $A$-specific N-quota | g N $g^{-1}$ dw |
| $\widetilde{Q}(t)$ | N-quota | g N $g^{-1}$ dw |
| $H(t)$ | chlorophyll $a$ quota | g Chl $a$ $g^{-1}$ dw |
| $I_0$ | irradiance | $\mu$mol photons $m^{-2}$ $d^{-1}$ |
| $z$ | light path | m |
| $a$ | optical cross section of chl a | $m^2$ $g^{-1}$ Chl $a$ |
| $\Phi$ | quantum efficiency | g C $mol^{-1}$ photons |
| $q$ | minimum/subsistence N quota | g N $g^{-1}$ dw |
| $q_m$ | maximum N quota | g N $g^{-1}$ dw |
| $c$ | C subsistence quota | g C $g^{-1}$ dw |
| $v_m$ | maximum uptake rate of nitrogen | g N g $dw^{-1}$ $d^{-1}$ |
| $v_h$ | half-saturation coefficient | g N $m^{-3}$ |
| $\rho_m$ | maximum chl:N | g Chl $a$ $g^{-1}$ N |
| $\mu_m$ | maximum N-limited growth rate | $d^{-1}$ |
| $p_0$ | maximum photosynthesis rate | g C $g^{-1}$ Chl $a$ $d^{-1}$ |

**Table 2.1:** Parameter and variable descriptions.

Combining Model (2.3) with Eqs. (2.14), (2.19), (2.15), (2.12), and (2.5) yields

the complete model,

$$\begin{aligned} A' &= \min\{\mu_N, \mu_L\} A, \\ L' &= \max\{(\mu_L - \mu_N) cA, 0\}, \\ H' &= \left(\frac{\rho_m v}{\mu_L} - H\right) \min\{\mu_N, \mu_L\}, \\ Q' &= v_m \frac{q_m - Q}{q_m - q} \frac{N}{N + v_h} - \min\{\mu_N, \mu_L\} Q, \end{aligned} \tag{2.20}$$

where

$$\begin{aligned} &\mu_N(Q) = \mu_m \left(1 - \frac{q}{Q}\right), \quad \mu_L(A, L, Q, H) = p(A, H, \widetilde{Q})/c, \\ &p(A, H, \widetilde{Q}) = H p_m(\widetilde{Q}) \left[1 - \exp\left(-\frac{a\Phi I(A, H)}{p_m(\widetilde{Q})}\right)\right], \\ &I(A, H) = \frac{I_0}{aHAz} \left[1 - \exp\left(-aHAz\right)\right], \\ &p_m(\widetilde{Q}) = p_0 \frac{\widetilde{Q}^2}{\widetilde{Q}^2 + q^2}, \quad \widetilde{Q} = \frac{AQ}{A + L}, \\ &v(Q, A) = v_m \frac{q_m - Q}{q_m - q} \frac{N}{N + v_h}, \quad N = T - QA. \end{aligned} \tag{2.21}$$

### *2.4.1 Properties*

System (2.20) was formulated for short-term batch cultures. However, mathematical properties are presented then used to discuss and justify the model's strengths and shortcomings. These results also justify otherwise speculative reasoning based on the data and simulations. Define $T = Q(t)A(t) + N(t)$. Note that $T' = 0$ and $T$ is constant, as expected for the closed system. The set

$$\Omega = \left\{(A, L, Q, H) : 0 < A < T/q, 0 < L, q < Q < q_M, 0 < H < \rho_m Q\right\} \tag{2.22}$$

consists of biologically reasonable solutions and is positively invariant. First, however, it needs to be checked that System (2.20) is well defined on the boundary $\partial\Omega$. In

particular, that $I(A,H)$ and $H'(t)$ are well defined as $H \to 0$ and as $A \to 0$.

**Lemma 1.** *System* (2.20) *is well defined on both* $\Omega$ *and* $\overline{\Omega}$ *as* $H \to 0$ *or* $A \to 0$.

*Proof.* It is readily apparent that if $p$ is well defined then so are $A'(t)$, $L'(t)$, $Q'(t)$, and $N'(t)$. To confirm that $p$ is well defined on $\overline{\Omega}$, it suffices to show that $I(A,H)$ is well defined as $A \cdot H \to 0$. It follows from l'Hôpital's rule that

$$\begin{aligned}\lim_{A\cdot H\to 0} I(A,H) &= \lim_{S\to 0} \frac{I_0}{azS}\left(1-e^{-azS}\right)\\ &= I_0.\end{aligned}$$

Thus $p = Hp_m\left(1-e^{-a\Phi I/p_m}\right) \to 0$ as $H \to 0$ or as $A \to 0$, with the latter because $p_m \to 0$ as $A \to 0$. So $p$ is well defined on $\overline{\Omega}$.

To show that $H'$ is well defined as $p \to 0$, rewrite

$$\frac{dH}{dt} = \frac{\mu}{\mu_L}\rho_m v(Q) - \mu H = \min\left\{\frac{\mu_N}{\mu_L}, 1\right\}(\rho v - \mu_L H).$$

Then the result follows from $\lim_{p\to 0} \min\left\{\frac{\mu_N}{\mu_L}, 1\right\} = 1$. □

Next, the minimum function that appears in the growth rate function $\mu$ may raise questions whether or not the system is Lipschitz and hence guaranteed to have unique solutions via an application of the Picard-Lindelof theorem. The following theorem, while simple, is useful for such assurance.

**Theorem 1.** *Let* $F_1 : A \to \Re, F_2 : A \to \Re$ *where* $A \subseteq \Re^n$ *and* $F_1 \in C^1, F_2 \in C^1$ *and* $H(x) = \min\{F_1(x), F_2(x)\}$. *Then* $H$ *is Lipschitz continuous.*

*Proof.* Since $F_1 \in C^1, F_2 \in C^1$, there are $L_1 > 0, L_2 > 0$ such that for all $x_1, x_2 \in A$, $\|F_1(x_2) - F_1(x_1)\| \leq L_1\|x_2 - x_1\|$ and $\|F_2(x_2) - F_2(x_1)\| \leq L_2\|x_2 - x_1\|$. There are four cases that need consideration:

I. $H(x_2) - H(x_1) = F_1(x_2) - F_1(x_1)$. Then $\|H(x_2) - H(x_1)\| \leq L_1\|x_2 - x_1\|$.

II. $H(x_2) - H(x_1) = F_2(x_2) - F_2(x_1)$. Similarly, $\|H(x_2) - H(x_1)\| \leq L_2\|x_2 - x_1\|$.

III. $H(x_2) - H(x_1) = F_1(x_2) - F_2(x_1)$. Let $x(t) : [0,1] \to [x_1, x_2]$ be defined as $x(t) = x_1 + t(x_2 - x_1)$. Since $F_1, F_2$ are continuous and $F_2(x(0)) < F_1(x(0))$ but $F_2(x(1)) > F_1(x(1))$, there is a $t^* \in (0,1)$ such that $F_2(x^*) = F_1(x^*)$ where $x^* = x(t^*)$. Then

$$\begin{aligned}
\|F_1(x_2) - F_2(x_1)\| &= \|F_1(x_2) - F_1(x^*) + F_2(x^*) - F_2(x_1)\| \\
&\leq \|F_1(x_2) - F_1(x^*)\| + \|F_2(x^*) - F_2(x_1)\| \\
&\leq L_1\|x_2 - x^*\| + L_2\|x^* - x_1\| \\
&= (1-t)L_1\|x_2 - x_1\| + tL_2\|x_2 - x_1\| \\
&\leq L_1\|x_2 - x_1\| + L_2\|x_2 - x_1\|.
\end{aligned}$$

IV. $H(x_2) - H(x_1) = F_2(x_2) - F_1(x_1)$. Similarly, we have that $F_2(x_2) - F_1(x_1) \leq (L_1 + L_2)\|x_2 - x_1\|$.

Thus $H$ is Lipschitz continuous with Lipschitz constant $L_1 + L_2$. □

**Theorem 2.** *System* (2.20) *has unique solutions with respect to initial conditions in* $\Omega$.

*Proof.* Applying Theorem 1 to each component's derivative in System (2.20), we see that each is Lipschitz continuous. The Picard-Lindelof theorem for existence and uniqueness can be applied for the result. □

**Theorem 3.** $\Omega$ (2.22) *is positively invariant for the semi-flow generated by system* (2.20).

*Proof.* Let $\mathbf{x_0} \in \Omega$ and define $\mathbf{x}(t) = [A(t), L(t), Q(t), H(t)]^\top$ as the solution $\mathbf{x}(t) = \phi(t, \mathbf{x_0})$ to System (2.20). Suppose that $\Omega$ is not invariant; that is, there exists $t_1 > 0$ such that

$$\{\mathbf{x}[t < t_1]\} \subseteq \Omega, \qquad \mathbf{x}(t_1) \notin \Omega.$$

Note that since $\Omega$ is open,

$$\Omega = \Omega^{\circ}, \qquad \mathbf{x}(t_1) \in \partial\Omega,$$

which means $\mathbf{x}(t_1)$ must be on a hyperplane generated by fixing a coordinate to one of its boundary values; for example, $\{H = 0\} \cap \overline{\Omega}$. Therefore it suffices to consider the following seven cases. Unless specified otherwise, assume that $0 \leq t \leq t_1$.

Case I. $H(t_1) = 0$. Let $\hat{\mu} = \max\{\mu(\mathbf{x}(t)) : t \in [0, t_1]\} < \infty$, which exists since $\mathbf{x}(t)$ is continuous on $[0, t_1]$. Also note that $\dfrac{\mu}{\mu_L}\rho_m v \geq 0$ on $\overline{\Omega}$. Thus for $t \in [0, t_1]$,

$$\begin{aligned} H' &= \frac{\mu}{\mu_L}\rho_m v - \mu H \\ &= \min\left\{\frac{\mu_N}{\mu_L}, 1\right\}(\rho_m v - \mu_L H) \\ &\geq -\bar{\mu} H, \end{aligned}$$

and from Gronwall's inequality $H(t) \geq H(0)e^{-\bar{\mu}t} > 0$, contradicting $H(t_1) = 0$. So $H(t) > 0 \forall t \geq 0$, and the semi-flow through $x_0 \in \Omega$ cannot leave $\Omega$ through the hyperplane $\{H = 0\} \cap \overline{\Omega}$.

Case II. $A(t_1) = 0$. But $A' > 0$, contradicting $A(0) > 0$.

Case III. $L(t_1) = 0$. Similarly, $L' > 0$ arriving at a contradiction.

Case IV. $Q(t_1) = q$. By property of the minimum function, $\mu \leq \mu_N = \mu_m(1 - q/Q)$. Then

$$\begin{aligned} Q' &\geq v_m \frac{q_m - Q}{q_m - q}\frac{N}{N + v_h} - \mu_m(1 - \frac{q}{Q})Q \\ &> -\mu_m(Q - q). \end{aligned}$$

Gronwall's inequality gives $Q(t) \geq q + (Q(0) - q)e^{-\mu_m t} > q$, contradicting $Q(t_1) = q$.

Case V. $Q(t_1) = q_M$. Then continuity of $Q$ implies $Q'(t_1) \geq 0$. But,

$$Q'(t_1) = -\min\{\mu_L, \mu_N\} Q \ < 0,$$

contradicting $Q'(t_1) \geq 0$. Thus any semi-flow through $\Omega$ cannot leave $\Omega$ through the hyperplane $Q = q_m$. Note that the strict inequalities $\mu_L(t_1) > 0$ and $\mu_N(t_1) > 0$ are possible here since the previous cases have shown that $Q(t) > q$, $A(t) > 0$, and $H(t) > 0$ for all $t$.

Case VI. $A(t_1) = T/q$. It suffices to show that $A(t_1)Q(t_1) < T$ since $q < Q$ implies $T/Q(t_1) < T/q$. Indeed,

$$\begin{aligned}(QA)' &= v_m \frac{q_m - Q}{q_m - q} \frac{N}{N + v_h} A, \\ &\leq \frac{v_m}{v_h} NA \;=\; \frac{v_m}{v_h} A(T - QA), \\ &\leq \frac{v_m}{v_h} \frac{T}{q}(T - QA) \;:=\; k(T - QA).\end{aligned}$$

Then it follows from $Q(0)A(0) < T$ and Gronwall's inequality that $T > T + (Q(0)A(0) - T)e^{-kt} \geq Q(t)A(t)$, a contradiction.

Case VII. $H(t_1) = \rho_m Q(t_1)$. Define the function

$$w(t) = A(t)H(t) - \rho_m A(t)Q(t).$$

Recall that, by assumption, $H(t) - \rho_m Q(t) < 0$ and $A(t) > 0$ for $t < t_1$ with $\mathbf{x}(\mathbf{t}) \in \Omega$. Then $w(t_1) = 0$ implies $w'(t_1) \geq 0$. By definition $\mu_L \leq \mu$, and from Case II $A(t_1) > 0$. It follows that

$$\frac{dw}{dt} = \frac{\mu}{\mu_L} \rho_m v A - \rho_m v A < 0,$$

contradicting $w'(t_1) \geq 0$ and $H(t_1) = \rho_m Q(t_1)$.

It has been shown that for any $x_0 \in \Omega$, the semi-flow $\Phi(t, x_0)$ through $x_0$ is cannot leave $\Omega$. □

**Remark 1.** *Observe that* $I(A, H) = \frac{I_0}{aHAz} \left[1 - \exp\left(-aHAz\right)\right]$ *is a strictly decreasing, non-negative function and that on* $\overline{\Omega}$, $H < \rho_m Q$ *implies* $H < \rho_m q_m$. *Thus*

$$\inf_{\Omega} \{I(A, H)\} \geq I(T/q, \rho_m q_m) > 0.$$

*Further,* $p_m(\widetilde{Q}) = p_0 \frac{\widetilde{Q}^2}{\widetilde{Q}^2+q^2} > 0$ *and so*

$$p(A, H, \widetilde{Q}) = H p_m(\widetilde{Q}) \left[1 - \exp\left(-\frac{a\Phi I(A,H)}{p_m(\widetilde{Q})}\right)\right] > 0.$$

Though the extracellular nitrogen $N(t)$ is decoupled from System (2.20), the following results are useful when proving later results.

**Remark 2.** *The bounds* $0 < N < T$ *for the uncoupled variable* $N$ *now follow from* $A > 0$, $Q > q > 0$, *and* $QA < T$*:*

$$QA < T \implies 0 < T - QA = N,$$
$$0 < QA \implies T > T - QA = N.$$

**Lemma 2.** *For solutions to System* (3.1) *with initial conditions in* $\Omega$*,*

$$\lim_{t\to\infty} N(t) = 0,$$

*where the limit is approached monotonically.*

*Proof.* Recall from Theorem 3 and Remark 2 that $A(t) > 0$, $Q(t) < q_m$, and $0 < N(t)$. Thus

$$N' = -\left[v_m \frac{q_m - Q}{q_m - q} \frac{A}{N + v_h}\right] N < 0.$$

□

**Corollary 1.** *It follows from Lemma 2 and* $N = T - QA$ *that*

$$\lim_{t\to\infty} Q(t)A(t) = T.$$

Corollary 1 is unsurprising given the model's formulation and conservation of mass. It is similarly easy to conjecture the asymptotic behavior of $A$ and $Q$: once N is depleted from the growth medium, non-lipid biomass production will continue

until $Q = q$, at which point the growth rate given by the cell quota model is zero. At this point, $A$ will reach $T/q$, the theoretical maximum non-lipid biomass density supported by the available N in the bioreactor. Although it is not proven here that $A \to T/q$, the following Lemma, combined with the facts that $N \to 0$ and $Q'$ is only positive when $N > 0$, suggest $Q \to q$. If so $A \to T/q$ would immediately follow.

**Lemma 3.** *Suppose there is a $t_0 \geq 0$ such that $Q'(t_0) > 0$. Then there exists $t_1 > t_0$ such that $Q'(t) > 0$ on $[t_0, t_1)$ and $Q'(t_1) = 0$.*

*Proof.* Let $t_0 > 0$ with $Q'(t_0) > 0$. Suppose instead that such a $t_1$ does not exist; in other words, $Q'(t) > 0$ for all $t \geq t_0$ and so $Q$ is monotonically increasing on $[t_0, \infty)$. Since $\sup\{Q\} = q_m$, it must follow that $\lim_{t\to\infty} Q(t) = q_m$.

$Q''$ is bounded, and so it follows from Barbalat's Lemma that $\lim_{t\to\infty} Q'(t) = 0$. Then

$$\begin{aligned}
\lim_{t\to\infty} Q'(t) &= \lim_{t\to\infty} v_m \frac{q_m - Q}{q_m - q}\frac{N}{N + v_h} - \min\{\mu_N, \mu_L\} Q \\
&= 0, \\
\iff \quad \lim_{t\to\infty} \min\{\mu_N, \mu_L\} &= 0 \qquad \left(\text{since } \lim_{t\to\infty} \frac{q_m - Q}{q_m - q}\frac{N}{N + v_h} = 0\right) \\
\iff \quad \lim_{t\to\infty} \mu_L &= 0 \qquad (\text{since } \mu_N(q_m) > 0) \\
\iff \quad \lim_{t\to\infty} I(A, H) &= 0 \ \textbf{ or } \ \lim_{t\to\infty} p_m(\widetilde{Q}) = 0.
\end{aligned}$$

However, as shown in Remark 1, $I(A, H)$ is bounded below by a strictly positive value. Therefore,

$$\begin{aligned}
\lim_{t\to\infty} \mu_L &= 02 \\
\iff \quad \lim_{t\to\infty} p_m(\widetilde{Q}) &= 0 \\
\iff \quad \lim_{t\to\infty} \widetilde{Q} &= \lim_{t\to\infty} \frac{QA}{QA + L} \\
&= 0, \\
\iff \quad \lim_{t\to\infty} A &= 0 \ \text{ or } \ \lim_{t\to\infty} L = \infty.
\end{aligned}$$

But from Corollary 1, $\lim_{t\to\infty} QA = T$ means $\lim_{t\to\infty} A \neq 0$. This leaves $\lim_{t\to\infty} L = \infty$ which implies $L'(t) > 0$ for all $t > t_n$. But

$$\begin{aligned} L' &= \max\{(\mu_L - \mu_N)\, cA, 0\} \\ &> 0 \\ \iff \mu_L &> \mu_N, \end{aligned}$$

contradicting $\mu_L \to 0$. Hence $Q$ can only be increasing on finite intervals of $t$. Continuity therefore implies that there must exist a $t_1 > t_0$ such that $Q'(t_1) = 0$. □

## 2.5 Parameter values

| **Parameter** | **Value** |
|---|---|
| $k_a^T$ | 600 $\mu$mol photon $m^{-2}$ $d^{-1}$ |
| $z$ | 0.03 m |
| $a$ | 4.82 $m^2$ $g^{-1}$ chl |
| $c$ | 0.610 g C $g^{-1}$ dw |
| $q$ | 0.0277 g N $g^{-1}$ dw |
| $q_m$ | 0.0935 g N $g^{-1}$ dw |
| $v_m$ | $5.96 \times 10^{-1}$ g N $g^{-1}$ dw $d^{-1}$ |
| $v_h$ | $1.03 \times 10^{-5}$ g N $m^{-3}$ |
| $\rho$ | 0.283 g chl $g^{-1}$ N |
| $\mu_m$ | 3.26 $d^{-1}$ |
| $p_0$ | 90.1 g C $g^{-1}$ chl $d^{-1}$ |
| $\Phi$ | $9.84 \times 10^{-3}$ mol C $mol^{-1}$ photon |

**Table 2.2:** Parameter values.

All parameter values are consistent with those established in the literature. Best-fit parameters were found by minimizing the mean square error. Table 2.2 lists

parameter values and initial conditions.

Observed values for $q$ vary considerably across and within species of microalgae. For example, single studies have found $q$ to range from 0.02 to 0.07 g N $g^{-1}$ C (Ho et al., 2003). It is important to consider the units for $q$ when comparing and using measured values. Originally the cell quota was expressed as intracellular nutrient normalized to cell count (e.g. pg nutrient $10^{-6}$ cells) but it is often expressed as the N:C ratio of biomass with units of g N $g^{-1}$ C or mol N $mol^{-1}$ C (Droop, 1973, 2003; Ho et al., 2003). Using the cell quota as a stoichiometric ratio is useful in the context of Ecological Stoichiometry or measuring biomass in terms of carbon dry weight in the field. Since *Pseudochlorococcum* sp. biomass was measured by its dry weight, $Q$ and $\widetilde{Q}$ have units of g N $g^{-1}$ dw. These units are technically equal to the common formulation g N $g^{-1}$ C but data measured with respect to dry weight are not equal to data measured with respect to carbon. Further, as illustrated by the data (Fig. 2.1), *Pseudochlorococcum* sp. exhibit extreme plasticity, with NL content of biomass that ranges from below measurable to over 50% on the order of days. Since NLs mostly consist of carbon, it is assumed that cellular mass varies with respect to NL content. As such, the C-content of biomass dry weight should also vary with respect to NL content. The data support this assumption: when N was replete, biomass-specific growth was not due to NL synthesis. When N was depleted, NL synthesis constituted nearly all biomass-specific growth. Coupled with arrested cellular reproduction, cellular mass should have simultaneously increased primarily due to carbon assimilation and storage.

For purposes of the model, it is assumed that there is a constant conversion factor $\hat{c}$ (g C $g^{-1}$ dw) for dry weight of non-NL biomass and dry weight in carbon. That is, $\hat{c}A(t)$ is the intracellular carbon not associated with neutral lipids. The parameter $c$ is the sum of $\hat{c}$ and the additional metabolic costs in carbon per unit of non-NL growth. Therefore $\hat{c}/c$ represents the efficiency of cell growth with respect to carbon.

The photosynthesis model as formulated in Eq. (2.14) has three parameters (excluding $q$): $p_0$, $a$, and $\Phi$. Measured values of $p_0$ vary depending on units and measurement methods. Here $p_0$ is parameterized as the net carbon fixation rate normalized to chlorophyll $a$. Maximum photosynthesis rates may also be measured in terms of net oxygen evolution and/or normalized to algal C or cells. An example range of reported $p_0$ values is 0.5 to 29.3 g C $g^{-1}$ Chl $a$ $h^{-1}$ (Behrenfeld et al., 2004; MacIntyre et al., 2002). Measured values of the absorption coefficient $a$ ($m^2$ $g^{-1}$ Chl) similarly vary across a wide range of values. When absorption is normalized to chlorophyll $a$, as done in this model, the absorption due to other pigments is only implicitly considered. If the relative proportion of chlorophyll $a$ to other pigments changes then $a$ ($m^2$ $g^{-1}$ Chl $a$) may also change. Measured values of $a$ are reported as low as under 1 $m^2$ $g^{-1}$ Chl $a$ and as high as 40 $m^2$ $g^{-1}$ Chl $a$ (Falkowski, Dubinsky and Wyman, 1985; Behrenfeld et al., 2004).

The theoretical quantum yield for fully efficient photosynthesis can be mechanistically derived. Each molecule of $O_2$ evolved requires 8 photons, so $\Phi$ has the theoretical maximum value of 0.125 mol $O_2$ $mol^{-1}$ photons. Of course, the realized efficiency is typically lower. For example, light absorption by photoprotective pigments and non-photochemical quenching direct photons from oxygen evolution. Actual values of $\Phi$ have been measured between 0.077 mol $O_2$ $mol^{-1}$ photons and 0.12 mol $O_2$ $mol^{-1}$ photons (MacIntyre et al., 2002). When $\Phi$ is parameterized as the quantum efficiency of net carbon fixation (mol C $mol^{-1}$ photons), it decreases further from its theoretical maximum as there are multiple electron sinks downstream of PSII. Observed values have been reported to vary by as much as two orders of magnitude, from 0.001 mol C $mol^{-1}$ photons to 0.1 mol C $mol^{-1}$ photons (Sakshaug et al., 1997; MacIntyre et al., 2002; Behrenfeld et al., 2004). Converted to units consistent with the model gives the range $1.2 \times 10^{-8}$ g C $\mu mol^{-1}$ photons to $1.2 \times 10^{-6}$ g C $\mu mol^{-1}$ photons.

### N Uptake and $\theta$ Synthesis

Nitrogen uptake and chlorophyll-related parameters are readily available in the literature (Droop, 2003; Geider, MacIntyre and Kana, 1998; Li et al., 2008; Sakshaug, Andresen and Kiefer, 1989). Since N-uptake rates are often normalized to algal carbon (for example, g N $g^{-1}$ C $d^{-1}$), values for $v_m$ from the literature were converted to g N $g^{-1}$ dw $d^{-1}$ using $\hat{c}$. Chlorophyll $a$ content was not measured for *Pseudochlorococcum*; however, by finding best-fit parameters, variations in $H(t)$ from observed values for *Pseudochlorococcum* can be compensated for with parameters $a$ and $\Phi$. Initial values for $H(t)$ were taken from the range 0.005 g dw $g^{-1}$ Chl $a$ to 0.03 g dw $g^{-1}$ Chl $a$ (Li et al., 2008; Geider, MacIntyre and Kana, 1998). Initial guesses for $\rho$ chosen from the range 0.2 g Chl $a$ $g^{-1}$ N to 0.4 g Chl $a$ $g^{-1}$ N, consistent those reviewed in Geider, MacIntyre and Kana (1998).

## 2.6 Results

Optimized parameters were found by minimizing the residual sum of squares for extracellular nitrogen, biomass dry weight, and neutral lipid content. The model was unable to accurately fit data from the 100% culture while also fitting data from the N-limited 0% and 25% cultures. Therefore the residual sum of squares was subsequently minimized with respect to data for the N-limited cultures only, and those results are presented here. Parameter values and MSE values are presented in Table 2.2. Simulation results for available data are presented in Fig. 2.4), while results for $Q$ and $H$ are presented in Fig. 2.5).

The model greatly agrees with the 12-day observations for 0% and 25%. As expected, the model overestimates biomass for the 100% cultures due to the assumption that growth is only N- or light-limited. Since the average maximum non-NL biomass

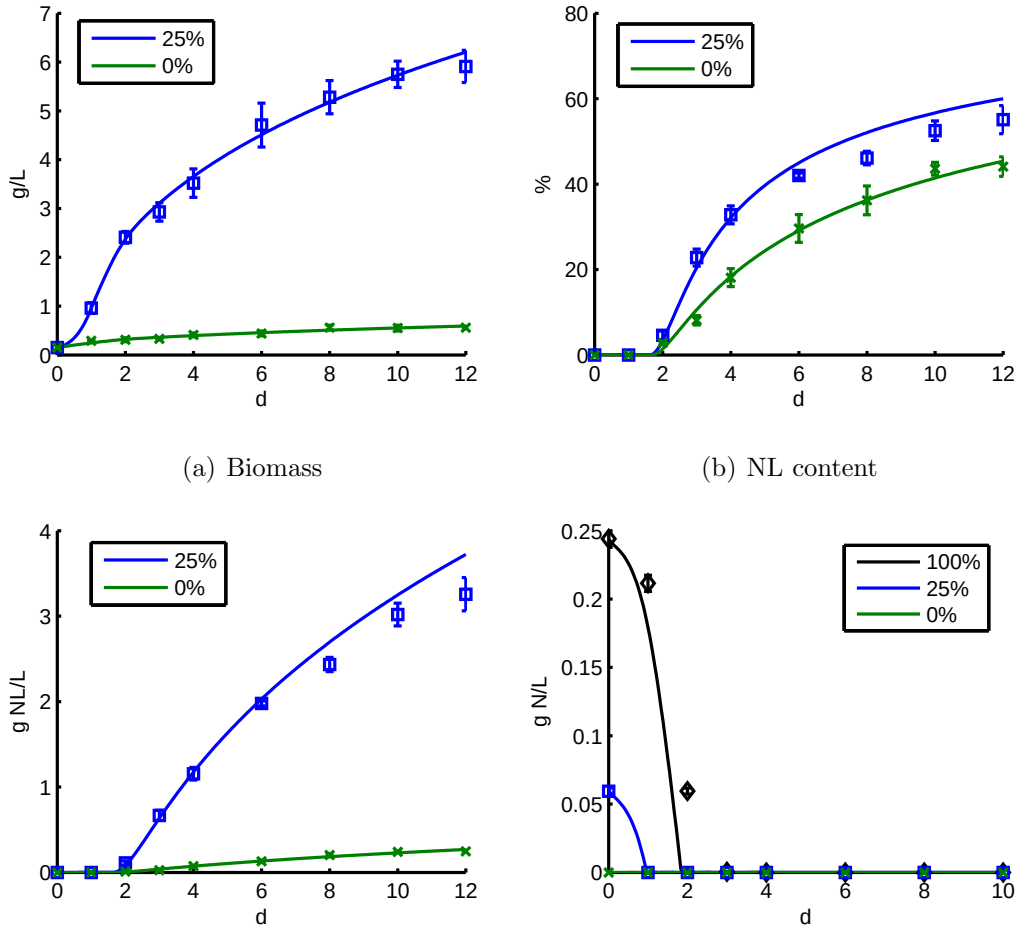


(a) Biomass

(b) NL content

(c) NL concentration

(d) Extracellular N concentration

**Figure 2.4:** Model results. (a) Biomass dryweight. (b) NL content of biomass. (c) NL concentration. Note the overestimation for the %25 cultures. (d) Extracellular nitrogen concentration. The model was not fitted to the 100% culture data—it is displayed here for illustrative purposes.

in the 100% cultures was only 1.7 times greater than that in the 25% cultures, but the 100% cultures had four times as much nitrate, it is likely that growth in the 100% cultures was limited by another nutrient.

An inherent property of the model is that it does not accommodate long-term dynamics; it is formulated for batch cultures up until stationary phase. For example, there is no mechanism for cell death or explicit consideration for respiration and cellular upkeep. As such, biomass and neutral lipids are overestimated after stationary

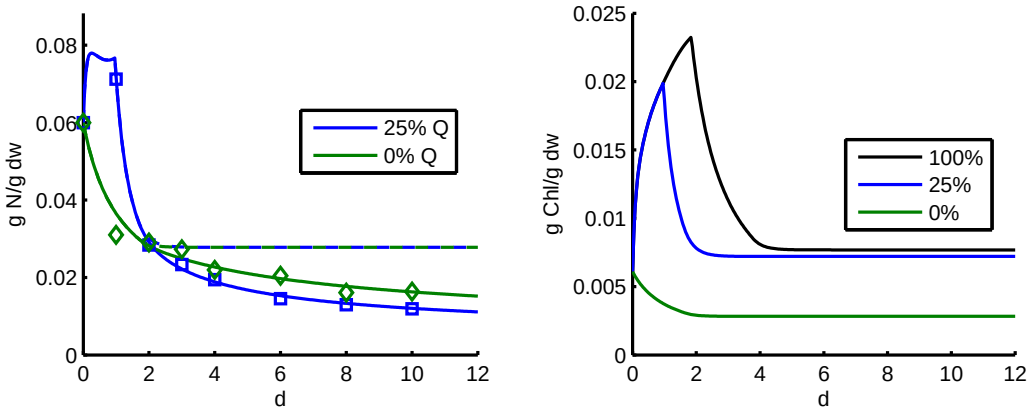


(a) $Q$ and $\widetilde{Q}$

(b) Chlorophyll $a$ content

**Figure 2.5:** (a) Simulation results for $Q$ and $\widetilde{Q}$ are shown along with calculated $\widetilde{Q}$ from data. The dashed lines are $Q$. (b) Results for $H$. The 100% culture results are shown to demonstrate the interrelated dynamics of $N$ assimilation and chlorophyll $a$ synthesis.

phase. Theorem 3 and Remark 1 reveal the causes for this behavior.

## 2.7 Conclusion and Future Work

A novel model of neutral lipid synthesis in green microalgae was carefully derived and validated against parallel experiments. Existing, empirically-driven mathematical formulations for modeling in phycology were combined with very specific and relevant concepts in theoretical biology. Model (2.20) provides a framework in and of itself for modeling neutral lipid production in green microalgae. This work demonstrates how ecological stoichiometry may be used as an effective model for describing neutral lipid production in green oleaginous algae. In particular, the N:C of algal biomass quantifies the metabolic transition from "normal" carbon assimilation and storage to the extreme upregulation of biosynthesis of neural lipids. Splitting biomass into separate compartments for functional biomass and neutral lipids is a useful conceptualization for stoichiometric models. Assumption 4, which posits that lipid synthesis is an energy sink under nutrient stress, combined with the decoupling

of carbon fixation from growth, form the basis for improved and more sophisticated models. Klok et al. (2013), for example, further distinguishes biomass in terms of both starch and neutral lipid content and models how nutrient availability affects the degree to which each is used as an energy sink for excess carbon.

# Chapter 3

# PRODUCER-GRAZER SYSTEMS IN AQUACULTURE

## 3.1 Introduction

Chapter 2 saw the cell quota applied to a very specific problem motivated by both data and theory. While the model may not necessarily be interesting from a dynamical systems perspective, its direct applications and influence on later research are significant. This chapter adopts a more theoretical approach to modeling, one which relies more on mathematics to explore and answer questions. The model exhibits rich, complex dynamics which leave several open mathematical questions.

A producer-grazer model with nutrient recycling is developed based on ecology stoichiometry and the cell quota model. It incorporates a novel feedback loop to account for animal toxicity due to accumulation of nitrogen waste. While this model design has many applications, it was conceived within the context of aquaculture.

Aquaculture systems are microcosms for larger ecosystems and present a number of interesting applications for mathematical ecologists, particularly ecological stoichiometry. Aquaculture is an international industry that is responsible for a large proportion of all consumed fish and shrimp. It can also have detrimental effects on the environment. There are ongoing efforts for sustainable implementations (Naylor, Williams and Strong, 2001).

Increasing feed in order to try to increase yield in aquaculture systems can have an inhibitory effect on the animals due to the accumulation of excessive waste concentrations. Ammonia has been found to decrease animal survival and growth at both high (Jamu and Piedrahita, 1998; Tomasso, 1994) and even low levels (Lemarie

et al., 2004). As such, there has been significant attention in the literature towards modeling the nitrogen cycle in various aquaculture systems (Burford and Lorenzen, 2004; Lorenzen, Struve and Cowan, 1997; Jamu and Piedrahita, 2002a,b).

## 3.2 "Toxicity" Model

The following model considers systems in which nitrogen (N) is the limiting nutrient. It is based on that of Loladze, Kuang and Elser (2000) and its later extensions, e.g. Wang, Kuang and Loladze (2008). These models developed a simple structure for incorporating nutrient recycling in the context of ecological stoichiometry, one which has a natural extension to simple aquaculture systems.

| | | |
|---|---|---|
| $y(t)$: | grazer C concentration | (g C $L^{-1}$) |
| $x(t)$: | algal (producer) C concentration | (g C $L^{-1}$) |
| $Q(t)$: | producer N:C | (g N $g^{-1}$ C) |
| $N(t)$: | free nitrogen concentration | (g N $L^{-1}$) |

$$\begin{aligned} x' &= m\left(1-\frac{q}{Q}\right)x - f(x)y \\ y' &= r\min\left\{1,\frac{Q}{\theta}\right\}f(x)y - dy - h\left(T-Qx-\theta y\right)y \\ Q' &= v(T-Qx-\theta y) - m\left(Q-q\right) \\ \left[N' = -v(N)x + \Big(Q - r\min\left\{\theta, Q\right\}\Big)f(x)y + d\theta y + h\left(N\right)\theta y\right] \end{aligned} \tag{3.1}$$

Rather than explicitly model the nitrogen cycle, it is assumed that the free N is constituted of ammonia, nitrate, and other N-containing compounds (e.g. nitrite).

| Parameter | Description | Units |
|---|---|---|
| $T$ | total system nitrogen | g N $L^{-1}$ |
| $m$ | producer maximum growth rate | $d^{-1}$ |
| $q$ | producer minimum N:C quota | g N $g^{-1}$ C |
| $\theta$ | grazer homeostatic N:C | g N $g^{-1}$ C |
| $r$ | grazing/digestion efficiency | scalar |
| $d$ | grazer natural death rate | $d^{-1}$ |

| Function | Description | Units |
|---|---|---|
| $f(x)$ | functional response | g C $g^{-1}$ C $d^{-1}$ |
| $v(N)$ | producer-specific N uptake rate | g N $g^{-1}$ C $d^{-1}$ |
| $v(N)$ | grazer toxicity death rate | $d^{-1}$ |
| $A$ | $A = \min\left\{1, \frac{Q}{\theta}\right\}$ (notational convenience) | scalar |

**Table 3.1:** Model parameters and generalized functions

The free N concentration thus represents the potential for toxicity of the grazer. The system is also closed under N, so the total N in the system is a constant value.

Since the system is closed with constant $T$, the free nitrogen $N(t) = T - Q(t)x(t) - \theta y(t)$ is decoupled and so $N'$ is not needed. The equation for $N'$, however, is useful for emphasizing how nitrogen flows throughout the system.

### *3.2.1 Derivation*

**Ecological stoichiometry.** The model's derivation is based on ecological stoichiometry and its existing applications to producer-grazer systems which consider both nutrient recycling and food quality (Kuang, Huisman and Elser, 2004; Loladze, Kuang and Elser, 2000). The grazer N:C is assumed to be constant over the time scale of

the model. The parameter $\theta$ represents this homeostatic N:C of the animals. The producers (phytoplankton) have a variable N:C which is modeled using the cell quota model. The minimum cell quota $q$ is assumed to satisfy $q < \theta$.

**Closed system.** The system is closed with respect to nitrogen and its total nutrient concentration, denoted by $T$, is constant. Nitrogen can be in one of three pools: producer, grazer, and free. The producer pool is given by $Qx$, the grazer pool by $\theta y$, and the free pool by $T - Qx - \theta y$ (using conservation of mass).

**Producer growth dynamics.** The model is applied to theoretical ecosystems or aquaculture implementations in which phytoplankton are the producers. Producer growth is nitrogen limited and modeled using the cell quota model.

**Producer nutrient uptake.** The algal-specific uptake rate function, $v(N)$, is left as a general function with the properties $v(0) = 0$, $v' > 0$, and $v'' \leq 0$.

**Functional response.** The functional response $f(x)$ is any (continuous) function which satisfies $f(0) = 0$, $f' > 0$, and $f'' \leq 0$. The ingestion rate is assumed to be a constant proportion of $f$, denoted by the parameter $r < 1$. $r$ represents the feeding/ingesting efficiency of the animals.

**Grazer biomass production.** The grazer growth rate is proportional to the rate of ingestion. However, it is also limited by the homeostatic N:C value of $\theta$. Each unit of grazer C requires $\theta$ units of N. Thus the feeding rate $f(x)$ does not directly translate to the growth rate in case of an imbalance between the food's N:C and the grazer's homeostatic N:C. Animal growth is dependent on both the feeding rate and the actual nutrient content of the food. (Note that regardless of the producer N:C, a constant proportion of ingested food is always assumed to be lost/wasted due to the imperfect efficiency $r < 1$.)

To derive the grazer growth rate, there are three cases to consider with respect to the difference between the food N:C and grazer N:C ($Q$ and $\theta$, respectively). This mechanistic derivation, originated in Loladze, Kuang and Elser (2000), is significant because it encapsulates both food quantity and food quality. Both are essential to processes governing not only growth dynamics but also nutrient recycling–and thus waste accumulation. The model 3.1 proposed here extends these processes to the toxicity potential of such waste accumulation.

In each case, a portion of ingested food is excreted as waste. Since the model only considers N-limited growth and N-induced toxicity, the total N excreted is important to model explicitly. The N excretion from the grazer's feeding can be calculated as

$$\begin{aligned}\text{N waste} &= \text{total N of ingested food} \\ &\quad - \text{N actually assimilated from food},\end{aligned}$$

where the exact values vary based on whether the food has excessively high N:C or excessively low N:C, the details of which follow below.

$\boldsymbol{Q = \theta}$. In this case every unit C of food that is consumed can sustain a unit C of animal growth (less the constant proportion lost due to $r$). Instantaneous growth therefore equals $rf(x)y$, since $f(x)y$ is the total instantaneous ingested C, all of which can support animal growth.

$$\begin{aligned}\text{net growth} &= rf(x)y, \\ \text{N waste} &= (1-r)\,Qf(x)y.\end{aligned} \qquad \text{(optimal quality food, } Q = \theta)$$

$\boldsymbol{Q < \theta}$. In this case each unit C of food cannot sustain a unit C of grazer growth. The animals ingest excess C which lacks the required N for growth. This excess C is assumed to be excreted instantaneously. Therefore the growth rate is the feeding

rate decreased by the proportion $Q/\theta$ (and the feeding efficiency $r$). More precisely,

$$\begin{aligned} \text{net growth} &= r\frac{Q}{\theta}f(x)y, \\ \text{N waste} &= (1-r)\,Qf(x)y. \end{aligned} \qquad \text{(low quality food, } Q < \theta\text{)}$$

$\boldsymbol{\theta < Q}$. Here the food is *too* nutrient rich–the grazer cannot utilize all of the ingest N for biomass production. Since it can utilize all of the C, the growth rate is the same as the case when $Q = \theta$. However, now there is excess N from the ingested food which must be excreted. It is assumed that the excess N is recycled instantaneously back into the free nutrient pool.

$$\begin{aligned} \text{net growth} &= rf(x)y, \\ \text{N waste} &= (Q - r\theta)\,f(x)y. \end{aligned} \qquad \text{(low quality food, } Q < \theta\text{)}$$

Combining these three cases yields the simple yet powerful numerical response formulation used in the model. If $Q < \theta$ then the net instantaneous growth is $r\frac{Q}{\theta}f(x)y$. If $\theta \leq Q$, then it is $rf(x)y$. The result immediately follows:

$$\text{net instantaneous growth} = r\min\left\{1, \frac{Q}{\theta}\right\}f(x)y. \tag{3.2}$$

With this function, it is simple to derive the instantaneous rate of N waste by the grazer. First, note that the functional response $f(x)$ gives the intake rate in terms of C. The total N of ingested food is therefore $Qf(x)y$ since $Q$ is the N:C of the food $x$ being eaten. The total N of ingested food that was actually used for growth is similarly calculated. The net instantaneous growth function (3.2) is in terms of C. Since grazer biomass is assumed to be fixed at $\theta$, their product yields

$$\text{N used for instantaneous growth} = r\min\{\theta, Q\}\,f(x)y. \tag{3.3}$$

Subtracting (3.3) from the total ingested N gives the N waste,

$$\text{N waste by grazer} = \big(Q - r\min\{\theta, Q\}\,\big)f(x)y. \tag{3.4}$$

**Nutrient recycling.** In addition to waste from feeding and growth, grazer death also recycles N back into the environment. It is assumed that N from dead grazer biomass is instantaneously released back into the free-N pool. Multiplying the grazer death rate (which is in terms of C) by $\theta$ gives the rate of N recycled via death.

**Toxicity** To account for the toxic effect of ammonia and nitrate, the grazer death rate increases with the free N concentration. The function $h$ in Model (3.1) represents the functional relationship between accumulated N in the environment and grazer toxicity. The only assumption on $h$ is that it satisfies $h(0) = 0$, $h' > 0$, and $h'' \leq 0$.

## 3.3 Model Properties

**Remark 3.** *Applying Theorem 1 from Chapter 2, we see that System* (3.1) *has unique solutions on the set* $\Omega$*, given below.*

**Theorem 4.** *Let* $\Omega \subset \mathbb{R}^3$ *be the open set given by*

$$\Omega = \{(x, y, Q) : 0 < x < T/q, 0 < \theta y + Qx < T, q < Q < q + v(T)/m\}. \tag{3.5}$$

*Then* $\Omega$ *is positively invariant for the semi-flow generated by system* (3.1)*.*

*Proof.* Let $\mathbf{x_0} \in \Omega$ and denote by $\mathbf{x}(t) = [x(t), y(t), q(t)]^\top$ the solution $\mathbf{x}(t) = \phi(t, \mathbf{x_0})$ to System (3.1). Suppose that $\Omega$ is not invariant; that is, there exists $t_1 > 0$ such that

$$\{\mathbf{x}[t < t_1]\} \subseteq \Omega, \qquad \mathbf{x}(t_1) \notin \Omega.$$

Note that since $\Omega$ is open,

$$\Omega = \Omega^\circ, \qquad \mathbf{x}(t_1) \in \partial\Omega,$$

which means $\mathbf{x}(t_1)$ must be on a hyperplane generated by fixing a coordinate to one of its boundary values on $\partial\Omega$; for example, $\{(x, y, Q) \in \mathbb{R}^3 : x = 0\} \cap \overline{\Omega}$. Therefore there are six cases to consider. For the following, $0 \leq t \leq t_1$ unless specified otherwise.

I. $y(t_1) = 0$

Since $q \leq Q$ and $y \leq T/\theta$, $x'(t) \geq -f'(0)T/\theta x$. From Gromwall's Inequality, $x(t) \geq x(0)e^{-f'(0)T/\theta t} > 0$, a contradiction.

II. $y(t_1) = 0$

$T - Qx - \theta y \leq T$ and monotonicity of $g$ yield $y'(t) \geq -(d + h(T))y$. Applying Gromwall's Inequality gives $y(t) > 0$, a contradiction

III. $y(t_1) = 0$

From Cases I and II, $x > 0$ and $y > 0$ which yields the strict inequality $x'(t) < m\,(1 - q/Q)$. Since $Qx \leq T$, $x'(t) < m\,(1 - qx/T)$. Thus $x(t) < T/q$, a contradiction.

IV. $Q(t_1)x(t_1) + \theta y(t_1) = T$

Recall that $N = T - Qx - \theta y$ and that

$$N' = -v(N)x + (Q - r\min\{Q, \theta\})\, f(x)y + d\theta y + h(N)\theta y.$$

Thus $N(t_1) = 0$. But $N'(t) > -v'(0)xN$, so Gromwall's Inequality gives $N(t) > 0$, a contradiction.

V. $Q(t_1) = q$

$Q'(t) \geq -m(Q - q)$ and so $Q(t) \geq q + (Q(0) - q)e^{-mt}$, a contradiction.

VI. $Q(t_1) = q + v(T)/m$

Let $U = 1/Q$. Then

$$U' = mU\left[1 - (v(T - Qx - \theta y)/m + q)\, U\right].$$

From Cases I and II, $x > 0$ and $y > 0$ which yields the strict inequality $T > T - Qx - \theta y$. Strict monotonicity of $v$ gives $U' > mU\left[1 - (v(T)/m + q)\, U\right]$ and so $U(t) > (v(T)/m + q)^{-1}$. Therefore $Q(t) < v(T)/m + q$, a contradiction.

It has been shown that solutions starting in the open set $\Omega$ remain so for all forward time and cannot reach $\partial\Omega$ in finite time. $\square$

### *3.3.1 Equilibria*

System (3.1) has two distinct boundary equilibria on $\partial\Omega$,

$$E_0 = (0, 0, q + v(T)/m) \qquad \text{(Extinction)} \tag{3.6}$$

$$E_1 = (T/q, 0, q) \qquad \text{(Grazer extinction)} \tag{3.7}$$

and the internal equilibrium

$$E_2 = (x, y, Q) \in \Omega^\circ \qquad \text{(Coexistence)} \tag{3.8}$$

When discussing a particular equilibrium, the notation $(x, y, Q)$ should be understood to denote the fixed point in question. It is worthwhile to reiterate here that $N$ is a function defined on the phase space as $N(x, y, Q) = T - Qx - \theta y$. This is important when calculating partial derivatives for the Jacobian, e.g. $\partial_x v(N)$. $N$ is written in place of $T - Qx - \theta y$ (and vice versa) for readability or when interpreting results and thus $\partial_x N = -Q$, etc. Define

$$A = \min\left\{1, \frac{Q}{\theta}\right\},$$

$$N \coloneqq N(x(t), y(t), Q(t)) = T - Q(t)x(t) - \theta y(t).$$

The Jacobian of system (3.1) is given by

$$J = \begin{pmatrix} m\left(1 - \frac{q}{Q}\right) - f'(x)y & -f(x) & \dfrac{mqx}{Q^2} \\ rAf'(x)y + h'(N)Qy & \begin{matrix} rAf(x) + h'(N)\theta y \\ -h(N) - d \end{matrix} & h'(N)xy + \underbrace{\dfrac{r}{\theta}f(x)y}_{Q<\theta} \\ -v'(N)Q & -v'(N)\theta & -v'(N)x - m \end{pmatrix} \tag{3.9}$$

Calculating explicit conditions for stability of the boundary equilibria is straightforward. Such is not the case for $E_2$.

**Theorem 5.** *The extinction equilibrium* $E_0 = \left(0, 0, q + \frac{v(T)}{m}\right)$ *is an unstable saddle whose unstable manifold is the plane*

$$y = 0, \quad x = \frac{m + \frac{v(T)}{q+v(T)/m}}{v'(T)(q + v(T)/m)} \left(Q - q - \frac{v(T)}{m}\right)$$

*and whose stable manifold consists of the* $Q$*-axis and the plane*

$$x = 0, \quad y = \frac{m - d - h(T)}{v'(T)\theta} \left(Q - q - \frac{v(T)}{m}\right).$$

*Proof.* From Eq. (3.9) it follows that

$$J(E_0) = \begin{pmatrix} m\left(1 - \frac{q}{q+v(T)/m}\right) & 0 & 0 \\ 0 & -d - h(T) & 0 \\ -v'(T)(q + \frac{v(T)}{m}) & -v'(T)\theta & -m \end{pmatrix} \tag{3.10}$$

which has eigenvalues

$$\lambda_1 = m\left(1 - \frac{q}{q + v(T)/m}\right), \quad \lambda_2 = -d - h(T), \quad \lambda_3 = -m$$

and corresponding eigenvectors

$$v_1 = \begin{pmatrix} \frac{mq+2v(T)}{v'(T)(q+v(T)/m)^2} \\ 0 \\ 1 \end{pmatrix}, \quad v_2 = \begin{pmatrix} 0 \\ \frac{m-d-h(T)}{v'(T)\theta} \\ 1 \end{pmatrix}, \quad v_3 = \begin{pmatrix} 0 \\ 0 \\ 1 \end{pmatrix}.$$

□

**Theorem 6.** *Grazer extinction* $E_1 = (T/q, 0, q)$ *is locally asymptotically stable if and only if*

$$rf\left(\frac{T}{q}\right) < \frac{d\theta}{q} \tag{3.11}$$

*Proof.* From Eq. (3.9) it follows that

$$J(E_1) = \begin{pmatrix} 0 & -f(T/q) & mT/q^2 \\ 0 & r\frac{q}{\theta}f(T/q) - d & 0 \\ -v'(0)q & -v'(0)\theta & -v'(0)T/q - m \end{pmatrix} \tag{3.12}$$

which has characteristic equation

$$\lambda^3 - \mathrm{tr}(J)\lambda^2 + \left[\sum_{i=1}^{3} M_i\right]\lambda - \det(J) = 0, \tag{3.13}$$

where $M_i$ denotes the $i$th principal minor of order two of $J$. From the Routh-Hurwitz stability criterion, all three roots of Eq. (3.13) have strictly negative real part if and only if

$$\mathrm{tr}(J) < 0, \qquad \det(J) < 0, \qquad \mathrm{tr}(J)\left[\sum_{i=1}^{3} M_i\right] < \det(J).$$

It is readily apparent that

$$\det(J) = v'(0)mT/q\left(r\frac{q}{\theta}f(T/q) - d\right) < 0$$

if and only if Eq. (3.11) is satisfied. Then

$$\mathrm{tr}(J) = r\frac{q}{\theta}f(T/q) - d - v'(0)T/q - m < 0$$

immediately follows. The third relation then similarly follows since

$$\begin{aligned} 0 < M_1 &= \left(d - r\frac{q}{\theta}f(T/q)\right)\left(v'(0)T/q + m\right), \\ 0 < M_2 &= v'(0)mT/q, \\ 0 &= M_3, \end{aligned}$$

and so

$$\begin{aligned} \mathrm{tr}(J)\left[\sum_{i=1}^{3} M_i\right] < tr(J)M_2 &= \det(J) - \left(v'(0)T/q + m\right)v'(0)mT/q \\ &< \det(J). \end{aligned}$$

□

### 3.3.2 Coexistence

While the coexistence equilibrium $E_2$ cannot be explicitly calculated, general conditions for its existence and stability may be deduced. From the nullclines of system (3.1), a fixed point $E_2 = (x, y, Q) \in \Omega^\circ$ is the solution to the nonlinear system

$$\begin{aligned} \frac{f(x)}{x} y &= m\left(1 - \frac{q}{Q}\right), \\ r \min\left\{1, \frac{Q}{\theta}\right\} f(x) &= d + h(T - Qx - \theta y), \\ v(T - Qx - \theta y) &= m(Q - q). \end{aligned} \tag{3.14}$$

Define

$$A = \min\left\{1, \frac{Q}{\theta}\right\}, \qquad \widetilde{A} = \frac{\theta}{Q} A = \min\left\{\frac{\theta}{Q}, 1\right\}.$$

The $Q$-value of solutions to (3.14) may be calculated from

$$T = N(Q) + \left[Q + \frac{r\widetilde{A} m(Q-q)}{d + h\left(N(Q)\right)}\right] f^{-1}\left(\frac{d + h\left(N(Q)\right)}{rA}\right), \tag{3.15}$$

$$N(Q) = v^{-1}(m\left(Q - q\right)) \tag{3.16}$$

or equivalently,

$$T = N + \left[v(N)/m + q + \frac{r\widetilde{A} v(N)}{d + h(N)}\right] f^{-1}\left(\frac{d + h(N)}{rA}\right), \tag{3.17}$$

$$Q = v(N)/m + q. \tag{3.18}$$

Then $x$ and $y$ are given in terms of $Q$ (or, equivalently, $N$) by the expressions

$$x = f^{-1}\left(\frac{d + h(N(Q))}{rA}\right), \tag{3.19}$$

$$y = \frac{rAm(Q-q)/Q}{d + h(N(Q))} x \tag{3.20}$$

Therefore, existence of $E_2$ is depends on the existence of some $Q \in (q, q + v(T)/m)$ such that both

$$0 < \frac{d + h\left(N(Q)\right)}{rA} < f\left(\frac{T}{q}\right)$$

and Eq. (3.15) are satisfied. Finding analytical conditions for such $Q$ to exist is not possible in general; however, given explicit functions $f$, $v$, and $h$ and parameter values, any $Q$ that satisfies these conditions can be found numerically.

### *3.3.3 Global Stability of $E_1$*

In (Liu, Packer and Kuang, 2014) it was shown that $\frac{rf(T/q)}{d} < 1$ is sufficient for global asymptotic stability of the grazer-only extinction equilibrium $E_1$. It is also possible to show that $\frac{rTf'(0)}{d\theta} < 1$ is sufficient for global stability. Which condition is stronger depends on the function $f$; later it will be seen that $\frac{rTf'(0)}{d\theta} < 1$ is particularly useful for the case when $f$ is a linear. It is important to note that both conditions are weaker than that of local stability.

**Theorem 7.** *If $\frac{rf(T/q)}{d} < 1$ or $\frac{rTf'(0)}{d\theta} < 1$ then the grazer-only extinction equilibrium $E_1 = (T/q, 0, q)$ is globally asymptotically stable.*

*Proof.* It is first shown that when either condition is satisfied, $y(t)$ decreases monotonically toward 0. Observe that $f(x) \leq f'(0)x$ and $Qx < T$ gives

$$\begin{aligned} r\min\{1, Q/\theta\} f(x) &\leq r\min\{1, Q/\theta\} f'(0)x \\ &\leq r\frac{T}{\theta}f'(0), \end{aligned}$$

while $f(x) < f(T/q)$ gives

$$r\min\{1, Q/\theta\} f(x) \leq rf(T/q).$$

Therefore if $rTf'(0) < d\theta$ then

$$\begin{aligned} y' &< r\frac{T}{\theta}f'(0)y - dy \\ &< 0, \end{aligned}$$

while if $rf(T/q) < d$ then

$$\begin{aligned} y' &< rf(T/q)y - dy \\ &< 0, \end{aligned}$$

where in both cases the strict inequality comes from $-h(T-Qx-\theta y)y < 0$. Therefore $y(t)$ is strictly monotonically decreasing and

$$\lim_{t\to\infty} y(t) = 0.$$

Consider now the system given by

$$\begin{aligned} x' &= m\left(1 - \frac{q}{Q}\right)x \\ Q' &= v(T - Qx) - m(Q - q) \end{aligned} \tag{3.21}$$

defined on $\{(x, Q)|0 < x < T/q, q < Q < q + v(T)/m\}$. Showing that solutions to this system (3.21) converge to $(T/q, q)$ is straightforward thanks to monotonicity. Observe that system (3.21) can be rewritten as

$$\begin{aligned} x' &= m\left(1 - \frac{qx}{T - N}\right)x \\ N' &= (T - Qx)' = -v(T - Qx)x. \end{aligned}$$

Then $N' < 0$ and so $\lim_{t\to\infty} N(t) = 0$. Let $\epsilon > 0$. Then there is a $t_1$ such that $N(t) < \epsilon$ for all $t > t_1$. Further,

$$x' > m\left(1 - \frac{qx}{T - \epsilon}\right)x,$$

which by a simple comparison argument gives $\lim_{t\to\infty} x(t) > (T - \epsilon)/q$. Combined with the upper bound $x < T/q$ and taking $\epsilon \to 0$, it follows that $\lim_{t\to\infty} x = T/q$. Thus $\lim_{t\to\infty} Q(t) = q$ and solutions to system (3.21) converge to the point $(T/q, q)$.

Applying Markus (1956) and Thieme (1992), the original model (3.1) is an asymptotically autonomous system with system (3.21) its limit system. For the asymptotically autonomous system (3.1), let $\omega$ be the $\omega$-limit set for an orbit through some

point in $\Omega$. Then $\omega$ is nonempty and attracts the orbit (Thieme, 1992). Since $y(t) \to 0$ and $E_0 = (0, 0, q + v(T)/m)$ is unstable, $\omega \subseteq \overline{\Omega} \setminus \{(0, 0, q + v(T)/m)\}$. Let $(x_0, 0, Q_0)$ be any point in $\omega$. Then the solution of the limit system (3.21) through $(x_0, Q_0)$ converges to $(T/q, q)$, which implies $\omega = \{(T/q, 0, q)\}$ (Thieme, 1992). □

Naturally one would ask whether or not the necessary and sufficient condition for LAS, Eq. (3.11) from Theorem 6, is also necessary and sufficient for GAS. Previously this was proposed as a Conjecture and left as an open question (Liu, Packer and Kuang, 2014). However, such is not the case unless additional assumptions are made on $f$. The next section examines such a case where local and global stability are equivalent, followed by a counter-example that disproves the conjecture.

## 3.4 $f(x) = ax$

First, the less-complex case is explored in which $f$ is explicitly defined as the linear function $f(x) = ax$. The functions $v$ and $h$ are still defined as any continuous functions which satisfy $v(0) = 0$, $v' > 0$, and $v'' \leq 0$ (similarly for $h$).

$$\begin{aligned} \frac{dx}{dt} &= m\left(1 - \frac{q}{Q}\right)x - axy \\ \frac{dy}{dt} &= \min\left\{1, \frac{Q}{\theta}\right\} axy - dy - h\left(T - Qx - \theta y\right)y \\ \frac{dQ}{dt} &= v(T - Qx - \theta y) - m\left(Q - q\right) \end{aligned} \tag{3.22}$$

### *3.4.1 Properties*

A linear functional response affords several properties to the model that are either untrue or unknown in the general case. As mentioned previously, it remained an open question whether or not local and global asymptotic stability of grazer-only extinction

were equivalent. As a corollary to theorems 6 and 7, it is trivial to show they are indeed the same for $f(x) = ax$.

**Corollary 2.** *If $f(x) = ax$ then the grazer-only extinction equilibrium $E_1$ is globally asymptotically stable if and only if $rqf(T/q) > d\theta$. In other words, local and global stability of $E_1$ are equivalent.*

*Proof.* From theorem 7, $rTf'(0) < d\theta$ is sufficient for global stability. Since $rTf'(0) = rqf(T/q)$, this condition is identical to $rqf(T/q) < d\theta$, the necessary and sufficient condition for local asymptotic stability. □

Another open problem is under what conditions a coexistence equilibrium exists and is asymptotically stable. In the general case, answering these questions analytically remains to be accomplished. The problem is compounded by the fact that it can not be assumed only one internal equilibrium exists for a single parameter set. Numerical simulations can be deceiving unless extra care is taken to account for possible nonuniqueness and dependence on initial conditions. Here these questions are explored for $f(x) = ax$. Doing so provides insight into not only the linear case but also the general and nonlinear cases.

**Remark 4.** *$f^{-1}(z)/z = 1/a$ greatly simplifies the system of equations for $E_2$ generated by the nullclines. Equation* (3.15) *for finding $Q$ becomes*

$$\begin{aligned} T &= N(Q) + \frac{Q}{ar \min\{1, Q/\theta\}} (d + h(N)) + \theta m \left(1 - \frac{q}{Q}\right) \\ &= N(Q) + \max\{Q, \theta\} \frac{d + h\big(N(Q)\big)}{ar} + \frac{\theta m}{a} \left(1 - \frac{q}{Q}\right) \end{aligned} \tag{3.23}$$

*where as before $N(Q) = v^{-1}\big(m(Q-q)\big)$. Also*

$$\begin{aligned} x &= \max\left\{\frac{\theta}{Q}, 1\right\} \frac{d + h\big(N(Q)\big)}{ar} \\ y &= \frac{m}{a}\left(1 - \frac{q}{Q}\right) \end{aligned} \tag{3.24}$$

**Theorem 8.** *For system* (3.22)*, the coexistence equilibrium* $E_2$ *exists if and only if* $d\theta < rqf(T/q)$*. Furthermore, if* $E_2$ *exists then it is unique.*

*Proof.* Recall that any $Q$-value at an $E_2$ equilibrium must satisfy Eq. (3.23). Let $F(Q)$ be the function given by the right hand side of Eq. (3.23) with domain $[q, q+v(T)/m]$. In other words, $E_2$ exists if there is some $\overline{Q}$ on $(q, q+v(T)/m)$ such that $F(\overline{Q}) = T$:

$$F(Q) = N(Q) + \max\{Q, \theta\}\frac{d + h\big(N(Q)\big)}{ar} + \frac{\theta m}{a}\left(1 - \frac{q}{Q}\right),$$

$$\textit{with} \qquad N(Q) = v^{-1}\big(m(Q-q)\big).$$

First observe that the derivative $F'(Q)$ exists and is positive. It follows from the positivity of $v$ and $c$ and the inverse function theorem. Namely,

$$\frac{d}{dQ}\left[v^{-1}\big(m\,(Q-q)\,\big)\right] = \frac{m}{v'\Big(v^{-1}\big(m(Q-q)\big)\Big)}$$

and

$$\frac{d}{dQ}h\big[v^{-1}\big(m\,(Q-q)\,\big)\big] = \frac{m}{v'\Big(v^{-1}\big(m(Q-q)\big)\Big)}h'\big(v^{-1}\big(m(Q-q)\big)\big)$$

are well-defined and strictly positive on $[q, q+v(T)/m]$. So $F(Q)$ is strictly increasing and if the solution to $F(Q) = T$ exists then it must be unique. Further, it exists if and only if $F(q) < T$ and $T < F(q+v(T)/m)$.

Denote $Q_m = q + v(T)/m$ for convenience. At $Q = Q_m$,

$$N(Q_m) = v^{-1}\big(m(Q_m - q)\big) = v^{-1}\big(v(T)\big) = T$$

and so

$$\begin{aligned} F(Q_m) &= T + \max\{Q_m, \theta\}\frac{d + h\big(T\big)}{ar} + \frac{\theta m}{a}\left(1 - \frac{q}{Q_m}\right) \\ &> T \end{aligned}$$

is always true. For $Q = q$, noting that $N(q) = v^{-1}(0) = 0$,

$$\begin{aligned} F(q) &= \frac{dq}{ar \min\{q/\theta, 1\}} \\ &= \frac{d\theta}{ar} \\ &= \frac{d\theta}{rqf(T/q)}T \\ &< T \\ \iff & \; d\theta < rqf(T/q). \end{aligned}$$

If $Q^* = F^{-1}(T)$ exists then so does $E_2 = (y^*, x^*, Q^*)$, where $x^*$ and $y^*$ are given by Eq. (3.24). $x^*$ and $y^*$ are guaranteed to satisfy $Q^*x^* + \theta y^* < T$ because $F(Q^*) = N(Q^*) + Q^*x^* + \theta y^*$ and $N(Q^*) > 0$. □

Theorem 8 is significant because it proves that the model's overall asymptotic behavior is governed by the same ratio $rqf(T/q)/(d\theta)$ which determines both LAS and GAS of $E_1$. If $E_2$ does not exist then $E_1$ is globally asymptotically stable. If $E_1$ is not stable then $E_2$ exists and is unique. However, as observed from simulations and confirmed analytically below, existence of $E_2$ does not guarantee asymptotic stability of $E_2$.

**Theorem 9.** *For system* (3.21) *with* $f(x) = ax$, *let* $d\theta < rqf(T/q)$ *and denote* $E_2 = (x^*, y^*, Q^*)$ *the unique interior equilibrium per Theorem 8. If* $Q^* < \theta$ *and*

$$mh'(N^*)\theta y < rf'(x^*)yv'(N^*)x$$

*with* $N^* = T - \theta y^* - Q^*x^*$, *then* $E_2$ *is locally asymptotically stable.*

*Proof.* For notational convenience, let $(x, y, Q) \equiv (x^*, y^*, Q^*)$ and $N = T - Qx - \theta y$. At $E_2$ the Jacobian simplifies to

$$J = \begin{pmatrix} 0 & -ax & \dfrac{mqx}{Q^2} \\ rAay + h'(N)Qy & h'(N)\theta y & h'(N)xy + \underbrace{\dfrac{r}{\theta}axy}_{Q<\theta} \\ -v'(N)Q & -v'(N)\theta & -v'(N)x - m \end{pmatrix} \tag{3.25}$$

The characteristic equation can be written

$$\lambda^3 - \mathrm{tr}(J)\lambda^2 + \left[\sum_{i=1}^{3} M_i\right]\lambda - \det(J) = 0 \tag{3.26}$$

where $M_i$ denotes the $i$th principal minor of order two of $J$:

$$\begin{aligned} M_1 &= -mh'(N)\theta y + \underbrace{rayv'(N)x}_{Q<\theta}, \\ M_2 &= v'(N)x\frac{mq}{Q}, \\ M_3 &= \Big(raA + h'\left(N\right)Q\Big)axy, \end{aligned}$$

and

$$\mathrm{tr}(J) = h'(N)\theta y - v'(N)x - m. \tag{3.27}$$

Computing and simplifying $\det(J)$ gives the explicit and mathematically tractable expression

$$\begin{aligned} \det(J) = {} & ax\left[-\left(v'(N)x + m\right)\left(rAay + h'(N)Qy\right) + v'(N)Q\left(h'(N)xy + \underbrace{\frac{r}{\theta}axy}_{Q<\theta}\right)\right] \\ & + \frac{mqx}{Q^2}\left[-v'(N)\theta\left(rAay + h'(N)Qy\right) + v'(N)h'(N)Q\theta y\right] \\ = {} & -\Big(v'(N)x + m\Big)M_3 + v'(N)Qax\left(h'(N)xy + \underbrace{\frac{r}{\theta}axy}_{Q<\theta}\right) \\ & - r\frac{\theta}{Q}AayM_2. \end{aligned} \tag{3.28}$$

From the Routh-Hurwitz stability criterion, all three roots of the characteristic equation. (3.26) have strictly negative real part if and only if

$$\text{I. } \operatorname{tr}(J) < 0, \qquad \text{II. } \det(J) < 0, \qquad \text{III. } \operatorname{tr}(J)\left[\sum_{i=1}^{3} M_i\right] < \det(J).$$

**I.** $\operatorname{tr}(J) < 0$ is satisfied if and only if

$$h'(N)\theta y < v'(N)x + m, \tag{3.29}$$

which is satisfied since

$$\begin{aligned} & mh'(N)\theta y < rayv'(N)x, \quad ray < m \\ \implies \quad & h'(N)\theta y < v'(N)x \\ \implies \quad & h'(N)\theta y < v'(N)x + m \end{aligned} \tag{3.30}$$

**II.** $\det(J) < 0$ is readily apparent after substituting $M_3$ into Eq. (3.28) then simplifying. Recall that $A = \frac{Q}{\theta}$ when $Q < \theta$ and so strict negativity of $\det(J)$ is always satisfied, as seen below:

$$\begin{aligned} \det(J) &= -\Big(v'(N)x + m\Big)M_3 + v'(N)Qax\left(h'(N)xy + \underbrace{\frac{r}{\theta}axy}_{Q<\theta}\right) - r\frac{\theta}{Q}AayM_2 \\ &= -\Big(v'(N)x + m\Big)\Big(raA + h'(N)\,Q\Big)axy + v'(N)Qax\left(h'(N)xy + \underbrace{\frac{r}{\theta}axy}_{Q<\theta}\right) \\ &\quad - r\frac{\theta}{Q}AayM_2 \\ &= -m\Big(raA + h'(N)\,Q\Big)axy - v'(N)axy\Big(raAx + \underbrace{ra\frac{Q}{\theta}x}_{Q<\theta}\Big) - r\frac{\theta}{Q}AayM_2 \\ &< 0. \end{aligned}$$

**III.** $\operatorname{tr}(J)\left[\sum_{i=1}^{3} M_i\right] < \det(J)$.

Assume now that $Q < \theta$. Then

$$\begin{aligned}\det(J) &= -\Big(v'(N)x + m\Big)M_3 + v'(N)xM_3 - rayM_2 \\ &= -mM_3 - r\frac{\theta}{Q}AayM_2,\end{aligned}$$

and so

$$\operatorname{tr}(J)\left[\sum_{i=1}^{3} M_i\right] - \det(J) = \operatorname{tr}(J)M_1 + \big(\operatorname{tr}(J) + ray\big)M_2 + \big(h'(N)\theta y - v'(N)x\big)M_3.$$

$M_2, M_3 > 0$ is always true, while $M_1 > 0$ by assumptions $mh'(N)\theta y < rayv'(N)x$ and $Q < \theta$. Also, as shown in Eqs. (3.30), $\operatorname{tr}(J) < 0$ and $h'(N)\theta y < v'(N)x$. Lastly, $\operatorname{tr}(J) + ray < 0$ because $ray < m$. Therefore,

$$\operatorname{tr}(J)\left[\sum_{i=1}^{3} M_i\right] - \det(J) < 0.$$

□

### *3.4.2 Results*

As shown in Corollary 2, the asymptotic behavior of the linear model is divided into two regions by the threshold value $qrf(T/q)/(d\theta) = 1$. In the parameter space $qrf(T/q)/(d\theta) < 1$, only the boundary equilibria exist. Grazer-only extinction $E_1$ is globally asymptotically stable and total extinction $E_0$ is unstable. In the space $qrf(T/q)/(d\theta) > 1$, only $E_0$ and the unique internal equilibrium $E_2$ exist. $E_0$ is unstable, and solutions either converge to $E_2$ or stable periodic orbits depending on the stability of $E_2$. Figure 3.1 illustrates this behavior using the bifurcation parameter $d$.

### *3.4.3 Discussion*

The model's asymptotic behavior has been explored in more detail for the simple functional response $f(x) = ax$. There are three possible outcomes for global

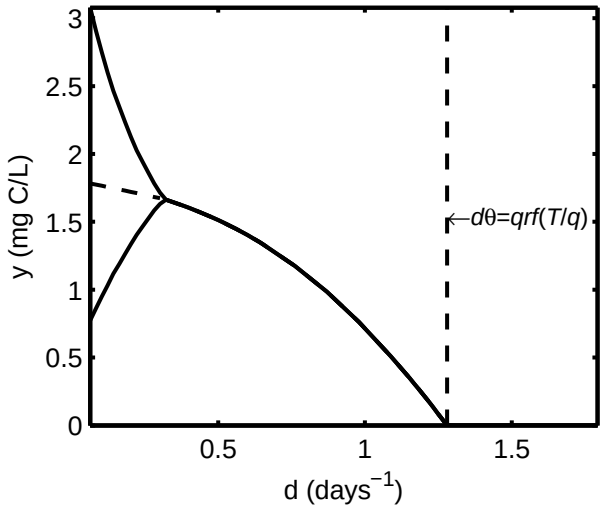


(a) y

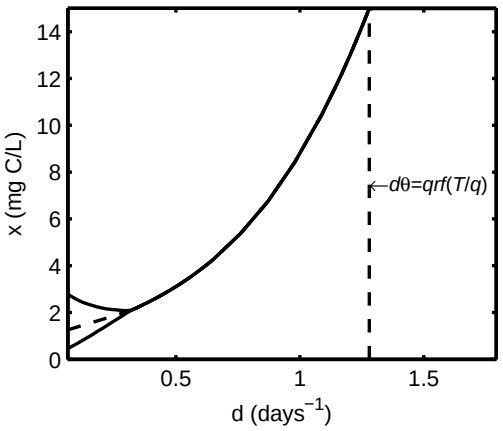


(b) x

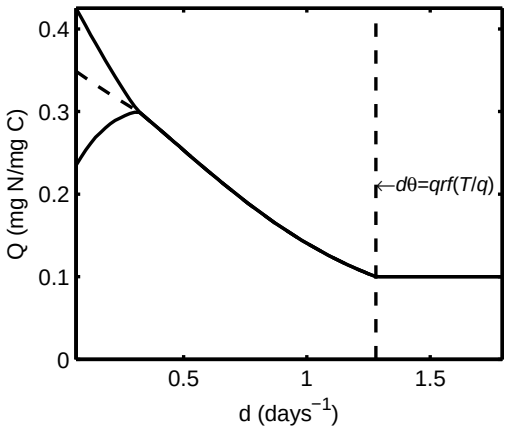


(c) Q

**Figure 3.1:** Bifurcation on $d$ with linear functional response $f(x) = ax$. For $d > qrf(T/q)/\theta$, the grazer-only extinction equilibrium $E_1$ is globally asymptotically stable. Otherwise, $E_1$ is unstable and the coexistence equilibrium $E_2$ is either asymptotically stable or unstable, with the latter giving rise to stable periodic orbits. In this example both $v$ and $h$ are Holling type II with $v(N) = v_m \frac{N}{N+v_k}$ and $h(N) = h_m \frac{N}{N+h_k}$. $T = 1.5$, $q = 0.1$, $\theta = 0.3$, $m = 0.8$, $r = 0.8$, $a = 0.32$, $v_m = 0.5$, $v_k = 0.8$, $h_m = 0.5$, $h_k = 0.5$.

asymptotic behavior. If $rqf(T/q) > d\theta$ then the producer and grazer coexist in either a stable limit cycle or a stable equilibrium. The boundary equilibria $E_0$ and $E_1$ exist and are unstable. There is also a single internal equilibrium whose stability varies. If $rqf(T/q) < d\theta$ then only the boundary equilibria exist, with $E_1$ globally asymptotically and $E_0$ unstable.

It is important to note that while $f$ was set to this explicit form, the functions $v$ and $h$ were kept in the generalized form without any additional assumptions made. By setting $f$ as linear, the model becomes substantially more tractable. In particular, $f^{-1}(z) = z/a$, $f(x)/x = f'(x)$, and constant derivative $f'$ facilitate straightforward analytical results. It was shown that the coexistence equilibrium exists and is unique when the grazer-only extinction equilibrium, $E_1$, is not stable. In fact, the local and global asymptotic stability of $E_1$ coincide. When $f(x) = ax$, the necessary and sufficient condition for LAS of $E_1$ is the same as the weaker, sufficient condition for global stability of $E_1$. This is a direct consequence of $f(x)/x = f'(x)$.

Such is not the case for general or nonlinear $f$, explored in the following sections. As expected, nonlinear $f$ gives rise to much more interesting and complex dynamics, and results from this section are not applicable to nonlinear or generalized $f$.

As a final segue into the next section, a quick look at the system's Jacobian provides a handwaving summary of why the linear functional response is special. For the general model (3.9),

$$\frac{\partial}{\partial x}\left[x'(x, y, Q)\right] = m\left(1 - \frac{q}{Q}\right) - f'(x)y.$$

Also recall that steady states with non-zero $x$ must satisfy

$$m\left(1 - \frac{q}{Q}\right)x - f(x)y = 0, \quad x > 0.$$

In this special case where $f(x)/x = f'(x)$, $\partial_x x' = 0$ at the internal equilibrium, which is unique, too—neither of which can be proven for the generalized function.

## 3.5 Nonlinear Functional Response

When $f$ is nonlinear the dynamics are more expectedly more complex. While deriving explicit conditions for stability may not be possible, insights can be drawn through comparisons with the case of linear $f$. In Theorem 8, proving existence and uniqueness of a coexistence equilibrium was possible because $f(x) = ax$ guaranteed the derivative of Eq. (3.15) with respect to $Q$ is positive (Eq. (3.23)). However, in general it is not necessarily true; for example, the derivatives

$$\frac{d}{dQ}\left[\min\left\{\frac{\theta}{Q},1\right\}\frac{rm(Q-q)}{d+h\big(N(Q)\big)}\right], \qquad \frac{d}{dQ}\left[f^{-1}\left(\frac{d+h(N(Q))}{r\min\{Q/\theta,1\}}\right)\right]$$

are not necessarily positive. The possibility for multiple internal equilibria to exist suggests more bifurcations and possible regions of bistability as compared to the case when $f$ is linear. For the general case, it was proven that $rqf(T/q) < d\theta$ is necessary and sufficient for **local** stability and that either of the weaker conditions $rf(T/q) < d$ or $rTf'(0) < d\theta$ is sufficient for global stability. If $f(x) = ax$ then $rTf'(0) < d = rqf(T/q) < d$. Now it will be shown that for different (nonlinear) $f$, grazer-only extinction can be locally but not globally stable.

Model (3.1) with nonlinear $f$, $v$, and $h$ (3.31) was explored numerically. Besides simulations of solutions, the coexistence equilibria and their local stability were computed numerically. In this section, the model discussed in System (3.1) with the following Holling type II equations (3.31) for $f$, $v$, and $h$:

$$\begin{aligned} f(x) &= a\frac{x}{x+a_k}, \\ v(N) &= v_m\frac{N}{N+v_k}, \\ h(N) &= h_m\frac{N}{N+h_k}. \end{aligned} \tag{3.31}$$

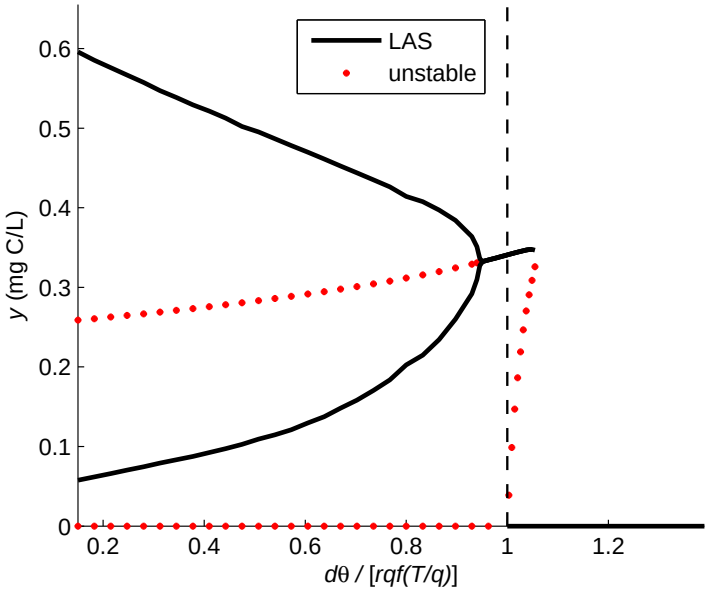


(a) y

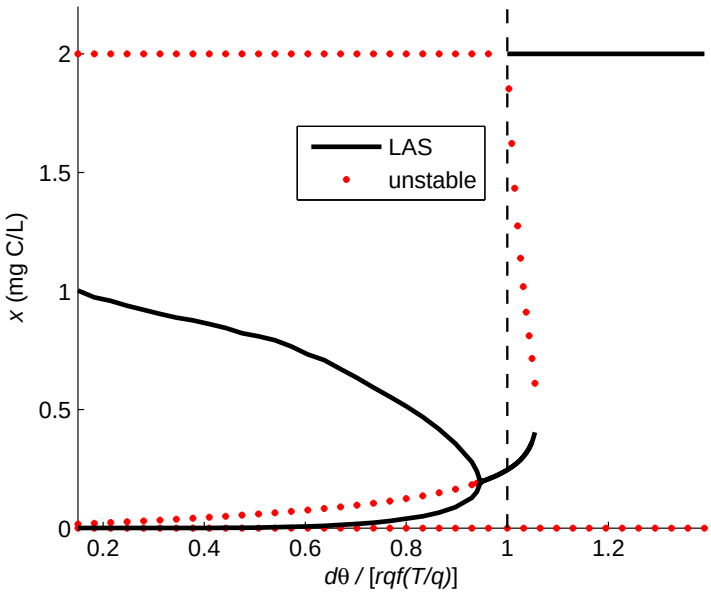


(b) x

**Figure 3.2:** Bifurcation on $d$ with Holling type II functional response $f(x) = ax/(x + a_k)$. For $d\theta < qrf(T/q)$, $E_1$ is unstable. Only one $E_2$ exists and is either LAS or unstable, the latter giving rise to stable periodic orbits. For $d\theta > qrf(T/q)$, $E_1$ is LAS. There is a region of bistability where one of the $E_2$ is also LAS. In this example, $v(N) = v_m \frac{N}{N+v_k}$, $h(N) = h_m \frac{N}{N+h_k}$, $T = 0.1$, $q = 0.05$, $\theta = 0.15$, $m = 1.2$, $r = 0.9$, $a = 0.8$, $a_k = 0.25$, $v_m = 1.6$, $v_k = 0.8$, $h_m = 0.03$, $h_k = 0.1$.

Figure 3.2 shows bifurcations on $d$ for $y$ and $x$. For $d < qrf(T/q)/\theta$, the behavior is nondifferent from the linear case: the coexistence equilibrium is unique and either stable or unstable, with the latter giving rise to stable periodic orbits. However, as $d$ increases past $qrf(T/q)/\theta$, another coexistence equilibrium forms that is unstable, while the other coexistence equilibrium remains locally asymptotically stable. Meanwhile, $E_1$ is also locally asymptotically stable. Thus this region is bistable, with solutions tending towards either $E_1$ or one of the $E_2$ depending on initial conditions.

To demonstrate the bistability, solutions to the model were computed at different initial conditions using fixed parameter values. $Q(0)$ was held fixed while $x(0)$ and $y(0)$ varied across $\Omega$. The computed solutions were projected into the $xy$-plane along with all existing equilibrium points. The internal equilibria $E_2$ were computed numerically, with their local stabilities determined by computing the eigenvalues of the corresponding Jacobian matrices. Figures 3.3 1and 3.4 contain the results for several different parameter sets. In Figure 3.3(a), $E_1$ and one of the two $E_2$ are locally asymptotically stable, and solutions can tend to either one depending on initial conditions. With respect to the $xy$-plane, it appears as though the stable manifold of the unstable $E_2$ separates the space of initial conditions into two distinct regions where either $E_1$ or the LAS $E_2$ are globally attractive. Figure 3.3(b) demonstrates the case where solutions can either converge to $E_1$ or a stable periodic orbit about one of the internal $E_2$ equilibria. Similarly, the other $E_2$ divides the space of initial conditions into two regions.

Figure 3.4 uses the same values as those of Figure 3.3(b) except $d$ is increased. In Figure 3.3(b), $d\theta/[qrf(T/q)] = 1.05$. In Figure 3.4(a), $d$ is increased such that this value is 1.15. While the system still has the stable equilibrium $E_1$ and a stable periodic orbit about an $E_2$, the two internal $E_2$ equilibria are nearer to one another. Finally, in Figure 3.4(b), where $d\theta/[qrf(T/q)] = 1.5$, the $E_2$ have already crossed

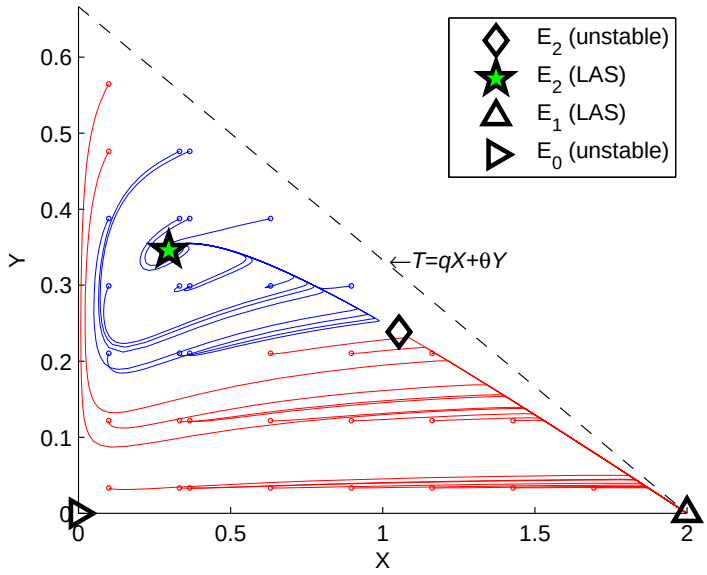


(a) Bistability: $E_1$ and an $E_2$ are LAS

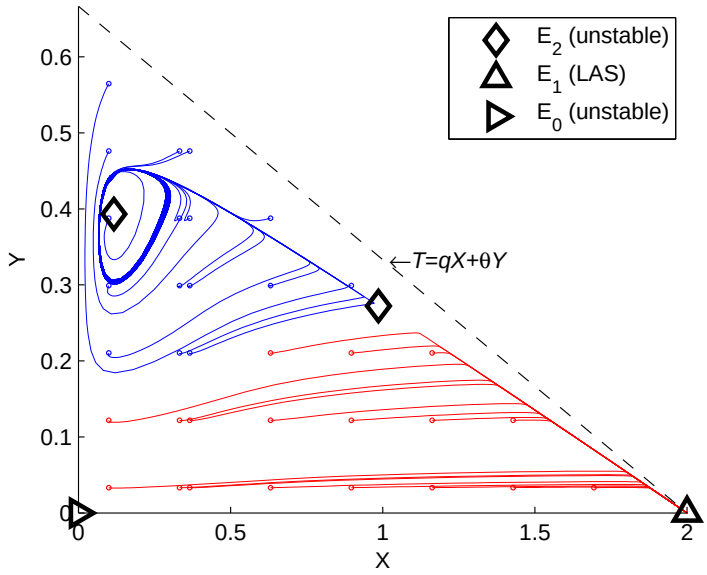


(b) $E_1$ is LAS; a stable periodic orbit also exists about one of the $E_2$

**Figure 3.3:** Orbits projected into the $xy$-plane, including all equilibria and their local stability. Solution curves are shown for various initial conditions. Red indicates convergence to $E_1$; blue indicates convergence to an $E_2$ or to a periodic orbit about an $E_2$. **(a)** $d\theta/[qrf(T/q)] = 1.03$, $v_m = 1.6$; **(b)** $d\theta/[qrf(T/q)] = 1.05$, $v_m = 6$. In both panels, $f(x) = ax/(x + a_k)$, $v(N) = v_m \frac{N}{N+v_k}$, $h(N) = h_m \frac{N}{N+h_k}$; $T = 0.1$, $q = 0.05$, $\theta = 0.15$, $m = 1.2$, $r = 0.9$, $a = 0.8$, $a_k = 0.25$, $h_m = 0.03$, $h_k = 0.1$, $v_k = 0.8$, $Q(0) = 0.055$.

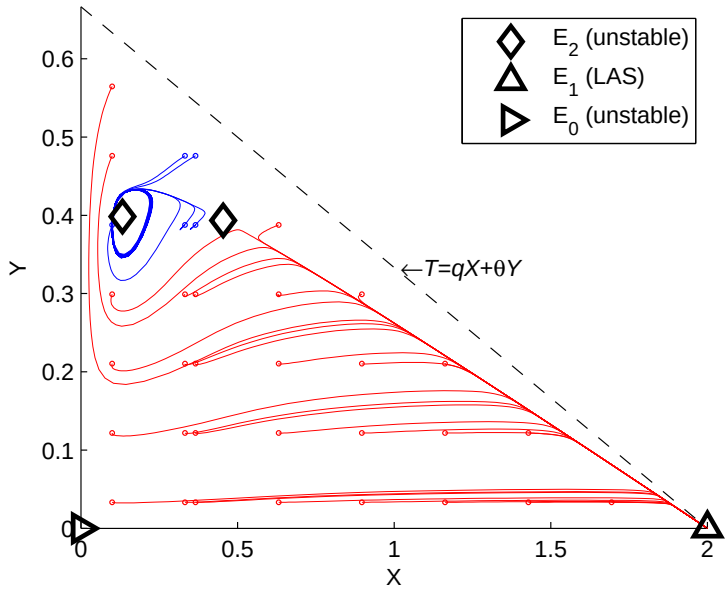


(a) $E_1$ is LAS; a stable periodic orbit also exists about one of the $E_2$

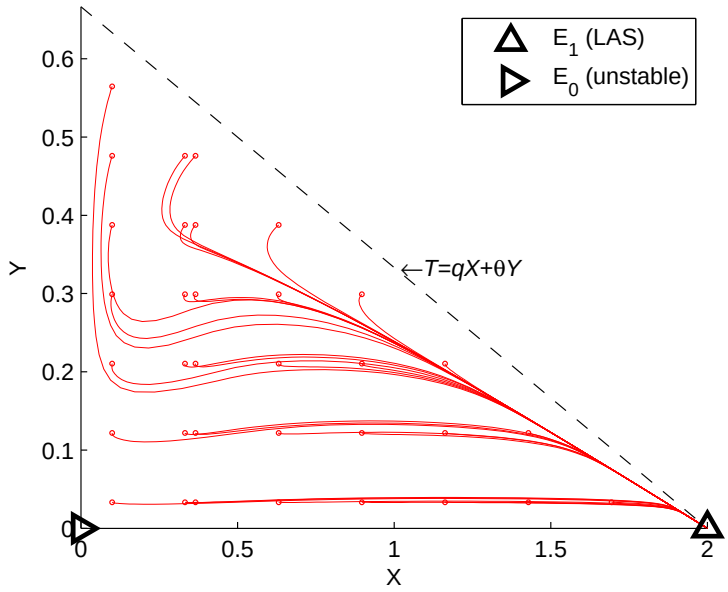


(b) No $E_2$ exist; $E_1$ is globally asymptotically stable

**Figure 3.4:** A continuation of Figure 3.3(b). Orbits projected into the $xy$-plane, including all equilibria and their local stability. **(a)** $d\theta/[qrf(T/q)] = 1.15$; **(b)** $d\theta/[qrf(T/q)] = 1.5$. In both panels, all parameters except for $d$ are fixed to the same values as those in Figure 3.3(b).

paths and annihilated one another, leaving $E_1$ as the only stable equilibrium point. This behavior is as to be expected from what is observed in the bifurcation diagrams of Figure 3.2. Namely, in the $d$-interval where both of the $E_2$ exist, the distance between these two interal equilibria decreases as $d$ increases. They eventually intersecting, after which there are no internal equilibria and $E_1$ is globally asymptotically stable.

## 3.6 Conclusion

Here a new feedback term was added to the grazer, one which introduces a cost to recycling nitrogen. Increased grazing and/or food quality creates positive feedback for grazer biomass production. However, it also increases N recycling, which in turn creates negative feedback on biomass production. Lastly, the producer assimilation rate of nutrient not only affects food quality and abundance but also plays a protective role for the grazer. As expected, this behavior is observed in the model; for example, even with the linear functional response the stability of the coexistence equilibrium requires a balance between feeding, producer uptake/cleaning, and sensitivity to N accumulation.

While the original motivation was to explore toxicity in closed aquaculture systems and the important knife edge phenomenon (Boersma and Elser, 2006; Peace et al., 2013), working on this project has also brought attention to more general problems in mathematical biology. For example, using the linear functional response $f(x) = ax$ to explore the dynamical behavior obfuscates the model's potential for richer and more interesting dynamics. It is important to be cognizant of how the choice of functions may affect qualitative behavior. If one were trying to validate the model with data, deriving "correct" functions for $f$, $v$, and $h$ is important. Here, these functions are considered more generally without a data-driven derivation. This approach is in direct contrast to the derivation of the lipid model in Chapter 2, which makes heavy usage

of empirically validated functions specific to the problem.

### *3.6.1 Future work*

The model assumes that the concentration of free N is directly correlated to the concentration of ammonia and nitrate. It also assumes instantaneous recycling of N from the grazer pool into the free-N pool. These assumptions neglect the intricacies of the nitrogen cycle, something which could be incorporated into a more complex model. Incorporating the relative concentrations of ammonia, nitrate, nitrite, etc., would allow for a more realistic derivation of a toxicity function $h$. Alternatively, one could derive a nitrification model and then apply quasi-steady states to the ammonia and nitrate concentrations, eliminating two differential equations. This would reduce the complexity while facilitating a more mechanistic construction of $h$.

# Chapter 4

# PROSTATE CANCER

## 4.1 Introduction

Prostate cancer has the highest incidence rate of non-skin cancers in men in the United States and the second highest mortality rate. It is projected that in 2013 there will be 238,590 newly diagnosed cases of prostate cancer in the United States, accounting for 28% of all newly diagnosed cases of cancer in men. Prostate cancer is projected to account for 29,720 deaths in the United States for 2013 (Siegel, Naishadham and Jemal, 2013).

In serious cases with aggressive or malignant tumors, hormonal therapy is a common option for treatment. The prostate cells' dependency on androgens for proliferation and apoptosis inhibition is exploited by blocking the patient's androgen production. Unfortunately, tumors can adapt to the low androgen environment, rendering androgen treatment ineffective.

Understanding the mechanisms responsible for the progression of prostate cancer to a recurrent, hormone-refractory stage has immediate clinical implications. Although hormonal ablation therapy significantly reduces tumor mass, many tumors recur in a more aggressive form and with a poorer prognosis. One theory is that androgen-deprivation aids in the development of these so-called androgen independent (AI) tumors by exhibiting strong selective pressure for AI phenotypes. As a result, it has been suggested and demonstrated experimentally that intermittent androgen suppression (IAS) therapy, as compared to continuous androgen suppression (CAS), may delay relapse (Sato et al., 1996; Bruchovsky et al., 1996, 2000, 2006).

Mathematical models have been proposed as possible tools to help determine optimal timing for androgen treatment. Given the fundamental role of androgen and androgen receptor (AR) in prostate cancer development and progression, it is important to have a clear understanding of their similarly important role in the healthy prostate. Quantitatively investigating how androgen and AR affect the healthy prostate may provide clues for developing a useful treatment model.

## 4.2 Background

Androgen regulates both proliferation and apoptosis of prostate cells through intracellular action of the AR (Gelmann, 2002; Feldman and Feldman, 2001; Heinlein and Chang, 2004). Testosterone enters prostate cells where it can bind to AR but is mostly converted to $5\alpha$-dihydrotestosterone (DHT) by the enzyme $5\alpha$-reductase. DHT instead more actively binds to AR, with a greater binding affinity. AR activated by DHT is more stable than when activated by testosterone and has a greater effect on prostate maintenance (Wright et al., 1996; Lee and Chang, 2003).

Androgen:AR complexes translocate to the nucleus where they play an active role in the regulation of gene transcription including genes involved in proliferation and apoptosis. The intracellular concentration of the androgen:AR complex is therefore reasonable for a quantitative predictor of cell death and proliferation rates. Indeed, this relationship has been demonstrated empirically () and used for mathematical models of the prostate (Eikenberry, Nagy and Kuang, 2010; Jain et al., 2011).

### *4.2.1 Treatment*

Treatment strategies depend on a number of factors such as disease stage and patient age. Radical prostatectomy is used as a curative therapy for cancer localized to the prostate through resection of the prostate gland and surrounding tissue

(Walsh, Lepor and Eggleston, 1983). Radical prostatectomy and radiation therapy are generally used for initial treatment of prostate cancer which is still localized to the prostate. However, a significant number of patients experience biochemical recurrence, as indicated by a rise in PSA levels. Alternative treatment methods are needed for these patients in addition to those diagnosed with metastatic cancer.

Huggins, Stevens and Hodges (1941) discovered that advanced prostate cancer responded to castration, and that injection of androgens exacerbated symptoms. Like healthy prostate cells, both local and metastatic prostate cancer cells depend on androgen for growth and survival. Androgen ablation therapy can effectively reduce tumor mass and PSA levels for some time by inducing castrate levels of androgen. Luteinizing hormone-releasing hormone (LHRH) agonists, which blocks release of luteinizing hormone (LH), and anti-androgens can achieve what is essentially reversible castration (Denmeade and Isaacs, 2002).

Although most prostate cancers are initially dependent on androgen, hormone treatment becomes ineffective as cancer cells develop resistance to the therapy (Denmeade and Isaacs, 2002; Taplin et al., 1995; Tran et al., 2009). Resistance has been observed to develop within months to years after treatment begins (Feldman and Feldman, 2001; Mcleod, 2003; Scher et al., 2004; Edwards and Bartlett, 2005a).

Identifying the exact mechanisms behind AI is still an open research area. Given the role of AR in cell proliferation and apoptosis, it is natural to suspect that modification related to AR or AR function plays a role in the evolution of hormone refractory cancer. AR is expressed in prostate cancer including the majority of treatment resistant cancers (Heinlein and Chang, 2004). There are indeed a number of known and proposed ways by which the cancer cells develop resistance; however, it is unknown exactly which pathway or combination thereof is the key step to AI (Taplin et al., 1995; Heinlein and Chang, 2004; Feldman and Feldman, 2001; Edwards and Bartlett,

2005b). Future treatment improvements may require classification of a specific patient's cancer, identifying then targeting whichever AI pathways are present.

It has been suggested and measured that AI cancer cells express higher levels of AR than AD cells (Taplin et al., 1995; Edwards and Bartlett, 2005a). Studies have found upwards of 30% of treatment resistant cancers have amplification of the AR gene which was not detected prior to therapy (Visakorpi et al., 1995; Heinlein and Chang, 2004; Koivisto et al., 1997). Increased expression of AR would increase sensitivity to androgen, an advantage in low androgen environments. However, AR gene amplification has been found not always to result in increased AR expression (Edwards and Bartlett, 2005a).

## 4.3 Modeling Androgen Deprivation Therapy

Modeling androgen deprivation therapy is an active research area. In general, these models consider tumors as consisting of two distinct subpopulations characterized by their responses to androgen. Before treatment, a tumor would consist (almost entirely) of cells that are completely dependent on androgen for survival and proliferation. These "androgen dependent" (AD) cells are responsible for the disease regression often observed during initial treatments. These sustained periods of androgen depletion create strong selective pressure for cells that are resistant to treatment by means of decreased androgen dependence. Expansion of this so-called androgen independent (AI) population reduces overall treatment effectiveness for the tumor; eventually, relapse occurs when a threshold is reached and the AI population outcompetes the AD population. In a basic model, expansion of the AI population is generally driven by two mechanisms. First, AD cells can mutate to become AI. Second, the AI population has a selective advantage during treatment. Models may also assume that AI cells mutate back to AD.

This model framework largely originate from a PDE-based model for continuous androgen suppression (Jackson, 2004b,a). Jackson considered a radially-symmetric tumor spheroid consisting of AD and AI cell subpopulations as well as the androgen levels in the prostate. Tumor volume and the relative fraction of AD and AI cells were used to investigate relapse under two modes of CAS corresponding to total and partial androgen blockade. Androgen levels were modeled depending on the simulated treatment type. There were no transitions between the AD and AI states, a fundamental difference from later adaptations. Instead, the AI population was initialized to 0.05% of the total cell population. Further, PSA levels were not deduced.

Ideta et al. (2008) later adapted the model from Jackson (2004b) as an ODE system for investigating intermittent androgen suppression. There have since been more ODE models based on the Jackson; Ideta et al. framework (Tanaka et al., 2008; Hirata, Bruchovsky and Aihara, 2010; Jain et al., 2011; Jain and Friedman, 2013; Portz, Kuang and Nagy, 2012; Suzuki, Bruchovsky and Aihara, 2010; Shimada and Aihara, 2008) in addition to PDE (Guo, Tao and Aihara, 2008; Tao, Guo and Aihara, 2010) and stochastic (Veestraeten, 2006; Dayananda, Kemper and Shvartsman, 2004; Tanaka et al., 2010) models.

## 4.4 Cell Quota Application - PKN Model

Portz, Kuang and Nagy (2012) proposed the first prostate cancer in the literature that adapts the Cell Quota framework. Interestingly, the model was in part motivated by the lipid model from Chapter 2, including its implementation of androgen "uptake" by the cancer cells. This model, henceforth referred to as the PKN model, is significant for numerous reasons. It demonstrated that existing, data-driven modeling methods from ecological stoichiometry may be applied to prostate cancer, both theoretically and qualitatively. The PKN model is rewritten here for reference and discussed in

detail because it is important for the original work presented later in this chapter.

| | | |
|---|---|---|
| $X_1$: | androgen dependent prostate cancer cells | (cells$\times 10^9$) |
| $X_2$: | androgen "independent" prostate cancer cells | (cells$\times 10^9$) |
| $Q_i$: | intracellular androgen concentration of $X_i$ | (nM) |
| $P$: | serum PSA concentration | (ng/mL) |
| $T_s$: | serum testosterone concentration | (nM) |

$$
\begin{aligned}
X_1' &= \underbrace{\mu_m\left(1-\frac{q_1}{Q_1}\right)}_{\text{proliferation}} X_1 - \underbrace{c_1\frac{K_1^n}{Q_1^n+K_1^n}X_1}_{X_1\to X_2 \text{ mutations}} + \underbrace{c_2\frac{Q_2^n}{Q_2^n+K_2^n}X_2}_{X_2\to X_1 \text{ mutations}} \\
X_2' &= \underbrace{\mu_m\left(1-\frac{q_2}{Q_2}\right)}_{\text{proliferation}} X_2 + \underbrace{c_1\frac{K_1^n}{Q_1^n+K_1^n}X_1}_{X_1\to X_2 \text{ mutations}} - \underbrace{c_2\frac{Q_2^n}{Q_2^n+K_2^n}X_2}_{X_2\to X_1 \text{ mutations}} \\
Q_i' &= \underbrace{v_m\frac{q_m-Q_i}{q_m-q_i}\frac{T_s}{T_s+v_h}}_{\text{"uptake"}} - \underbrace{\mu_m\left(Q_i-q_i\right)}_{\text{growth dilution}} - \underbrace{bQ_i}_{\text{androgen loss}} \qquad i=1,2 \\
P' &= \underbrace{\sigma_0\left(X_1+X_2\right)}_{\text{baseline secretion}} + \underbrace{\sigma_1 X_1\frac{Q_1^m}{Q_1^m+\rho_1^m}+\sigma_2 X_2\frac{Q_2^m}{Q_2^m+\rho_2^m}}_{\text{androgen dependent secretion}} - \underbrace{\delta P}_{\text{degredation}}
\end{aligned}
\tag{4.1}
$$

The underlying assumption of Model (4.1) is that the so-called AI cells can survive and proliferate with lower androgen levels. The property $q_2 < q_1$ is used to reflect this trait. Indeed, it has been empirically established that CR disease survives when serum testosterone is depleted. However, while serum testosterone may be essentially zero post (chemical) castration, rat and human data have revealed that intraprostatic androgen levels can remain relatively high, particularly those of DHT which is less likely than testosterone to leak from cells. In fact, it has been shown that during treatment intraprostatic DHT remains at 50% of pre-treatment levels while serum

testosterone levels decrease by over 90% (Heinlein and Chang, 2004). DHT constitutes the majority of intracellular androgen, with 90% of testosterone converted to DHT (Feldman and Feldman, 2001). While free intraprostatic androgens leak from the prostate, those which are bound to AR should remain in the cells. The T:AR and DHT:AR complexes are also highly stable and less susceptible to degradation. In conclusion, the relationship between serum and prostatic androgen concentrations during ablation is an important detail.

From this context we see that the use of $Q_i$ in this model is problematic. $Q_i$ is intracellular androgen but with no distinction between free cytoplasmic androgen and androgen bound to nuclear AR. In the model results, $Q_2(t) < Q_1(t)$ during homoeostatic conditions—both on and off treatment. It therefore predicts that tumors do not develop resistance by means of AR overexpression or amplification. The problem is that these very mechanisms have been implicated in a significant number of CR tumors, with one review concluding 30% all CR tumors exhibit increased AR expression post-treatment (Feldman and Feldman, 2001). Instead, the model formulation is such that tumors develop resistance only through pathways less dependent on androgen. That the model accurately fits data under the constraint $q_2 < q_1$ is not a criticism. Rather, it leaves open the question whether or not an ecological framework based on the cell-quota can fit data and provide biologically meaningful insight.

The model's uptake function of serum testosterone uses Michaelis–Menten kinetics but assumes there are maximum $Q_i$ that prevent excessive testosterone influx. This formulation stems from phytoplankton models (Geider, MacIntyre and Kana, 1998) and coincidentally is also in the neutral lipid model described earlier (2.20). While this model of nutrient uptake is widely used and empirically validated for phytoplankton models, its application here (4.1) may be problematic. It combines a first order chemical kinetics model with a higher level model, namely the cell quota. For

green algae it makes sense because observed phenomena such as "luxury uptake" and species-specific maximum N:C are consistent with using $Q$ to quantify regulation of N-uptake. That nitrate uptake is due to active transport, as opposed to simple diffusion, has long been known for algae (Halterman and Toetz, 1984). An important observation has been the uptake of nitrate and other nutrients against their concentration gradients.

This uptake process directly contrasts with that of prostate epithelial cells. Testosterone and DHT are exchanged across serum and cells via diffusion, in a two-way process dependent on the concentration gradient. A more mechanistic approach to modeling androgen uptake by prostate epithelium was described by Potter, Zager and Barton (2006). The functions for influx of testosterone and DHT followed from the blood flow rates to the prostate and the differences in the intracellular and extracellular concentrations of testosterone and DHT. For PCa models this formulation may prove difficult to parametrize when considering metastatic tumors. For Model (4.1) in particular the Potter, Zager and Barton (2006) uptake functions are not directly applicable. The reason is that Model (4.1) does not differentiate between androgens bound to nuclear AR and free cytoplasmic androgens.

Despite the problems with the implementation of the cell quota, the models and analysis by Portz, Kuang and Nagy (2012) remain an important step in empirically-driven, theoretical models of prostate cancer. Inherent to systems biology is the trade-off between detailed complexity and abstract simplification. The cell quota provided a simple link between complex biology and mathematics. It stands to reason, however, that the model can be improved with closer attention to the underlying AR dynamics which play an unprecedented role in prostate cancer progression and treatment. Along with the unresolved questions surrounding the uptake function, there are many opportunities for improvement upon the original PKN cell quota

model.

## 4.5 In Search of a Mechanistic Basis

In the PKN model (4.1), defining $Q$ too broadly leaves gaps with the underlying biology. These gaps include the interrelated dynamics of bound and free androgens, the retention or loss of intracellular androgens during ablation, and the capacity to predict known mechanisms of treatment resistance. Increasing the complexity of the model to include intracellular AR kinetics may provide a more descriptive model that is based on established biochemical principles and testable parameter ranges. The goal here is to connect these intracellular AR kinetics to a cell quota based population model akin to the PKN model.

This is accomplished by first "taking a step back" and considering a mechanistic model of intraprostatic AR-androgen kinetics. The AR-androgen model is then used as a building block to derive a simpler cell quota based model. The following steps are taken to derive a

### *4.5.1 Intracellular AR Kinetics*

The following AR model (4.2) is based on the system developed in Potter, Zager and Barton (2006) as part of a larger prostate model. Using basic biochemistry and experimentally supported parameterizations, Potter, Zager and Barton (2006) mechanistically derived a model for androgen-mediated proliferation and apoptosis in the prostate. The intracellular androgen and AR dynamical equations follow from first order principles in chemical kinetics. Eikenberry, Nagy and Kuang (2010) later adapted this system to derive a simpler, more tractable model of the prostate epithelium that translates intracellular androgen-AR activity to per-capita growth and death rates. The model combined theory with experiment to investigate how AR and androgen

parameters could shape the pre-malignant environment. In particular, it considered androgen-driven evolution of prostate AR with implications for the progression and severity of prostate cancer. This focus on AR and prostate cancer progression has provided a useful foundation for modeling the interplay of AR dynamics and ADT treatment for prostate cancer.

To derive a prostate cancer model for ADT that includes AR, begin with the following adaptation from Potter, Zager and Barton (2006), including its later extension in Eikenberry, Nagy and Kuang (2010). The notation used here is generally consistent with these existing works (more so with the latter) but also includes notation that is new or different. Unless explicitly stated or otherwise implied, discussions of cellular processes or intracellular chemical species are specific to prostatic epithelial cells. Define:

| | | |
|---|---|---|
| $C_T(t)$: | T:AR complex concentration | (nM) |
| $C_D(t)$: | DHT:AR complex concentration | (nM) |
| $R(t)$: | intracellular free AR concentration | (nM) |
| $D(t)$: | intracellular free DHT concentration | (nM) |
| $T(t)$: | intracellular free T concentration | (nM) |
| $T_s(t)$: | total serum T concentration | (nM) |

$$
\begin{aligned}
C_T' &= k_a^T TR - k_d^T C_T, \\
C_D' &= k_a^D DR - k_d^D C_D, \\
R' &= \lambda - k_a^T TR + k_d^T C_T - k_a^D DR + k_d^D C_D - \beta_R R, \\
D' &= \alpha k_{cat} \frac{T}{T+\alpha_k} - k_a^D DR + k_d^D C_D - \beta_D D, \\
T' &= K(T_s - T) - k_a^T TR + k_d^T C_T - \alpha k_{cat} \frac{T}{T+\alpha_k} - \beta_T T.
\end{aligned}
\tag{4.2}
$$

The AR kinetics model (4.2) mathematically describes the following system:

1. Testosterone exchange between serum and prostate is proportional to the blood flow rate to the prostate and the concentration gradient. Prostatic testosterone is uniformly distributed amongst the prostate cells.
2. Free testosterone is enzymatically converted to DHT by $5\alpha$-reductase.
3. Free testosterone and DHT bind to free AR in the cytoplasm by second order reaction kinetics.
4. Free AR, T, and DHT degrade by first order kinetics.
5. A fixed total AR concentration, $R_t$, is maintained at homeostasis.

Refer to Table 4.1 for a list of parameter descriptions and units. The uptake function $K(T_s - T)$ is based on the serum transport model in Potter, Zager and Barton (2006); its derivation is found in the following section. It is assumed DHT does not to leak from the prostate into serum. The AR production rate function $\lambda$ can be derived based on the assumed homeostatic total AR concentration, defined as $R_t$. Since the total AR concentration is $R(t) + C_D(t) + C_T(t)$, taking the derivative $R'(t) + C'_D(t) + C'_T(t)$ it readily follows that

$$\lambda = \beta_R \left( R_t - C_D(t) - C_T \right) \tag{4.3}$$

is sufficient for the steady state value $R_t = R + C_D + C_T$ of the total AR concentration. The enzymatic conversion of T to DHT by $5\alpha$-reductase is modeled with Michaelis–Menten kinetics. In absence of androgens, AR is unstable (Gregory et al., 2001). However the T:AR and DHT:AR complexes, which are highly stable, are assumed not to degrade. It has been suggested that disassociation from its ligand—rather than degradation of the bound protein—regulates AR activity (Tyagi et al., 2000; Lee and Chang, 2003). Along with the $5\alpha$-reductase enzyme rate constants, the on/off rate constants $k_{a,d}^{T,D}$ and degradation rates $\beta_{R,D,T}$ can be determined from existing data and models (Potter, Zager and Barton, 2006; Eikenberry, Nagy and Kuang, 2010).

The Potter, Zager and Barton model also included state variables and second order reaction equations for dimerization of the T:AR and DHT:AR complexes in

| Parameter | Description | Units |
|---|---|---|
| $R_t$ | homeostatic total AR concentration | nM |
| $k_a^T$ | T:AR association rate constant | $nM^{-1}$ $h^{-1}$ |
| $k_d^T$ | T:AR disassociation rate constant | $h^{-1}$ |
| $k_a^D$ | DHT:AR association rate constant | $nM^{-1}$ $h^{-1}$ |
| $k_d^D$ | DHT:AR disassociation rate constant | $h^{-1}$ |
| $\beta_R$ | free AR degradation rate | $h^{-1}$ |
| $\beta_T$ | free T degradation rate | $h^{-1}$ |
| $\beta_D$ | free D degradation rate | $h^{-1}$ |
| $k_{cat}$ | 5$\alpha$-reductase turnover number | nmol $mg^{-1}$ $h^{-1}$ |
| $\alpha$ | 5$\alpha$-reductase concentration | mg $L^{-1}$ |
| $\alpha_k$ | 5$\alpha$-reductase Michaelis constant | nM |
| $K$ | flow rate constant | $h^{-1}$ |
| $V$ | prostate volume | L |

**Table 4.1:** Parameters for AR kinetics model (4.2). These parameters also apply to the population level AR Quota Model (4.23)

addition to their subsequent binding to hormone response elements. Although not included here, these dimer-DNA dynamics are relevant to forthcoming discussions in this chapter. Similarly relevant is that prostate volume was nonconstant because the complete model was used to predict changes in volume and mass post-castration.

### Uptake

Testosterone and DHT diffuse past the cell membrane and are exchanged between serum and prostate (cancer) cells. The exchange rate should therefore depend on the concentration gradient and prostate volume, which Potter, Zager and Barton (2006) expresses as $KV(T_s - T)$ (variables renamed here for consistency). The volumetric

flow rate $KV$ (L $h^{-1}$) consists of a flow rate constant, $K$ ($h^{-1}$), and the prostate volume $V$ (L). $K$ can be considered as a combination of the volumetric flux (L $m^{-2}$ $h^{-1}$) and surface area per unit volume of prostate/tumor (e.g. $m^2$ $L^{-1}$). Therefore $KV(T_s - T)$ has units nmol $h^{-1}$, and

$$\begin{aligned}(VT)' &= KV(T_s - A) - k_a^T VTR + k_d^T VC_T - V\alpha k_{cat}\frac{T}{T + K_M} - \beta_T VT \\ &= VT' + TV'.\end{aligned}$$

If the volume $V$ is constant then $V' = 0$ and $T' = (VT)'/V$ gives the equation for $T'$ in Model (4.2).

## 4.6 A Closer Look at Uptake

On an abstract level, using a maximum $Q$ as in the PKN Model (4.1) is understandable, as the maximum free-androgen concentrations in the prostate would be limited by serum concentrations. Yet $Q$ may represent AR-bound androgen or total intracellular androgen, and so the meaning of $q_m$ is not straightforward. A novel derivation is provided here which links the uptake model to the underlying biochemistry. Testosterone that enters a prostate cell is mostly converted to DHT by the enzyme 5$\alpha$-reductase. It would be straightforward to use Michaelis–Menten kinetics to describe this process. This DHT and (to a lesser extent) testosterone in the cytosol may bind to AR, which ultimately results in a stable androgen:AR dimer that translocates to the nucleus and binds to DNA. It is here that the now-bound androgen would be involved in regulating transcription of genes for proliferation, survival, and PSA production, among other processes (Gelmann, 2002). Therefore androgen taken up by a cell must go through many intermediate steps before it (indirectly via AR signaling) regulates cellular processes.

While testosterone entering a cell can either convert enzymatically to DHT or

bind to AR, it can also leak out of the cell into serum. The same is true for DHT but at a decreased rate and not accounted for here. Hence a certain proportion of the testosterone taken into the cell ultimately leads to stable androgen:AR complexes localized to the nucleus. This proportion should vary based on the concentration of testosterone entering the cell, the concentration of free AR in the cytosol, and the concentration of 5$\alpha$-reductase. Consider the cell-specific uptake rate function

$$v_m \frac{q_m - Q}{q_m - q} \frac{T_s}{T_s + v_h} \tag{4.4}$$

as implemented in Model (4.1). If $Q$ is the androgen:AR complex concentration, then $q_m$ could represent the parameter $R_t$ defined for Model (4.2). If the total AR (bound and free) concentration is assumed constant, then the free AR concentration is given by $R_t - Q$. This interpretation is consistent with mass action for the binding of AR and androgen, where ${T_s}/{(T_s + v_h)}$ is somehow the association rate multiplied with the available androgen concentration. Indeed, for fixed $T_s$ the quantity ${v_m T_s}/{(T_s + v_h)}$ is the rate of androgen:AR complex formation when $Q = q$. This rate decreases linearly with $R_t - Q$, similar to a mass action process. At any given time, the cell nucleus has at least $q$ concentration of androgen:AR and free AR concentration in the range $[0, q_m - q]$. The fraction ${(R_t - Q)}/{(R_t - q)}$ is therefore the free AR concentration scaled to $[0, 1]$. Under this interpretation of Model (4.1), the uptake function represents the following processes:

1. Uptake of serum testosterone,
2. Conversion of testosterone to DHT,
3. Leaking of free testosterone from the cytoplasm,
4. Binding of free AR to testosterone and DHT.

It remains to derive ${T_s}/{(T_s + v_h)}$. Assume that the total AR concentration is in

quasi-steady state and denote $\overline{R}(t) = R(t) + C_T(t) + C_D(t)$. Then

$$\overline{R}' = \beta_R \left(R_t - C_T - C_D\right) - \beta_R R = 0 \tag{4.5}$$

$$\Leftrightarrow R + C_T + C_D = R_t. \tag{4.6}$$

Denote by $\overline{T}(t)$ and $\overline{D}(t)$ the total concentrations of testosterone and DHT, respectively. Namely, $\overline{T}(t) = T(t) + C_T(t)$ and $\overline{D}(t) = D(t) + C_D(t)$. Similarly assume that total testosterone and DHT are in quasi-steady state. Setting $\overline{T}' = \overline{D}' = 0$ yields the expressions (4.7)-(4.8),

$$0 = K(T_s - T) - \alpha k_{cat} \frac{T}{T + \alpha_k} - \beta_T T, \tag{4.7}$$

$$D = \frac{\alpha k_{cat}}{\beta_D} \frac{T}{T + \alpha_k}. \tag{4.8}$$

Thus both $T$ and $D$ can be expressed in terms of $T_s$ once Eq. (4.7) is solved for $T$. To simplify notation, define the following parameters,

| | |
|---|---|
| $h := K + \beta_T$ | ($\mathrm{h}^{-1}$), |
| $v := \dfrac{K}{h}$ | (dimensionless), |
| $\alpha_m := \alpha k_{cat}$ | (nM $\mathrm{h}^{-1}$). |

$h$ is sum of the specific loss rates of testosterone excluding conversion to DHT (blood flow and degradation). $v$ is the fraction of this flux due to testosterone exchange with serum. Also note that $vT_s$ is the steady state concentration of intracellular testosterone in absence of any conversion to DHT. $\alpha_m$ is simply a notational convenience for the maximum reaction rate for $5\alpha$-reductase. (This maximum rate is expressed as the product of the $5\alpha$-reductase concentration and turnover rate in order to maintain the Eikenberry, Nagy and Kuang model's connection to data.) Solving Eq. (4.7) for $T$ yields a quadratic with unique positive solution,

$$T = \frac{1}{2}\left(vT_s - \alpha_m/h - \alpha_k\right) + \frac{1}{2}\left[\left(vT_s - \alpha_m/h - \alpha_k\right)^2 + 4vT_s\alpha_k\right]^{1/2}. \tag{4.9}$$

Eq. (4.9) is a nonegative and strictly increasing function of $T_s$ with $T = 0$ when $T_s = 0$ and $T \geq vT_s - \alpha_m/h - s$ for all $T_s$. After rewritting the expression in the radical,

$$T = \frac{1}{2}\left(vT_s - \alpha_m/h - \alpha_k\right) + \frac{1}{2}\left[\left(vT_s + \alpha_m/h + \alpha_k\right)^2 - 4vT_s\alpha_m/h\right]^{1/2}, \tag{4.10}$$

$$= \frac{1}{2}\left[\left(vT_s - \alpha_m/h - \alpha_k\right) + \left(vT_s + \alpha_m/h + \alpha_k\right)\left(1 - \frac{4vT_s\alpha_m/h}{\left(vT_s + \alpha_m/h + \alpha_k\right)^2}\right)^{1/2}\right], \tag{4.11}$$

and a simple approximating function can be found with a Taylor Series expansion that converges for all $T_s \geq 0$. The relation $\dfrac{4vT_s\alpha_m/h}{(vT_s + \alpha_m/h + \alpha_k)^2} < 1$ is already established by the fact that the expression under the radical in Eq. (4.9) is nonnegative. Thus

$$\begin{aligned}\left(1 - \frac{4vT_s\alpha_m/h}{\left(vT_s + \alpha_m/h + \alpha_k\right)^2}\right)^{1/2} &= \sum_{n=0}^{\infty} \frac{(-1)^n(2n)!}{(1-2n)(n!)^2 4^n} \frac{(-4vT_s\alpha_m/h)^n}{\left[vT_s + \alpha_m/h + \alpha_k\right]^{2n}} \\ &= \sum_{n=0}^{\infty} \frac{(2n)!}{(1-2n)(n!)^2} \frac{(vT_s\alpha_m/h)^n}{\left[vT_s + \alpha_m/h + \alpha_k\right]^{2n}}\end{aligned} \tag{4.12}$$

The quasi-steady state approximation $T^{(n)}$ for $T$ can now be written as

$$\begin{aligned}T^{(n)} = vT_s - \frac{vT_s\alpha_m/h}{vT_s + \alpha_m/h + \alpha_k} - \frac{(vT_s\alpha_m/h)^2}{\left[vT_s + \alpha_m/h + \alpha_k\right]^3} - \\ \cdots - \frac{(2n)!}{2(1-2n)(n!)^2} \frac{(vT_s\alpha_m/h)^n}{\left[vT_s + \alpha_m/h + \alpha_k\right]^{2n-1}}.\end{aligned} \tag{4.13}$$

The error for $T^{(n)}$ is 0 if $T_s = 0$ and is an increasing function of $T_s$. For the $n$th approximation, error is approximated by the usual Taylor Series remainder and bounded by Eq. (4.14) since $\dfrac{4vT_s\alpha_m/h}{(vT_s + \alpha_m/h + \alpha_k)^2} < 1$ and

$$\begin{aligned}\|T - T^{(n)}\| &\approx \frac{(vT_s + \alpha_m/h + \alpha_k)}{2} \frac{(2n+2)!}{(1+2n)((n+1)!)^2 4^{n+1}} \frac{(4vT_s\alpha_m/h)^{n+1}}{\left[vT_s + \alpha_m/h + \alpha_k\right]^{2n+2}} \\ &\leq \frac{2vT_s\alpha_m/h}{vT_s + \alpha_m/h + \alpha_k} \left[\frac{4vT_s\alpha_m/h}{\left(vT_s + \alpha_m/h + \alpha_k\right)^2}\right]^n \\ &< \frac{2vT_s\alpha_m/h}{vT_s + \alpha_m/h + \alpha_k} 4^{-n} \\ &< \frac{\max\left\{\alpha_m/h, vT_s\right\}}{\alpha_k} 4^{-n}.\end{aligned} \tag{4.14}$$

Therefore $T^{(1)}$ and $T^{(2)}$ are good approximations for $T$ if $\max\{\alpha_m/h, vT_s\}$ is sufficiently small or $\alpha_k$ is sufficiently large. Since $v < 1$ and $T_s < \alpha_k$ for applications to rat and human, the value $\alpha_m/h$ is more pertinent.

The quasi-steady state value for $D$ is also computed in terms of $T_s, K, \beta_T, \alpha, \alpha_k$, and $\beta_D$ using Eq. (4.8) and the approximation (4.13) for $T$. Explicit consideration is given to $T^{(n)}$ for $n = 1, 2$ and the exact form in Eq. (4.9). With $T$ and $D$ explicitly defined in terms of $T_s$, the extracellular testosterone, uptake can be modeled as a direct process from serum to AR binding. Specifically, "uptake" now constitutes binding of T and DHT with free AR. The reason the reaction rate constants for AR binding do not appear is that the total prostatic testosterone concentration was assumed to be in quasi-steady state. This detail made possible the straightforward equations (4.7)-(4.8) without the parameters $k_a^{T,D}$, $k_d^{T,D}$ or the variables $R(t)$, $C_D(t)$, $C_T(t)$. The only other quasi-steady state assumption has similarly been for total AR concentration but not free AR or androgen:AR complexes. The implications of this approach, including the associated problems, are discussed later.

$$T^{(1)} = vT_s \quad D_I^{(1)} = \frac{\alpha_m}{\beta_D}\frac{vT_s}{vT_s + \alpha_k} \tag{4.15a}$$

$$T^{(2)} = vT_s\frac{vT_s + \alpha_k}{vT_s + \alpha_k + \alpha_m/h} \quad D_I^{(2)} = \frac{\alpha_m}{\beta_D}\frac{vT_s}{vT_s + \alpha_k}\frac{(vT_s + \alpha_k)^2}{(vT_s + \alpha_k)^2 + \alpha_k\alpha_m/h}. \tag{4.15b}$$

The new uptake models follow from the same second-order reaction kinetics and parameters of model (4.2). From Assumption (4.5) the free AR concentration may be written $R_t - Q$, and Eqs. (4.15) gives free DHT and T concentrations. Use $V$ and

$V^{(1,2)}$ to denote the uptake rate function and its first two approximations, respectively.

$$V(T_s) = (R_t - Q)\left(k_a^T T(T_s) + k_a^D D(T_s)\right) \tag{4.16}$$

$$V^{(1)}(T_s) = vT_s\left[k_a^T + k_a^D \frac{\alpha_m}{\beta_D}\frac{1}{vT_s + \alpha_k}\right] \tag{4.17}$$

$$V^{(2)}(T_s) = vT_s \frac{vT_s + \alpha_k}{vT_s + \alpha_k + \alpha_m/h}\left[k_a^T + k_a^D \frac{\alpha_m}{\beta_D}\frac{vT_s + \alpha_k + \alpha_m/h}{(vT_s + \alpha_k)^2 + \alpha_k\alpha_m/h}\right] \tag{4.18}$$

**Remark 5.** *The steady state concentrations of bound AR (T:AR, DHT:AR) and free AR can be written as functions* (4.19) *of* $T_s$.

$$C_T + C_D = R_t\frac{\theta}{1+\theta}, \quad R = R_t\frac{1}{1+\theta}, \quad \theta = \frac{k_a^T}{k_d^T}T + \frac{k_a^D}{k_d^D}D. \tag{4.19}$$

*Proof.* At steady state, $C_T' = 0$ and $C_D' = 0$ yield the respective identities $C_T = \frac{k_a^T}{k_d^T}TR$ and $C_D = \frac{k_a^D}{k_d^D}DR$. Set $\theta = \frac{k_a^T}{k_d^T}T + \frac{k_a^D}{k_d^D}D$. Substituting them into the identity $C_T + C_D = R_t - R$ gives

$$C_T + C_D \;=\; \left(\frac{k_a^T}{k_d^T}T + \frac{k_a^D}{k_d^D}D\right)R \;=\; R_t - R. \tag{4.20}$$

The results quickly follow by solving for $R$ with the middle equation and RHS, or by substituting $R_t - C_T - C_D$ for $R$ in the middle equation then using the LHS to solve $C_T + C_D$. □

In Figure 4.1 the steady states in Eq. (4.19) are calculated using the quasi-steady state approximations for $T$ and $D$. Compared with the "actual" values, the difference is negligible for the 2nd-order approximation as expected from the error bound in Eq. (4.14). Although the steady state expressions suggest that asymptotically (with respect to serum T) activated AR is mostly comprised of T:AR (and intracellular androgen of T). However, such behavior is predicted for unreasonably high serum T concentrations. Figure 4.1 shows the steady state behavior for physiologically feasible concentrations of serum T in humans (and rats) using experimentally-derived parameters which were assembled for modeling AR in Potter, Zager and Barton (2006);

Eikenberry, Nagy and Kuang (2010). The general behavior as $T_s \to \infty$ is also shown but does not represent behavior that would occur in modeling applications.

It remains to connect the new uptake function (4.16) with the phytoplankton nutrient-uptake model as adapted by the PKN model. In doing so, the reasons for focusing so closely on the uptake function will become more apparent. Thus far the only relationship is $q_M = R_t$. Observe from Eqs. (4.15) and Figure 4.1 that for physiological ranges of $T_s$, the (approximate) intracellular concentration of free DHT is either equal to or approximated by a Michaelis–Menten function of serum T. Since DHT has an order of magnitude greater binding affinity than T, around 90% of bound AR is comprised of DHT:AR. AR binding with DHT also induces greater physiological response (Wright et al., 1996) than with testosterone. Recall that, while $Q$ was defined originally in Portz, Kuang and Nagy (2012) as the androgen quota, it is defined here instead as the intracellular DHT:AR and T:AR complex concentrations. Hence the Michaelis–Menten function used for uptake in the Portz, Kuang and Nagy model may now be explained as a simplified approximation to Eqs. (4.16).

In summary, the mechanistically derived uptake function (4.16), together with established molecular biology, provides a much greater phenomenological basis for deriving a "cell quota" model of prostate cancer and ADT. Further reasons for giving special attention to uptake are severalfold. First, it provides a degree of clarity on how the mathematics connects with (or were intended to have connected with) the biology. Although it follows from the simple process of assuming quasi-steady states, deriving functions through this approach makes better interpretation of results. It has explicit consideration of mechanisms which would, for example, affect the T→DHT rate or relative binding activity. In fact, the major pathways to treatment resistance can all be separately expressed by the AR quota $Q$ and "uptake" function provide.

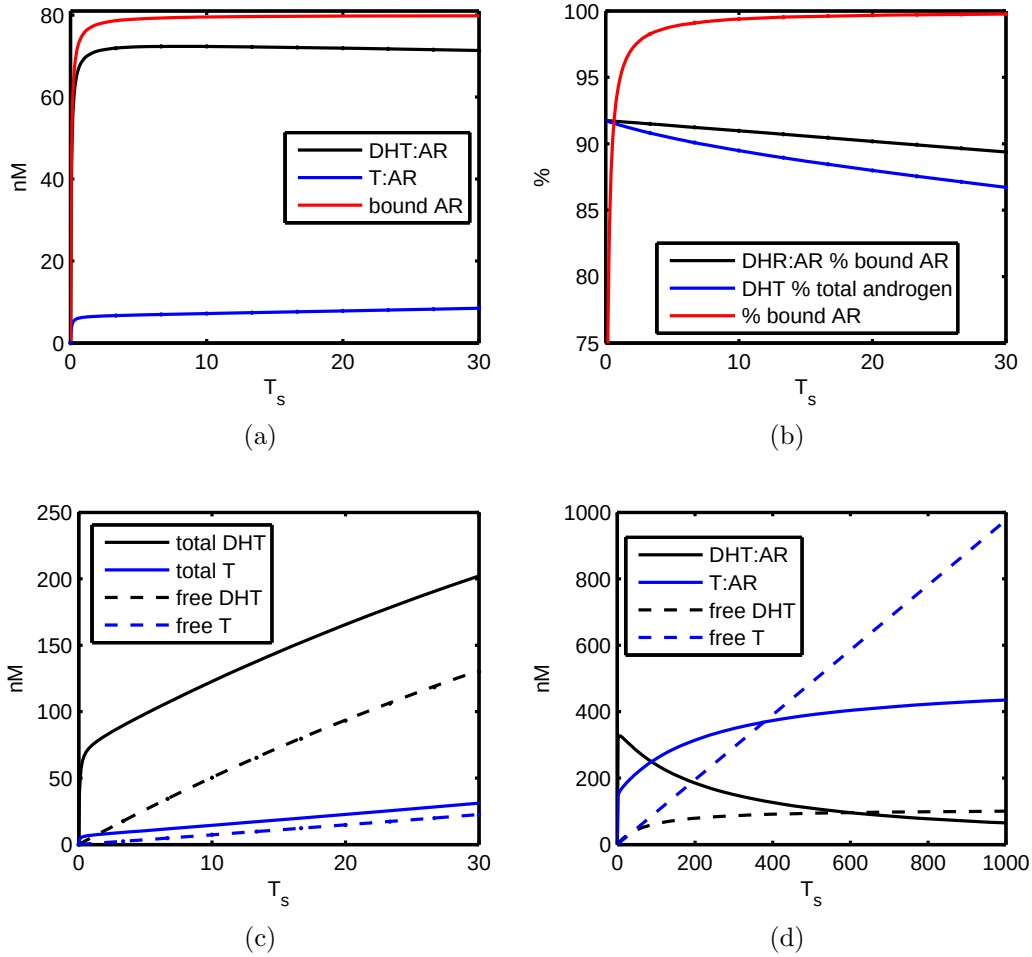


**Figure 4.1:** Steady states of Model (4.2) calculated with the quasi-steady state approximations of $T$ and $D$ and $R_t = 80$, $\alpha = 5$, $k_{cat} = 8.276$, $\alpha_k = 70$, $k_a^D = 0.053$, $k_d^D = 0.018$, $k_a^T = 0.14$, $k_d^T = 0.069$, $\beta_D = 0.077$, $\beta_T = 0.231$, $K = 2$. (a)-(c) Steady state dynamics over a physiological range of $T_s$ for humans. (d) Snapshot over an unrealistic range of $T_s$. As $T_s \to \infty$, the proportion of bound AR constituted by T:AR approaches 100% while free T increases indefinitely. The free and bound DHT concentrations are bounded above due to finite 5$\alpha$-reductase and its saturating reaction rate.

## 4.7 AR Quota Model for ADT

Now the intracellular AR system (4.2) is used to establish a simple but descriptive prostate cancer model suitable for interpreting numerical results within a biological context. The goal is to derive a simple "cell quota" model such as (Portz, Kuang and Nagy, 2012) but in such a way that the functions and parameters are explicitly connected to the underlying biology. For example, in the Portz, Kuang and Nagy model, free intracellular T and DHT are combined into a single variable represented as a function of the serum testosterone concentration. Similarly the intracellular T:AR and D:AR complexes are combined to represent the cell quota. If one were to model a single cell population, it would take the form

$$\begin{aligned} X' &= \mu X - \delta_m \frac{(q_\delta)^n}{Q^n + (q_\delta)^n} X - \delta_0 X, \\ Q' &= (R_t - Q)(k_a^T T + k_a^D D) - \left((1-f_D)k_d^T - f_D k_d^D\right) Q - \mu Q, \\ P' &= \sigma \frac{Q^p}{Q^p + (q_\sigma)^p} X - \beta_P P, \end{aligned} \tag{4.21}$$

where

$$\begin{aligned} T &= vT_s \frac{vT_s + \alpha_k}{vT_s + \alpha_k + \alpha_m/h}, \\ D &= \frac{\alpha_m}{\beta_D} \frac{vT_s}{vT_s + \alpha_k} \frac{(vT_s + \alpha_k)^2}{(vT_s + \alpha_k)^2 + \alpha_k \alpha_m / h}. \\ \mu(Q) &= \mu_m \frac{Q^m}{Q^m + (q_\mu)^m}. \end{aligned} \tag{4.22}$$

Of course, to model the development of treatment resistance during androgen deprivation therapy, model (4.21) is extended to a two-population system. Doing so creates a system of 5 ODEs, as defined below. Let

| | | |
|---|---|---|
| $X_i(t)$: | CS ($i=1$) and CR ($i=2$) cancer cells | ($1\times10^6$ cells) |
| $Q_i(t)$: | "AR Quotas" | (nM) |
| $P(t)$: | serum PSA concentration | (ng mL$^{-1}$) |
| $T_s$: | serum testosterone concentration | (nM) |

$$\begin{aligned}
X_1' &= \mu_1 X_1 - \delta_1 X_1 - \Lambda X_1 + \lambda X_2 \\
X_2' &= \mu_2 X_2 - \delta_2 X_2 + \Lambda X_1 - \lambda X_2 \\
Q_i' &= (R_t^i - Q_i)(k_a^{T_i} T_i + k_a^{D_i} D_i) - \beta_i Q_i - \mu_i Q_i, \\
P' &= \sigma_1 \frac{Q_1^p}{Q_1^p + q_{\sigma_1}^p} X_1 + \sigma_2 \frac{Q_2^p}{Q_2^p + q_{\sigma_2}^p} X_2 + \sigma_0^1 X_1 + \sigma_0^2 X_2 - \beta_P P,
\end{aligned} \tag{4.23}$$

where

$$\begin{aligned}
\mu_i &= \mu_m^i \frac{(Q_i)^m}{(Q_i)^m + (q_\mu^i)^m}, & \delta_i &= \delta_m^i \frac{(q_\delta^i)^n}{(Q_i)^n + (q_\delta^i)^n} + \delta_0^i, \\
\Lambda &= c_1 \frac{(s_1)^b}{(Q_1)^b + (s_1)^b}, & \lambda &= c_2 \frac{(Q_2)^b}{(Q_2)^b + (s_2)^b}, \\
T_i &= v_i T_s \frac{v_i T_s + \alpha_k^i}{v_i T_s + \alpha_k^i + \alpha_m^i / h_i}, & D_i &= \frac{\alpha_m^i}{\beta_D^i} \frac{v_i T_s \left(v_i T_s + \alpha_k^i\right)}{\left(v_i T_s + \alpha_k^i\right)^2 + \alpha_k^i \alpha_m^i / h_i}.
\end{aligned} \tag{4.24}$$

Model (4.23) has the same structure and number of equations as the PKN model (4.1). However, there are many differences in its implementation. First, the proliferation rates $\mu_i$ are no longer given by the Droop model for phytoplankton growth. The reason is that the concepts of $Q$ and the minimum quota in the PKN model are problematic (as discussed in section 4.4). Next, the model has androgen-dependent death rate functions in addition to the constant baseline death rates.

Finally, the equation for $Q'$ includes the mechanistically derived "uptake" equation. While this adds more parameters and slightly increased computational complexity, it may be simplified by rewriting $\frac{\alpha_m^i}{\beta_D^i}$ and $\alpha_m^i/h_i$ as two separate parameters, reducing the model's total parameters by 4 (2 for each cell subpopulation). The

| Parameter | Description | Units |
|---|---|---|
| $\mu_m^i$ | maximum specific proliferation rate | $h^{-1}$ |
| $\mu_q^i$ | proliferation function constant | nM |
| $\delta_m^i$ | maximum specific death rate | $h^{-1}$ |
| $\delta_q^i$ | apoptosis function constant | nM |
| $\delta_0^i$ | baseline specific death rate | $h^{-1}$ |
| $\sigma_i$ | maximum specific PSA secretion rate | ng $mL^{-1}$ $1\times10^6$ $cell^{-1}$ $h^{-1}$ |
| $\sigma_q^i$ | PSA production function constant | nM |
| $\sigma_0^i$ | baseline PSA secretion rate | ng $mL^{-1}$ $1\times10^6$ $cell^{-1}$ $h^{-1}$ |
| $c_1$ | maximum $X_1 \to X_2$ mutation rate | $h^{-1}$ |
| $c_2$ | maximum $X_2 \to X_1$ mutation rate | $h^{-1}$ |
| $s_1$ | $X_1 \to X_2$ mutation function constant | nM |
| $s_2$ | $X_2 \to X_1$ mutation function constant | nM |
| $\mu_q^i$ | proliferation function constant | nM |
| $m$ and $n$ | proliferation and death rate coefficients | dimensionless |
| $p$ and $b$ | PSA secretion and mutation rate coefficients | dimensionless |
| $\beta_i$ | T and DHT loss rate* | $nM^{-1}$ $h^{-1}$ |

**Table 4.2:** Parameters for the AR quota model (4.23). *$\beta_i$ is equal to the value $(1 - f_D^i)k_d^{T_i} - f_D^i k_d^{D_i}$, where $f_D^i$ is the steady state fraction of intracellular androgens in the form of DHT.

| Case | PKN model | AR Quota model | AR Quota model (one population) |
|---|---|---|---|
| 1 | 2.96 | 1.74 (1.81)* | 4.67* |
| 2 | 2.79 | 2.77 (3.18)* | 6.85* |
| 3 | 46.42 | 35.5 | 67.4 |
| 4 | 3.924 | 3.38 | 25.5 |
| 5 | 41.81 | 0.62 | 0.579 |
| 6 | 0.40 | 0.98 | 1.17 |
| 7 | 3.71 | 1.92 (1.62)* | 1.73* |

**Table 4.3:** MSE values from fitting the AR Quota Model (4.23) and PKN Model (4.1) to the seven-patient clinical data from Akakura et al. (1993). Values with * are the corrected MSEs which disregard serum PSA assays below the 2 ng $mL^{-1}$ detection level during the initial part of the study. All other serum PSA assays were made with a lower limit of 0.2 ng $mL^{-1}$ (Akakura et al., 1993).

parameter $\beta_i$ is actually equal to $(1 - f_D^i)k_d^{T_i} - f_D^i k_d^{D_i}$ where $f_D^i$ is the steady state fraction of intracellular androgens that are DHT. This reason is that $Q_i = C_T^i + C_D$ and so $Q'$ has the term $-k_d^{T_i}C_T^i - k_d^{D_i}C_D^i$. The AR quota model (4.23) therefore gives a strong basis for including the loss term for $Q'$, including what biochemical parameters it represents.

### *4.7.1 Results*

The seven-patient clinical data from Akakura et al. (1993) were used to validate the AR Quota model and to provide a means for comparison with the PKN quota model (4.1). Results for each patient are found in Figures 4.2 and 4.3. The mean squared error (MSE) values, including those reported for the PKN model, are listed in Table 4.3. Overall the new model provided better fits to the data. Besides achieving improved or (marginally) different MSE values, the mechanistic derivation

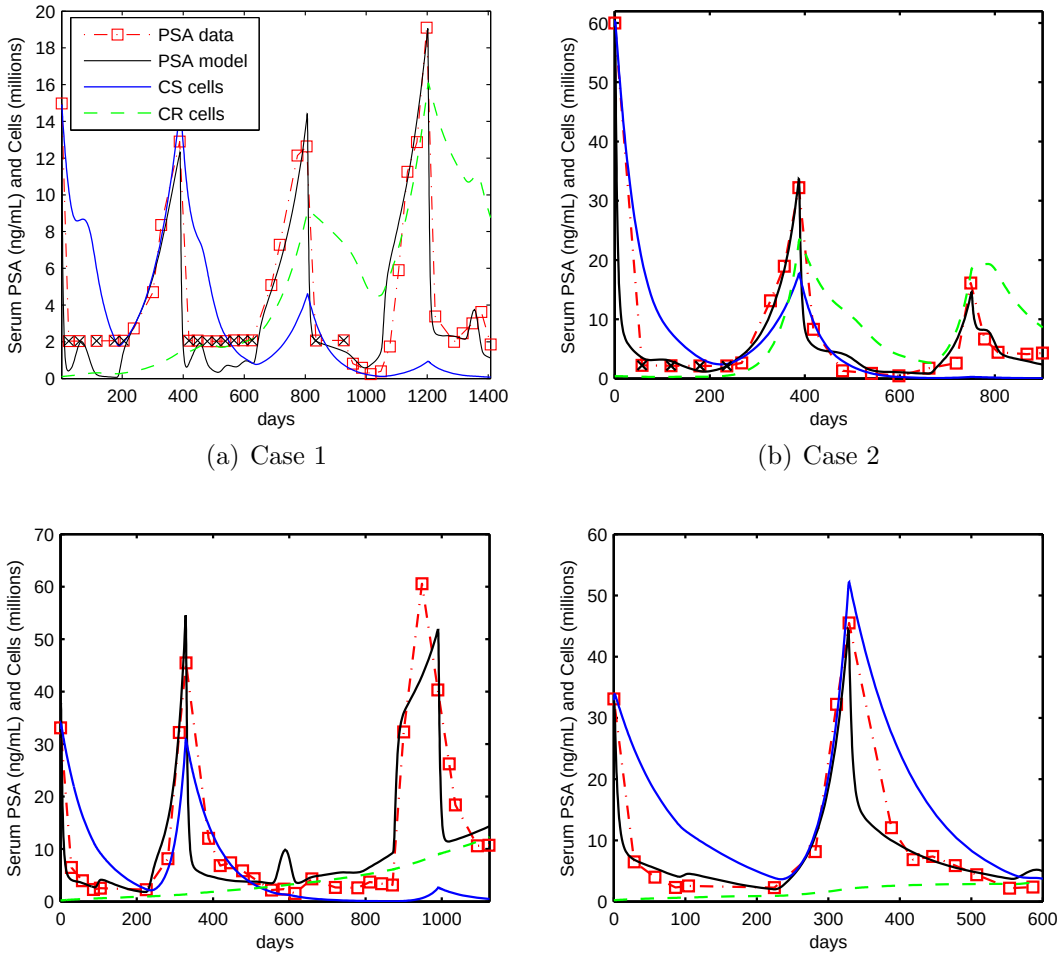


(a) Case 1

(b) Case 2

(c) Case 3

(d) Case 3 (1.5 treatment cycles)

**Figure 4.2:** Fitting the AR Quota Model (4.23) to the seven patient clinical data from Akakura et al. (1993). Data points marked with "x" indicate serum PSA values below the $2\,\mathrm{ng\,mL^{-1}}$ detection level which existed during the beginning of the study. (a) Case 1: localized stage C, 3.5 cycles. (b) Case 2: localized stage C, 2.5 cycles. (c) Case 3: stage C, 2.5 cycles. As with the PKN model (Portz, Kuang and Nagy, 2012), it was difficult to fit case 3 data. (d) Case 3, first 1.5 cycles.

It was found that the model with a single cell population is sufficient for describing the observed dynamics for several cases. During the numerical tests there were a number of interesting results that are worth noting. If the initial parameter guesses are set so that expansion of the CR population is not possible then only the CS population is used to fit the data. Figure 4.4 contains selected results of fitting with

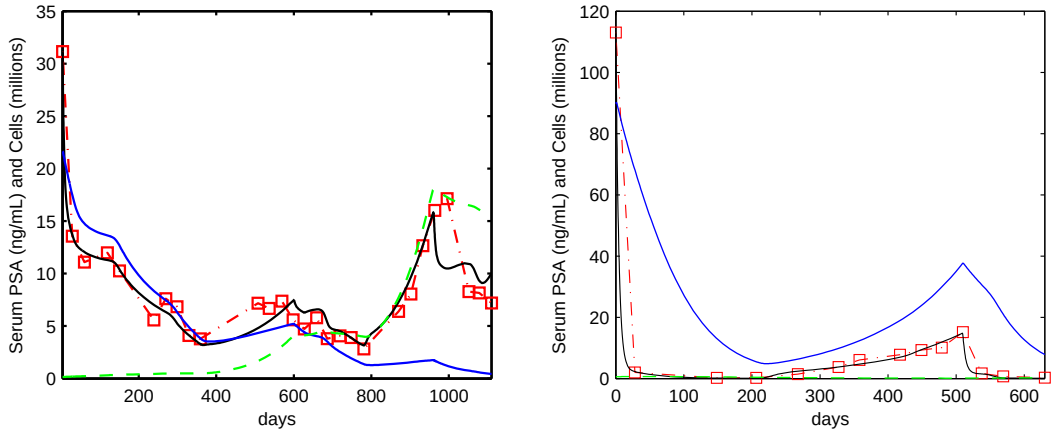


(a) Case 4




(b) Case 5

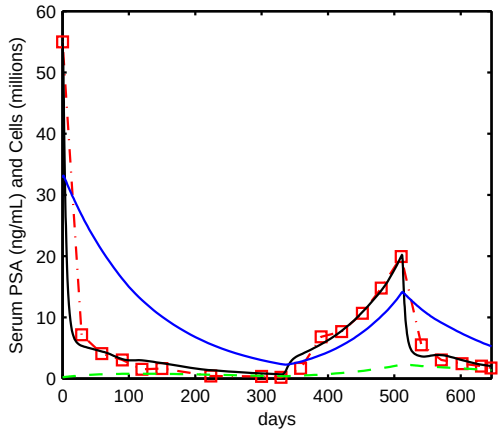


(c) Case 6

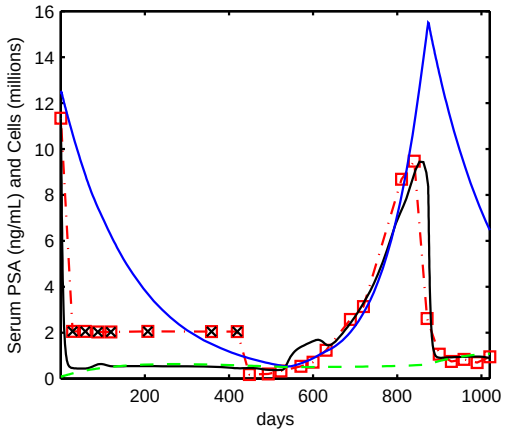


(d) Case 7

**Figure 4.3:** Fitting the AR Quota Model (4.23) to Akakura et al. (1993), continued. (a) Case 4: stage D1 with metastases, 2.5 cycles. (b) Case 5: stage C, 1.5 cycles. (c) Case 6: stage D2, 1.5 cycles. (d) Case 7: stage D2 with bone metastases, 1.5 cycles.

one cell population. The results were obtained while testing various initial parameter values for optimization and reflect "quick" tests. The single population is able to fit the data from Case 1 relatively well.

## 4.8 Conclusion

Starting from the AR chemical kinetics models established in Potter, Zager and Barton (2006); Eikenberry, Nagy and Kuang (2010), a relatively simple PCa model

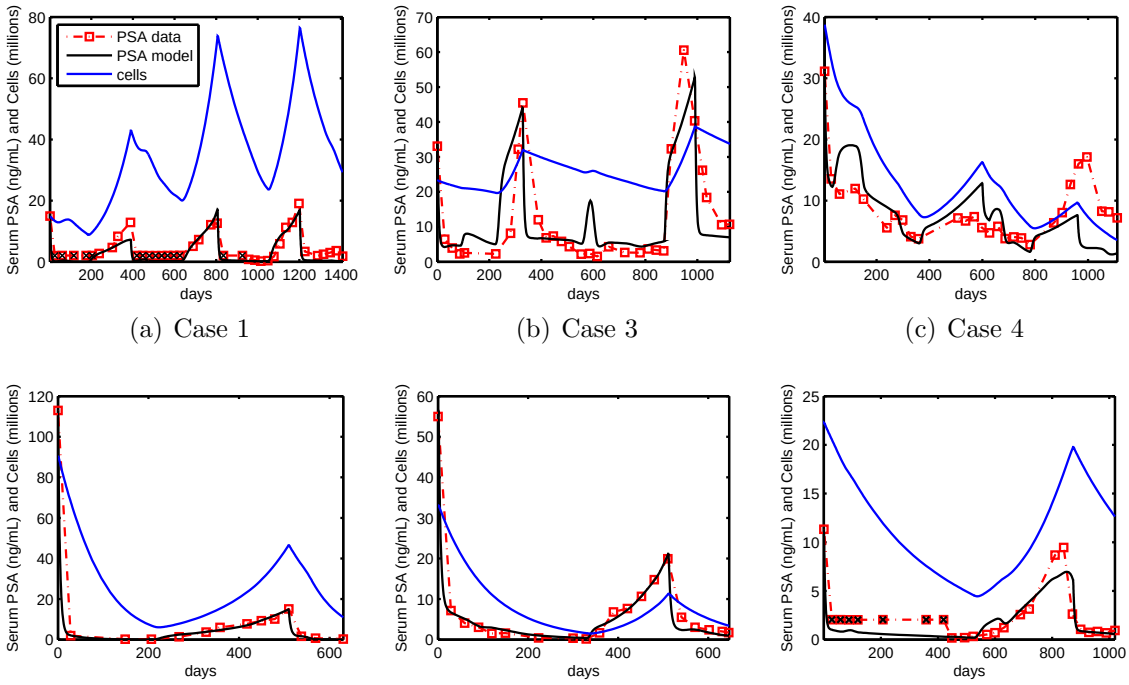


(a) Case 1 (b) Case 3 (c) Case 4

(d) Case 5 (e) Case 6 (f) Case 7

**Figure 4.4:** One population model. (a)-(b) Case 1. The model appears to fit the PSA data well. Note the cell population size more than doubles and halves each cycle. Further, the total androgen:AR complex concentration is upwards of 800 nM. (c) Case 3. An extreme example of changes in PSA levels due to changes in AR signaling but not tumor size. (d)-(e). Case 4. Indications are that CR was developing. These particular data suggest the need for a second population in the model.

has been derived. In particular, a mechanistic basis has been established for the higher-level "cell quota" framework from Portz, Kuang and Nagy (2012). This new model maintains the PKN model's ability to fit clinical data (Akakura et al., 1993) while providing a stronger link to the underlying biology. It can also fit the same data using only one cell population, raising many interesting questions for future modeling work.

A problem with ADT models is that only the PSA output is readily verifiable. A model's predictions for the two (or more) cancer cell subpopulations is largely based on theoretical assumptions and parameterizations. These model outputs certainly may be verified experimentally; however, regularly profiling tumors to determine, e.g., $X_1$

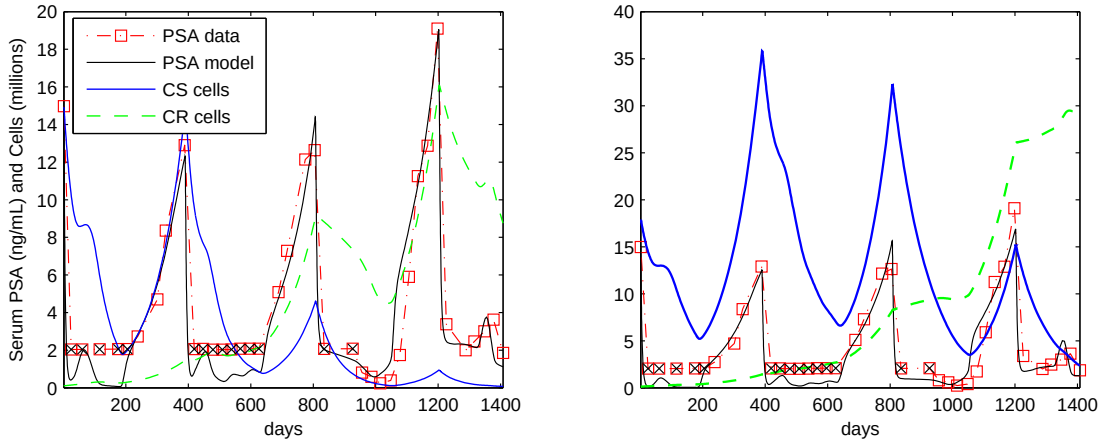


(a) Case 1a (b) Case 1b

**Figure 4.5:** One problem with the two-subpopulation approach is that two solutions can fit the same clinical data but with significantly different predictions. An illustrative example is Model (4.23) fit to clinical case 1 from Akakura et al. (1993). (a) predicts a disease state that remains largely sensitive to treatment for proliferation, PSA secretion, and survival. However, (b) predicts that the disease escapes dependence on androgen for survival. While both solutions explain the observed PSA dynamics, they have vastly different implications for effectiveness of continued treatment.

and $X_2$ is not plausible for practical or clinical purposes. Thus for clinical applications and *in vivo* data in general, the classification and relative sizes of the different subpopulations is theoretical. Consequently it is a problem that these theoretical outputs add many degrees of freedom to the models. These model constructions enable many different explanations for a single set of data.

How inter-subpopulation transitions are modeled may also exacerbate these problems. Androgen-dependent "mutation" rates are essentially ad-hoc enforcements of observed behavior into models. Treatment resistance is treated as a binary phenomenon: cancer cells either are completely sensitive to or have a fixed degree of resistance to ADT. The transition to resistance is more likely a multi-step process with many different mechanisms of resistance expressed in a single tumor (Edwards and Bartlett, 2005b).

Figures 4.5 and 4.4 illustrate these points for the AR Quota Model (4.23). Fig-

ure 4.5 shows two different solutions of the same model for a single clinical case. Although both solutions provide relatively good fits of the PSA data, their theoretical outputs have vastly different implications. In figure 4.5(a), responsiveness to treatment is maintained but with a decreased apoptotic response. In figure 4.5(a), apoptotic potential of the tumor is completely lost due to the CR population's independence from $Q$ for survival. Akakura et al. (1993) measured a 56% decrease in prostate volume during the final treatment cycle. Assuming that the prostate size is correlated to local tumor volume, then the first solution in figure 4.5(a) is more reasonable. Nonetheless, the general pattern of tumor growth and regression in both figures 4.5(a)–4.5(b) are consistent with observation.

In general, a good fit can be found for any single cycle. For multiple cycles, finding a good fit becomes increasingly difficult. This problem may be due to the aforementioned problems with the models. Figure 4.5 presents a comparison of the two- and one- subpopulation models for two clinical cases. It should be noted that these particular data represent only one and a half cycles of treatment. Hence the one-population model sufficient for predicting the observed PSA dynamics—a second cancer cell subpopulation is not necessary to fit the data. In fact, the two-population model is arguably worse when considering the cost of additional parameters and complexity.

### *4.8.1 Future Work*

In a separate project, both the PKN and new AR quota models were used to analyze clinical data from 86 patients treated with IAS for late-stage or biochemically recurrent prostate cancer (see Bruchovsky et al. (2006) for an overview of the study). The goal was to establish a feasible set or distribution of parameter ranges based on these data. A question was if the fitted parameters for an individual patient's

data can be an indicator of prognosis via comparison with the others' parameters and outcomes. Then, as a next step, to investigate whether or not fitting only partial data from a patient can predict the actual outcome. This ambitious project, not included here, led to the realization that more work is needed before a simple ODE model can aid in predicting clinical outcomes. While the model can fit these larger sets of data, no conclusive answers to these questions were found.

Hirata, Bruchovsky and Aihara (2010); Hirata et al. (2012a,b) investigated these questions with the same data but with a system of linear ODEs that are not readily linked to the underlying physical biology. The authors made an important first step in exploring the potential for PCa models to aid clinicians in treating patients with ADT. Similar questions were also discussed in (Morken et al., 2014; Everett, Packer and Kuang, 2014) but on a much smaller scale (using the 7 patient data in Akakura et al. (1993)) and with models that share the same underlying issues as the PKN model. It remains to be discovered how mathematical models of PCa can effect improvements in ADT for advanced or metastatic prostate cancer. Thus far, it has been demonstrated that models can successfully fit clinical data, albeit retroactively. Much work remains to be done in this interdisciplinary research area in order to realize the full potential of dynamical models of prostate cancer.

# REFERENCES


Akakura, K., N. Bruchovsky, S. L. Goldenberg, P. S. Rennie, A. R. Buckley and L. D. Sullivan, "Effects of intermittent androgen suppression on androgen-dependent tumors. apoptosis and serum prostate-specific antigen", Cancer **71**, 9, 2782–2790 (1993).

Archibald, P. A., "*Pseudochlorococcum*, a new chlorococcalean genus", Journal of Phycology **6**, 2, 127–132 (1970).

Behrenfeld, M. J. and P. G. Falkowski, "A consumer's guide to phytoplankton primary productivity models", Limnology and Oceanography **42**, 7, 1479–1491 (1997a).

Behrenfeld, M. J. and P. G. Falkowski, "Photosynthetic rates derived from satellite-based chlorophyll concentration", Limnology and Oceanography **42**, 1, 1–20 (1997b).

Behrenfeld, M. J., O. Prasil, M. Babin and F. Bruyant, "In search of a physiological basis for covariations in light-limited and light-saturated photosynthesis", Journal of Phycology **40**, 1, 4–25 (2004).

Berman-Frank, I. and Z. Dubinsky, "Balanced growth in aquatic plants: myth or reality?", BioScience **49**, 1, 29–37 (1999).

Boersma, M. and J. J. Elser, "Too much of a good thing: on stoichiometrically balanced diets and maximal growth", Ecology **87**, 5, 1325–1330 (2006).

Bruchovsky, N., L. Klotz, J. Crook, S. Malone, C. Ludgate, W. J. Morris, M. E. Gleave and S. L. Goldenberg, "Final results of the Canadian prospective phase II trial of intermittent androgen suppression for men in biochemical recurrence after radiotherapy for locally advanced prostate cancer", Cancer **107**, 2, 389–395 (2006).

Bruchovsky, N., L. Klotz, M. Sadar, J. Crook, D. Hoffart, L. Godwin, M. Warkentin, M. Gleave and S. Goldenberg, "Intermittent androgen suppression for prostate cancer: Canadian Prospective Trial and related observations", Molecular urology **4**, 3, 191 (2000).

Bruchovsky, N., R. Snoek, P. S. Rennie, K. Akakura, S. L. Goldenberg and M. Gleave, "Control of tumor progression by maintenance of apoptosis", The Prostate **29**, S6, 13–21 (1996).

Burford, M. A. and K. Lorenzen, "Modeling nitrogen dynamics in intensive shrimp ponds: the role of sediment remineralization", Aquaculture **229**, 1, 129–145 (2004).

Cullen, J. J., "On models of growth and photosynthesis in phytoplankton", Deap-Sea Research **37**, 667–683 (1990).

Dayananda, P., J. T. Kemper and M. M. Shvartsman, "A stochastic model for prostate-specific antigen levels", Mathematical biosciences **190**, 2, 113–126 (2004).

Denmeade, S. R. and J. T. Isaacs, "A history of prostate cancer treatment", Nature Reviews Cancer **2**, 5, 389396 (2002).

Droop, M., "Vitamin B12 and marine ecology. IV. the kinetics of uptake, growth and inhibition in monochrysis lutheri", J. Mar. Biol. Assoc. UK **48**, 3, 689–733 (1968).

Droop, M., "Some thoughts on nutrient limitation in algae", Journal of Phycology **9**, 3, 264–272 (1973).

Droop, M., "25 years of algal growth kinetics: A personal view", Botanica Marina **26**, 3, 99–112 (1983).

Droop, M., "In defence of the Cell Quota model of micro-algal growth", Journal of plankton research **25**, 1, 103–107 (2003).

Edwards, J. and J. Bartlett, "The androgen receptor and signal-transduction pathways in hormone-refractory prostate cancer. Part 1: modifications to the androgen receptor", BJU international **95**, 9, 1320–1326 (2005a).

Edwards, J. and J. Bartlett, "The androgen receptor and signal-transduction pathways in hormone-refractory prostate cancer. Part 2: androgen-receptor cofactors and bypass pathways", BJU international **95**, 9, 1327–1335 (2005b).

Eikenberry, S. E., J. D. Nagy and Y. Kuang, "The evolutionary impact of androgen levels on prostate cancer in a multi-scale mathematical model", Biology Direct **5**, 24 (2010).

Everett, R. A., A. M. Packer and Y. Kuang, "Can mathematical models predict the outcomes of prostate cancer patients undergoing intermittent androgen deprivation therapy?", Biophysical Reviews and Letters pp. 1–19 (2014).

Falkowski, P. G., Z. Dubinsky and K. Wyman, "Growth-irradiance relationships in phytoplankton", Limnology and Oceanography **30**, 2, 311–321 (1985).

Feldman, B. J. and D. Feldman, "The development of androgen-independent prostate cancer", Nature Reviews Cancer **1**, 34–45 (2001).

Friedrichs, M. A., M.-E. Carr, R. T. Barber, M. Scardi, D. Antoine, R. A. Armstrong, I. Asanuma, M. J. Behrenfeld, E. T. Buitenhuis, F. Chai *et al.*, "Assessing the uncertainties of model estimates of primary productivity in the tropical Pacific Ocean", Journal of Marine Systems **76**, 1, 113–133 (2009).

Geider, R., H. MacIntyre and T. Kana, "Dynamic model of phytoplankton growth and acclimation: responses of the balanced growth rate and the chlorophyll a: carbon ratio to light, nutrient-limitation and temperature", Marine ecology progress series. Oldendorf **148**, 1, 187–200 (1997).

Geider, R. J., H. L. MacIntyre and T. M. Kana, "A dynamic model of photoadaptation in phytoplankton", Limnology and Oceanography pp. 1–15 (1996).

Geider, R. J., H. L. MacIntyre and T. M. Kana, "A dynamic regulatory model of phytoplanktonic acclimation to light, nutrients, and temperature", Limnology and Oceanography **43**, 4, 679–694 (1998).

Gelmann, E. P., "Molecular biology of the androgen receptor", Journal of Clinical Oncology **20**, 13, 3001–3015 (2002).

Gregory, C. W., R. T. Johnson, J. L. Mohler, F. S. French and E. M. Wilson, "Androgen receptor stabilization in recurrent prostate cancer is associated with hypersensitivity to low androgen", Cancer research **61**, 7, 2892–2898 (2001).

Grobbelaar, J. U., *Mass Production of Microalgae at Optimal Photosynthetic Rates*, chap. 14 (InTech, 2013).

Guo, Q., Y. Tao and K. Aihara, "Mathematical modeling of prostate tumor growth under intermittent androgen suppression with partial differential equations", International Journal of Bifurcation and Chaos **18**, 12, 3789–3797 (2008).

Halterman, S. G. and D. W. Toetz, "Kinetics of nitrate uptake by freshwater algae", Hydrobiologia **114**, 3, 209–214 (1984).

Heinlein, C. A. and C. Chang, "Androgen receptor in prostate cancer", Endocrine Reviews **25**, 2, 276–308 (2004).

Hirata, Y., K. Akakura, C. S. Higano, N. Bruchovsky and K. Aihara, "Quantitative mathematical modeling of PSA dynamics of prostate cancer patients treated with intermittent androgen suppression", Journal of molecular cell biology **4**, 3, 127–132 (2012a).

Hirata, Y., N. Bruchovsky and K. Aihara, "Development of a mathematical model that predicts the outcome of hormone therapy for prostate cancer", Journal of Theoretical Biology **264**, 2, 517–527 (2010).

Hirata, Y., G. Tanaka, N. Bruchovsky and K. Aihara, "Mathematically modelling and controlling prostate cancer under intermittent hormone therapy", Asian journal of andrology **14**, 2, 270–277 (2012b).

Ho, T.-Y., A. Quigg, Z. V. Finkel, A. J. Milligan, K. Wyman, P. G. Falkowski and F. M. M. Morel, "The elemental composition of some marine phytoplankton", Journal of Phycology **39**, 6, 1145–1159 (2003).

Hu, Q., D. Han and M. Summerfeld, "Novel *Pseudochlorococcum* species and uses therefor", (2010).

Hu, Q., M. Sommerfeld, E. Jarvis, M. Ghirardi, M. Posewitz, M. Seibert and A. Darzins, "Microalgal triacylglycerols as feedstocks for biofuel production: perspectives and advances", The Plant Journal **54**, 4, 621–639 (2008).

Huggins, C., R. Stevens and C. V. Hodges, "Studies on prostatic cancer: II. the effects of castration on advanced carcinoma of the prostate gland", Archives of Surgery **43**, 2, 209–223 (1941).

Ideta, A. M., G. Tanaka, T. Takeuchi and K. Aihara, "A mathematical model of intermittent androgen suppression for prostate cancer", Journal of nonlinear science **18**, 6, 593–614 (2008).

Jackson, T. L., "A mathematical investigation of the multiple pathways to recurrent prostate cancer: comparison with experimental data", Neoplasia **6**, 6, 697–704 (2004a).

Jackson, T. L., "A mathematical model of prostate tumor growth and androgen-independent relapse", Discrete and Continuous Dynamical Systems-Series B **4**, 1, 187–202 (2004b).

Jain, H. V., S. K. Clinton, A. Bhinder and A. Friedman, "Mathematical modeling of prostate cancer progression in response to androgen ablation therapy", PNAS **108**, 49, 19701–19706 (2011).

Jain, H. V. and A. Friedman, "Modeling prostate cancer response to continuous versus intermittent androgen ablation therapy", Discrete and continuous dynamical systems series B **18**, 4, 945–967 (2013).

Jamu, D. and R. Piedrahita, "Nitrogen biogeochemistry of aquaculture ponds", Aquaculture **166**, 181–212 (1998).

Jamu, D. and R. Piedrahita, "An organic matter and nitrogen dynamics model for the ecological analysis of integrated aquaculture/agriculture systems: I. model development and calibration", Environmental Modelling & Software **17**, 6, 571–582 (2002a).

Jamu, D. and R. Piedrahita, "An organic matter and nitrogen dynamics model for the ecological analysis of integrated aquaculture/agriculture systems: II. model evaluation and application", Environmental Modelling & Software **17**, 6, 583–592 (2002b).

Klok, A. J., J. A. Verbaanderd, P. P. Lamers, D. E. Martens, A. Rinzema and R. H. Wijffels, "A model for customising biomass composition in continuous microalgae production", Bioresource technology **146**, 89–100 (2013).

Koivisto, P., J. Kononen, C. Palmberg, T. Tammela, E. Hyytinen, J. Isola, J. Trapman, K. Cleutjens, A. Noordzij, T. Visakorpi *et al.*, "Androgen receptor gene amplification: a possible molecular mechanism for androgen deprivation therapy failure in prostate cancer", Cancer research **57**, 2, 314–319 (1997).

Kuang, Y., J. Huisman and J. J. Elser, "Stoichiometric plant-herbivore models and their interpretation", Mathematical Biosciences and Engineering **1**, 2, 215–222 (2004).

Leadbeater, B., "The 'Droop Equation'–Michael Droop and the legacy of the 'Cell-Quota Model' of phytoplankton growth", Protist **157**, 3, 345 (2006).

Lee, D. K. and C. Chang, "Expression and degradation of androgen receptor: mechanism and clinical implication", Journal of Clinical Endocrinology & Metabolism **88**, 9, 4043–4054 (2003).

Lemarie, G., A. Dosdat, D. Covès, G. Dutto, E. Gasset and J. Person-Le Ruyet, "Effect of chronic ammonia exposure on growth of European seabass (Dicentrarchus labrax) juveniles", Aquaculture **229**, 1, 479–491 (2004).

Li, Y., D. Han, M. Sommerfeld and Q. Hu, "Photosynthetic carbon partitioning and lipid production in the oleaginous microalga *Pseudochlorococcum* sp. (Chlorophyceae) under nitrogen-limited conditions", Bioresource Technology **102**, 1, 123–129 (2011).

Li, Y., M. Horsman, B. Wang, N. Wu and C. Q. Lan, "Effects of nitrogen sources on cell growth and lipid accumulation of green alga Neochloris oleoabundans", Applied Microbiology and Biotechnology **81**, 4, 629–636 (2008).

Liu, H., A. Packer and Y. Kuang, "Stoichiometric producer-grazer models with varying nitrogen pools and ammonia toxicity", Discrete and Continuous Dynamical Systems - Series S **7**, 6, 1305–1320 (2014).

Loladze, I., Y. Kuang and J. J. Elser, "Stoichiometry in producer-grazer systems: linking energy flow with element cycling", Bulletin of Mathematical Biology **62**, 6, 1137–1162 (2000).

Lorenzen, K., J. Struve and V. Cowan, "Impact of farming intensity and water management on nitrogen dynamics in intensive pond culture: a mathematical model applied to Thai commercial shrimp farms", Aquaculture Research **28**, 7, 493–507 (1997).

MacIntyre, H. L., T. M. Kana, T. Anning and R. J. Geider, "Photoacclimation of photosynthesis irradiance response curves and photosynthetic pigments in microalgae and cyanobacteria", Journal of Phycology **38**, 1, 17–38 (2002).

Markus, L., "Asymptotically autonomous differential systems", Contributions to the theory of nonlinear oscillations **2**, 17 (1956).

Marshall, H. L., R. J. Geider and K. J. Flynn, "A mechanistic model of photoinhibition", New phytologist **145**, 2, 347–359 (2000).

Mata, T. M., A. A. Martins and N. S. Caetano, "Microalgae for biodiesel production and other applications: a review", Renewable and Sustainable Energy Reviews **14**, 1, 217–232 (2010).

Mcleod, D. G., "Hormonal therapy: historical perspective to future directions", Urology **61**, 2, 3 – 7 (2003).

Morken, J., A. Packer, R. Everett, J. Nagy and Y. Kuang, "Mechanisms of resistance to intermittent androgen deprivation in prostate cancer patients identified by a novel computational method", Cancer research pp. 3673–83 (2014).

Naylor, R. L., S. L. Williams and D. R. Strong, "Aquaculture–a gateway for exotic species", Science **294**, 5547, 1655–1656 (2001).

Packer, A., Y. Li, T. Andersen, Q. Hu, Y. Kuang and M. Sommerfeld, "Growth and neutral lipid synthesis in green microalgae: A mathematical model", Bioresource Technology **102**, 1, 111–117 (2011).

Peace, A., Y. Zhao, I. Loladze, J. J. Elser and Y. Kuang, "A stoichiometric producer-grazer model incorporating the effects of excess food-nutrient content on consumer dynamics", Mathematical Biosciences **244**, 2, 107–115 (2013).

Platt, T., C. Gallegos and W. Harrison, "Photoinhibition of photosynthesis in natural assemblages of marine phytoplankton", Journal of Marine Research **38**, 687–701 (1980).

Portz, T., Y. Kuang and J. D. Nagy, "A clinical data validated mathematical model of prostate cancer growth under intermittent androgen suppression therapy", AIP Advances **2**, 1, 011002 (2012).

Potter, L. K., M. G. Zager and H. A. Barton, "Mathematical model for the androgenic regulation of the prostate in intact and castrated adult male rats", American Journal of Physiology-Endocrinology And Metabolism **291**, 5, E952–E964 (2006).

Rawat, I., R. R. Kumar, T. Mutanda and F. Bux, "Biodiesel from microalgae: A critical evaluation from laboratory to large scale production", Applied Energy **103**, 0, 444–467 (2013).

Sakshaug, E., K. Andresen and D. A. Kiefer, "A steady state description of growth and light absorption in the marine planktonic diatom Skeletonema costatum", Limnology and Oceanography **34**, 1, 198–205 (1989).

Sakshaug, E., A. Bricaud, Y. Dandonneau, P. G. Falkowski, D. A. Kiefer, L. Legendre, A. Morel, J. Parslow and M. Takahashi, "Parameters of photosynthesis: definitions, theory and interpretation of results", Journal of Plankton Research **19**, 11, 1637–1670 (1997).

Sato, N., M. E. Gleave, N. Bruchovsky, P. S. Rennie, S. Goldenberg, P. H. Lange and L. D. Sullivan, "Intermittent androgen suppression delays progression to androgen-independent regulation of prostate-specific antigen gene in the LNCaP prostate tumour model", The Journal of Steroid Biochemistry and Molecular Biology **58**, 2, 139 – 146 (1996).

Scher, H. I., G. Buchanan, W. Gerald, L. M. Butler and W. D. Tilley, "Targeting the androgen receptor: improving outcomes for castration-resistant prostate cancer", Endocrine-Related Cancer **11**, 3, 459–476 (2004).

Shimada, T. and K. Aihara, "A nonlinear model with competition between prostate tumor cells and its application to intermittent androgen suppression therapy of prostate cancer", Mathematical biosciences **214**, 1, 134–139 (2008).

Siegel, R., D. Naishadham and A. Jemal, "Cancer statistics, 2013", CA: A Cancer Journal for Clinicians **63**, 1, 11–30 (2013).

Stanier, R., R. Kunisawa, M. Mandel and G. Cohen-Bazire, "Purification and properties of unicellular blue-green algae (order *Chroococcales*)", Bacteriological Reviews **35**, 2, 171 (1971).

Sterner, R. and J. Elser, *Ecological Stoichiometry: The Biology of Elements from Molecules to the Biosphere* (Princeton University Press, 2002).

Sukenik, A., J. Bennett and P. Falkowski, "Light-saturated photosynthesis—limitation by electron transport or carbon fixation?", Biochimica et Biophysica Acta (BBA)-Bioenergetics **891**, 3, 205–215 (1987).

Suzuki, T., N. Bruchovsky and K. Aihara, "Piecewise affine systems modelling for optimizing hormone therapy of prostate cancer", Philosophical Transactions of the Royal Society A: Mathematical, Physical and Engineering Sciences **368**, 1930, 5045–5059 (2010).

Tanaka, G., Y. Hirata, S. L. Goldenberg, N. Bruchovsky and K. Aihara, "Mathematical modelling of prostate cancer growth and its application to hormone therapy", Philosophical Transactions of the Royal Society A: Mathematical, Physical and Engineering Sciences **368**, 1930, 5029–5044 (2010).

Tanaka, G., K. Tsumoto, S. Tsuji and K. Aihara, "Bifurcation analysis on a hybrid systems model of intermittent hormonal therapy for prostate cancer", Physica D: Nonlinear Phenomena **237**, 20, 2616–2627 (2008).

Tao, Y., Q. Guo and K. Aihara, "A mathematical model of prostate tumor growth under hormone therapy with mutation inhibitor", Journal of nonlinear science **20**, 2, 219–240 (2010).

Taplin, M.-E., G. J. Bubley, T. D. Shuster, M. E. Frantz, A. E. Spooner, G. K. Ogata, H. N. Keer and S. P. Balk, "Mutation of the androgen-receptor gene in metastatic androgen-independent prostate cancer", New England Journal of Medicine **332**, 21, 1393–1398 (1995).

Thieme, H. R., "Convergence results and a Poincar-Bendixson trichotomy for asymptotically autonomous differential equations", Journal of Mathematical Biology **30**, 7, 755–763 (1992).

Tomasso, J., "Toxicity of nitrogenous wastes to aquaculture animals", Reviews in Fisheries Science **2**, 291–314 (1994).

Tran, C., S. Ouk, N. J. Clegg, Y. Chen, P. A. Watson, V. Arora, J. Wongvipat, P. M. Smith-Jones, D. Yoo, A. Kwon *et al.*, "Development of a second-generation antiandrogen for treatment of advanced prostate cancer", Science Signaling **324**, 5928, 787 (2009).

Tyagi, R. K., Y. Lavrovsky, S. C. Ahn, C. S. Song, B. Chatterjee and A. K. Roy, "Dynamics of intracellular movement and nucleocytoplasmic recycling of the ligand-activated androgen receptor in living cells", Molecular Endocrinology **14**, 8, 1162–1174 (2000).

Veestraeten, D., "An alternative approach to modelling relapse in cancer with an application to adenocarcinoma of the prostate", Mathematical biosciences **199**, 1, 38–54 (2006).

Visakorpi, T., E. Hyytinen, P. Koivisto, M. Tanner, R. Keinänen, C. Palmberg, A. Palotie, T. Tammela, J. Isola and O.-P. Kallioniemi, "In vivo amplification of the androgen receptor gene and progression of human prostate cancer", Nature genetics **9**, 4, 401–406 (1995).

Walsh, P. C., H. Lepor and J. C. Eggleston, "Radical prostatectomy with preservation of sexual function: anatomical and pathological considerations", The Prostate **4**, 5, 473–485 (1983).

Wang, H., Y. Kuang and I. Loladze, "Dynamics of a mechanistically derived stoichiometric producer-grazer model", Journal of Biological Dynamics **2**, 3, 286–296 (2008).

Wright, A., L. Thomas, R. Douglas, C. Lazier and R. Rittmaster, "Relative potency of testosterone and dihydrotestosterone in preventing atrophy and apoptosis in the prostate of the castrated rat", J Clin Invest **98**, 2558–2563 (1996).